Titre: Title:	Cutting Conditions Optimisation of Titanium Metal Matrix Composites in Turning and Face Milling.
Auteur: Author:	Alireza Asgari
Date:	2015
Type:	Mémoire ou thèse / Dissertation or Thesis
Référence: Citation:	Asgari, A. (2015). Cutting Conditions Optimisation of Titanium Metal Matrix Composites in Turning and Face Milling. [Mémoire de maîtrise, École Polytechnique de Montréal]. PolyPublie. https://publications.polymtl.ca/1950/

URL de PolyPublie: PolyPublie URL:	https://publications.polymtl.ca/1950/
Directeurs de recherche: Advisors:	Marek Balazinski
Programme: Program:	Génie mécanique

UNIVERSITÉ DE MONTRÉAL

CUTTING CONDITIONS OPTIMISATION OF TITANIUM METAL MATRIX COMPOSITES IN TURNING AND FACE MILLING

ALIREZA ASGARI

DÉPARTEMENT DE GÉNIE MÉCANIQUE

ÉCOLE POLYTECHNIQUE DE MONTRÉAL

MÉMOIRE PRÉSENTÉ EN VUE DE L'OBTENTION

DU DIPLÔME DE MAÎTRISE ÈS SCIENCES APPLIQUÉES

(GÉNIE MÉCANIQUE)

DÉCEMBRE 2015

UNIVERSITÉ DE MONTRÉAL

ÉCOLE POLYTECHNIQUE DE MONTRÉAL

Ce mémoire intitulé :

CUTTING CONDITIONS OPTIMISATION OF TITANIUM METAL MATRIX COMPOSITES IN TURNING AND FACE MILLING

présenté par: ASGARI Alireza

en vue de l'obtention du diplôme de : Maîtrise ès sciences appliquées

a été dûment accepté par le jury d'examen constitué de :

M. VADEAN Aurelian, Doctorat, président

M. BALAZINSKI Marek, Doctorat ès sciences, membre et directeur de recherche

M. MAYER René, Ph. D., membre

DEDICATION

I would like to dedicate this thesis to my little daughter.

ACKNOWLEDGEMENTS

I would like to express my sincere gratitude to my advisor, Professor Marek Balazinski, for the opportunity he has given me to work at the “laboratoire de recherché en fabrication virtuelle (LRFV) 'of École Polytechnique de Montréal.” Without his thrust, guidance, patience and supports, my research would not have been successful. Undoubtedly, he was the most influential person during my M.Sc. and I hope the bond that we established will continue for many years to come.

My immense appreciation extends to Professor Aurelian Vadean and Professor René Mayer serving as members of jury of my M.Sc. defense committee and for providing valuable comments.

I appreciate National Sciences and Engineering Research Council of Canada (NSERC) Innovation in Machining Technology (CANRIMT) for their financial supports.

Sincere thanks are extended to Dr. Seyed Ali Niknam for the time and efforts he spent to edit and improve my thesis.

Special thanks go to manufacturing laboratory technicians, Mr. Guy Gironne and Mr. Vincent Mayer for their excellent cooperation.

I really appreciate Mrs. Martine Bénard and Mrs. Carole Fraser for all the helps.

I wish to give my wholehearted thanks to my parents for their unwavering supports, kind words, well-wishing and patience for abiding by my absence. Special thanks go to my beloved wife Shilla and my children Anahita and Jasmine for their patience and for burden of life during the final stages of this thesis.

Finally, I express my deep feelings to my God for giving me the will to do this work.

RÉSUMÉ

Il y a quelques décennies, les industries ont utilisé les composites à matrice métallique de titane (Ti-MMC) dans les valeurs limitées. Chacune des industries s'intéresse à la caractéristique particulière du Ti-MMC. Les constructeurs de voitures s'intéressent à la résistance à l'usure et à la fatigue de ce matériau dans la fabrication des composantes de moteur et de transmission pour ainsi diminuer le poids des véhicules. Les fournisseurs d'accessoires et de matériel médicaux utilisent le Ti-MMC vu sa grande rigidité spécifique et sa résistance en compression élevée. De plus, dans les domaines aéronautique et aérospatiale, les fabricants sont intéressés par le gain en légèreté de ce matériau.

Mais il y a un problème avec le Ti-MMC, il a une faible usinabilité. Les aspects importants et acceptables pour l'usinage de pièces en industrie sont le coût de fabrication, de la finition de la surface et de la conformité au devis. Aussi, une dureté augmentée par les particules de céramique et une rigidité élevée du produit induisent un facteur de propagation élevée de fissures dans le corps du Ti-MMC. De plus, les particules fissurées ont tendance à éroder les arêtes des outils de coupe provoquant la dégradation de la finition de surface. Une très faible conductivité thermique, une haute résistance à la compression et une basse tendance à la déformation plastique devant l'arête de l'outil de coupe lors de son engagement avec ce matériau portent les contraintes mécaniques et thermiques à augmenter durant le processus d'usinage.

Il n'y a que peu d'études sur le Ti-MMC, en particulier sur l'usinage de ce matériau. En général, les outils PCD sont connus comme étant les outils les plus performants lors de l'usinage du MMC, mais le coût de production est fortement affecté par le prix élevé de ces outils. Cette étude fait suite à des expériences réalisées sur l'effet de trois sortes d'outils (carbure revêtu, PCBN et PCD) sur le tournage et (carbure et d'outils PCD) sur le surfaçage du Ti-MMC. Sur les conséquences de la productivité, le taux d'usure des outils et la rugosité de surface de la pièce. Les conditions de coupe optimales sont déterminées pour chaque outil au tournage et au fraisage en bout du Ti-MMC. Les effets des paramètres de coupe sont extraits par analyse de variance. Pour l'optimisation du processus de tournage et de fraisage avec chaque outil, la méthode Taguchi est utilisée. De plus, les données de performance de ces outils lors de ces expériences sont analysées.

ABSTRACT

World leading manufacturing sectors, in particular aerospace and automotive industries wish to have lighter materials with better physical, mechanical and chemical properties than the prevalent hard to cut heavier materials. This has brought much attention to alternative materials such as metal matrix composite (MMC). MMCs are composed of non-metallic reinforcements (i.e. ceramic) in metal matrices which feature high toughness, wear and fatigue resistance and relatively light weight. One of the metallic composite with remarkable mechanical properties is titanium metal matrix composite (Ti-MMC). Ti-MMC has been successfully incorporated into numerous of products in various industrial sectors. Each industrial sector has an interest in particular characteristics of Ti-MMC. Automotive and aerospace industries are craving for high wear and fatigue resistant materials with low weight for delicate applications in engine and power train component. Medical components suppliers utilize Ti-MMC in pursuance of its great specific stiffness and elevated compressive strength.

Despite having excellent features, various issues have emerged relate to the machining and machinability of Ti-MMCs. Due to the presence of hard and abrasive ceramic particles in metal matrices of Ti-MMCs, crack propagation appears on the Ti-MMC body. Furthermore, weak heat conductivity, low tendency to plastic deformation and high compressive resistance of the matrix exert large mechanical and thermal stresses to the cutting tool and the work-piece. This reveals that the principal machinability attributes of Ti-MMCs are rapid tool wear, low surface quality in Ti-MMC machined parts and excessive cost. According to the review of literature, there are few studies on the machining and machinability of Ti-MMCs. There is a lack of knowledge on appropriate setting levels of cutting process parameters for machining Ti-MMC, in particular milling and turning operations that deal with high material removal rate.

The main objectives of this work are to study the cutting parameters governing the tool wear and surface quality (finish) when machining (milling and turning) Ti-MMCs, as well as cutting factors optimization using Taguchi method to better reach the optimum or near optimum surface finish, tool wear and productivity. To that end, comprehensive experimental studies are arranged in multi-level full factorial design and orthogonal array design of experiment.

TABLE OF CONTENTS

LIST OF TABLES

LIST OF FIGURES

LIST OF SYMBOLS AND ABBREVIATIONS

MMC	Metal Matrix Composite
TiC	Titanium Carbide
TiN	Titanium Nitride
Ti-MMC	Titanium Metal Matrix Composite
γ_{wof}	Fracture-Work
K_{Ic}	Fracture Toughness
E	Modulus of Elasticity
Kr	specific Cutting Pressure
ρ	Mass Density
UTS	Ultimate Tensile Strength
Y	Yield Strength
BHN	Brinell hardness
HK	Knoop hardness
G	Shear Modulus
τ	Shear Strength
B	Bulk Strength
υ	Poisson Ratio
C	Coefficient of Thermal Expansion
k	Heat Conductivity
VB	Cutting Tool Flank Wear Width
PCD	Polycrystalline Diamond
CBN	Cubic Boron Nitride
PCBN	Polycrystalline Boron Nitride

RSM	Response Surface Methodology
Ra	Average Surface Roughness
SNR	Signal to Noise Ratio
SS	Sum of Squares
MS	Mean of Squares
y_{ij}	Observed Response
μ	Response Distribution Mean
ε_{ij}	Response Residual
TiAlN	Titanium Aluminum Nitride
TiSiN	Titanium Silicon Nitride
Co	Cobalt
Ru	Ruthenium
v_c	Cutting Speed
f_r	Cutting Feed Rate
a_p	Cutting Depth
MRR	Material Removal Rate
VB_{Bmax}	Maximum Wear of the Straight part of Cutting Edge
$\dot{VB}_{Bmax}$	The Rate of Maximum Wear of the Straight part of Cutting Edge

LIST OF APPENDICES

CHAPTER 1 INTRODUCTION

With growing the economy, the market demands more reliable and durable products with lightweights and less energy consumption at lower cost. This encourages industrial plants to improve their processes and materials. Significant amount of attentions has been paid to employ in alternative materials to the prevalent heavy materials, such as nickel alloys and steels. Thus, industries are interested in the new materials such as Metal Matrix Composite (MMC), which features high toughness, wear and fatigue resistance and relatively lightweight. One such metallic composite with remarkable mechanical properties is Titanium Metal Matrix Composite (Ti-MMC). It has been introduced to industry as an alternative to Ni-base alloys (Esslinger 1960) and since a few decades, it has been successfully incorporated into a vast number of products in various industrial sectors.

Automotive and aerospace industries typically use Ti-MMC in the rod connections and high wearing comportments. This strategy leads to lower weight and energy consumption in the products. Medical components suppliers employ the Ti-MMC in pursuance of great specific strength (Abkowitz, Abkowitz et al. 2004). The use of Ti-MMC in the thin structures (e.g. bicycle frame) tends to increase the stiffness of the products. Other feature of Ti-MMC, low elongation may help to establish a highly precise and rigid product (i.e. electronic devices). The main obstacle of Ti-MMC utilization is its poor productivity and machinability, which actually increases the machining and production cost. In fact, the hard particles in Ti-MMC generate cracks initiation and propagation in the work body. Moreover, the tool wear and ruining of the surface finish can be resulted.

Due to the above-mentioned difficulties hindering the applications of Ti-MMC, the industrial sectors seeking less expensive operations (e.g. automotive) have shown less interest on further investments on Ti-MMC (Ward-Close, Godfrey et al. 2001). Since 1990s, the automotive industries have had limited contributions in Ti-MMC, particularly in the engine components of sport and luxury cars (Froes, Friedrich et al. 2004). This recalls further investigations on evaluating the machinability of Ti-MMC. In the course of machinability evaluation, several criteria, including cutting force, surface quality and tool performance (wear) are of great importance.

Based on above-mentioned critics raised against the poor machinability and productivity of Ti-MMCs, this work plans to present a comprehensive investigation on the cutting factors governing the tool wear and surface quality (finish) when machining Ti- MMCs. Furthermore, the cutting parameters optimization using Taguchi method is presented to reach an optimum or near optimum surface quality, tool wear and productivity in milling and turning operations.

1.1. Problem Statement

Sever tool wear, short tool life and poor surface finish (quality) are considered the main concerns in machining Ti-MMCs. Due to aforementioned machining concerns, Ti-MMC is grouped as a difficult to cut material that suffer from poor machinability and productivity. Due to the very low thermal conductivity of Ti-MMCs, very high local temperatures are generated in a very small area around the cutting edge that result in high tool wear rate during machining operations. Moreover, oxidation and other chemical wear mechanisms are involved and further reduce the tool life. The performance of each individual tool material (i.e. Polycrystalline Diamond "PCD", carbide, and Cubic Boron Nitride "CBN") may vary under different machining operations and cutting parameters. Unfortunately, very limited experimental studies were reported on appropriate selection of tool materials and setting levels of cutting parameters (speed, feed rate) in milling and turning operations to achieve optimum or near optimum tool wear, tool life, surface finish and productivity. No work is reported yet on detailed comparison between the various tools materials used in machining Ti-MMCs. Furthermore, the optimization tools (e.g. Taguchi, GA, RSM) have not yet used to achieve optimum or near optimum tool life or surface finish when machining Ti-MMCs.

1.2. Objective

The main objectives of this work are to present a comprehensive investigation on the cutting parameters governing the tool wear and surface finish when machining Ti-MMCs, as well as cutting parameters optimization using Taguchi method to reach the optimum or near optimum surface finish, tool wear and productivity. In the course of this research project, the following specific objectives are defined:

- Understanding the cutting parameters governing the tool wear and surface quality (finish) when machining Ti-MMCs.

- Cutting parameters optimization by Taguchi method.

Each above-mentioned objective will be conducted in the case of milling and turning operations.

1.3. Scientific hypotheses

- Tool flank wear is the main aspect of tool wear and it will be used as an indicator of the tool wear.
- Average surface roughness (Ra) is the best surface quality parameter to specify the quality of the work-piece's surface finish.
- Due to specific mechanical and thermal properties of Ti-MMCs, wet (lubricated) machining is used for the machining of Ti-MMC.

1.4. Originality aspects and industrial benefits

This research project was initiated by the Canadian Network for Research and Innovation in Machining Technology (CANRIMT) and was financially supported by NSERC. The research outcomes can be used by local aerospace and automotive companies, which contributed in this project. This can be considered as the main industrial impacts on the feasibility of the project.

1.5. Thesis structure

This thesis consists of six chapters. It starts with an introduction chapter, followed by a literature review presented in chapter two. Chapter three was devoted to experimental methodology and method of analysis as well as experimental apparatus and materials used in this study. Chapter four and five present the research outcomes and they include comprehensive discussions on the research outcomes. Finally, some conclusions, recommendations and future plans are presented in Chapter 6. The experimental conditions and parameters used in this research work are presented at the beginning of Chapter 4 and Chapter 5.

Chapter 2 presents a comprehensive literature review on various machining operations, machinability aspects of Ti-MMCs including the chip morphology, surface integrity and tooling. This chapter also includes a review of the tool selection for machining Ti-MMCs. Furthermore, an overview of the most widely used optimization methods is presented. This chapter provides

insight into existing research studies, problems and missing links to be addressed. Moreover, this chapter ends with a conclusion of the literature review and a refining of the objectives.

Chapter 3 presents the experimental plan. An overview of Taguchi method as the desired optimization tool is presented. The method of analysis of experimental and optimization results is described. The work material used, along with its composition, mechanical and physical properties are introduced. The implemented tool materials and inserts are described. The CNC machines and other supporting tools including dynamometer, high resolution camera, and profilometer are presented.

Chapters 4 and **5** present the comprehensive experimental studies on evaluating the tool wear mechanisms in PCD, carbide and CBN inserts during turning and milling Ti-MMCs. The effects of each individual tool and cutting process parameter on the surface quality are described. The Taguchi optimization tool is then used to optimize the setting levels of cutting parameters to achieve optimum or near optimum surface quality and tool wear rate in turning and milling operations. Chapters 4 and 5 link the outcomes of this work and the previous studies, and help clarifying certain aspects and shortcomings that were identified in the problematic and research objectives. The discussion also shows the achievements of this research work on improving certain aspects in machining of Ti-MMCs.

Chapter 6 presents the concluding remarks and recommendations.

CHAPTER 2 LITERATURE REVIEW

2.1. Introduction

This chapter presents the literature review on the features and machinability of Titanium Metal Matrix Composite (Ti-MMC) and studies the existing research works on optimizing the cutting parameters when milling and turning Ti-MMCs.

2.2. Titanium Metal Matrix Composites (Ti-MMC)

The decreased fuel consumption is the most important issue for automotive and aerospace industries to avoid greenhouse gas emission and non-desirable expenses. These could be achieved by decreasing the weight of products and improving the efficiency of engines. Therefore, remarkable materials such as Ti-MMC with exceptional mechanical and physical properties and lightweight can ascertain those requests. Improved compressive strength would resist high loaded stressed on gears, connection rods, bearing and shaft in the engines, turbines and the other similar components. The high temperature resistance of Ti-MMC motivated NASA Glenn research center to examine Ti-MMC reinforced (Box 1953) which is identical to the material used in this study.

The Ti-MMC material, used in this study, was made by Dynamet Technology, Inc. and has been made of Ti-6Al-4V alloy matrix reinforced with 10-12% volume fraction of TiC particles with irregular shapes in 10-20 μm size. The mechanical and thermal properties as well as tribological behaviour of Ti-6Al-4V are enhanced by the ceramic reinforcement (Poletti, Merstallinger et al. 2004). Then, an adequate blend of ceramic and matrix material powders has been exposed to the process of a periodic cold and hot isolated pressing to yield bar stock. Knowing that Ti-MMCs are produced near net shape, finishing is generally required to obtain the adequate surface quality of the work-pieces.

However, these materials suffer from poor machinability due to the hard and abrasive nature of the reinforcing particles, in addition to the low thermal conductivity, low elastic modulus and high chemical reactivity of titanium alloy matrix (Niknam, Khettabi et al. 2014). The following sections present an overview of MMC and TiAl4V.

2.2.1. Metal matrix composite (MMC)

Metal matrix composite (MMC) has an essential base matrix of a light metal such as aluminium, magnesium or titanium. In order to reinforce the structure and enhance the matrix's tensile and temperature strength (Hunt 1997), 20% ceramic particles; fibres or whiskers are generally dispersed in the metal matrix. Moreover, reinforcement added, the base stiffness and wear resistance of the matrix as well as the fatigue strength at elevated temperature (Kainer 2006) are improved. Nonetheless, MMCs still suffer from poor machinability. In fact, the presence of hard particles, sever tool wear and poor surface finish are considered as the most important drawbacks in the case of machining MMCs.

Abrasion on the tool flank face seems to be the main wear mechanism of all sorts of carbide tool (Muthukrishnan and Davim 2011) used during machining the MMCs, although, adhesion plays the important role on tool wear when using CBN and PCD tools (Ciftci 2009). As observed in (Njuguna, Gao et al. 2013), adhesion on the flank face was the dominant wear mode when using coated and uncoated CBN tools. However, under similar cutting conditions when using PCD tools, less adhesion on the flank face was observed and the rake face chipping was mostly dominant in tool degradation.

Despite the static tests, reinforcements dislocating mechanism in the work-pieces plays different role at high strain rates. When an induced stress exceeds the material resistance limit, further damages propagate as cracks and crush into the reinforced particles. A procrustean stress by developing through the particles cluster creates nucleation and results into material failure. For instance, a crack follows reinforce particles through the cutting direction in turning as-cast aluminium metal matrix composite (Al6061+Al2O3). Indeed, on the voids growing and coalescence, the fracture occurs at a narrow band adjacent the surface (Ganguly, Poole et al. 2001). The reinforcements lead the MMC to yield before high strain appear (Irfan and Prakash 2000). Therefore, plastic deformation of chips abides more dominant on the ductile materials; further, crack propagation plays essential role for the brittle ones.

2.2.2. Ti6Al4V

In general, titanium alloys possess higher specific strength among other metals (Figure 2-1) by having around half the specific weight of stainless steel. They have acceptable fatigue strength

and turn not into brittle structure even under -200 C (Hurlich 1968). There are several titanium alloys, used in various industrial sectors. With the light specific weight and aesthetic feature, titanium is an attractive option for the luxury and high class artefacts including jewelleries, golf clubs, eyeglasses, bikes and watches (Taylor and Weidmann 2008). Among titanium alloys, Ti6Al4V inhabits almost 70% of market by having superior strength and lowest elongation percent (Welsch, Boyer et al. 1993). Two phases (α and β phases) of Ti6Al4V structure preserve strong mechanical and thermal properties than that is observed in other alloys at 315°C (Taylor and Weidmann 2008).

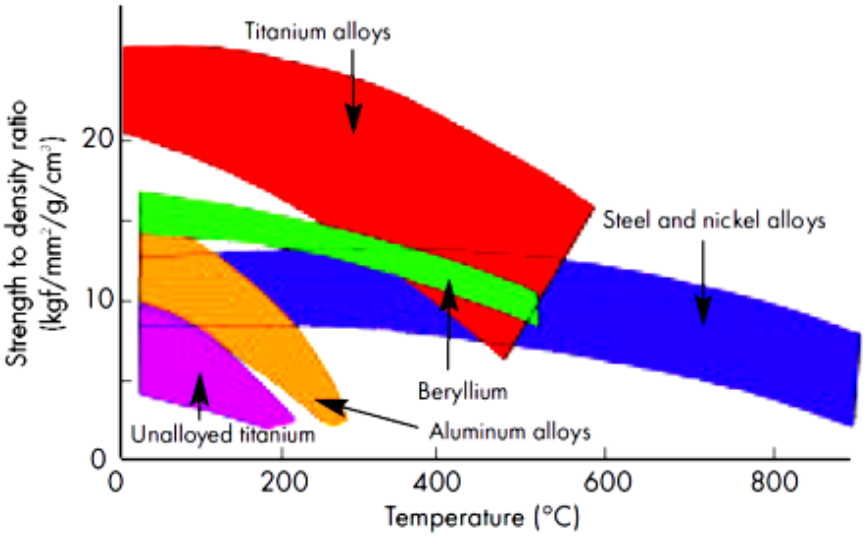

Figure 2-1: The strength to specific ratio of highly used metals (Hurless and Froes 2002)

Ti6Al4V has been widely used in prototyping and manufacturing race cars, aerospace products, biomedical components such as implants and prosthesis, marine applications, chemical industries and gas turbines (Leyens and Peters 2003) (Figure 2-2). Low modulus of elasticity and weak wear resistance restrict the applications of Ti-6Al-4V in the connection rods that require strong stiffness and high wear resistance (Ward-Close, Godfrey et al. 2001). Thus, reinforcements (e.g. ceramic particles as TiC) are added into the Ti6Al4V matrix structure to better improve its shortcoming. The TiC particles increase dislocations in the matrix structure. Therefore, the matrix hardness and stiffness are increased while ductility and toughness are decreased. Several delicate

metallic products, including the engine and transmission components endure massive thermal and mechanical stresses. Those comportments should be light to reduce energy consumption (Hurless and Froes 2002). Therefore, Ti-MMC with high specific strengths at elevated temperatures, great wear and corrosion resistances are ideal for those applications.

Figure 2-2: A race car's gearbox case (left), Hip implant (middle) and Bicycle frame (right) made with Ti-6AI-4V (AB , Taylor and Weidmann 2008)

By improved wear resistance, Ti-MMC can resist high stressed loads on gears, connection rods, bearing and shaft in the engines, turbines and similar components (Figure 2-3).

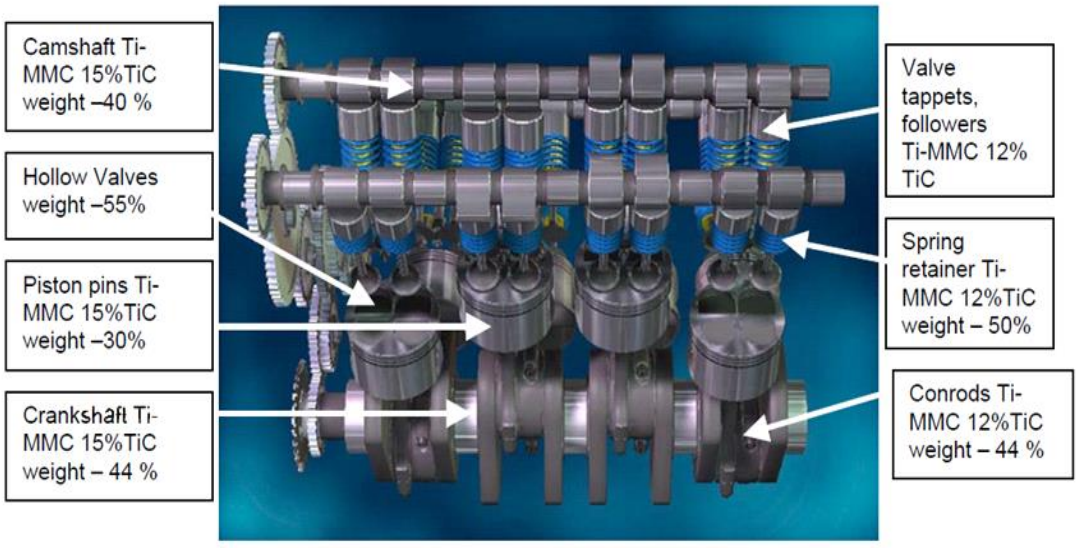

Figure 2-3: Ti-MMC parts under high pressure and temperature conditions in the car engine (Hurless and Froes 2002)

2.2.3. The machining difficulties of Ti-MMC

As a rule, for a same cutting tool life, a superior machinability allows cutting the related work-piece with higher speed. Table 2-1displays the mechanical and thermal properties of Ti-MMC, Ti6AL4V, Inconel 718 and AISI 4140H. It can be seem that Ti6Al4V has poorer machinability as compared to other materials, except nickel alloy-718.

Low elastic modulus of Ti6Al4V leads to serrated chip formation and cyclic cutting force. Cutting force fluctuation also induces chatter vibration (Antonialli, Diniz et al. 2010) and deteriorates the surface finish and increases the probability of tool failure.

Table 2-1: Mechanical and thermal properties of Ti-MMC, Ti6AL4V, Inconel 718 and AISI 4140H (www.aerospacemetals.com, www.rolledalloys.ca, www.alloywire.com) (Konig 1978)

		Ti 6AL 4V +12%TiC	Ti 6AL 4V (4.43 g/cm^3)	Inconel 718 (8.19 g/cm^3)	AISI 4140H Oil quenched (7.7 g/cm^3)
	Machinability	-	23	**12**	68
Mechanical Properties	Hardness, Brinell (BHN)	390	334	389	**520**
	Strength, Ultimate (UTS)	1082	950	1345	**1795**
	Strength, Yield (MPa)	1014	880	1100	**1515**
	Elongation at Break %	-	14	**22**	8
	Modulus of Elasticity (E) GPa	135	113.8	**205**	**205**
	Fracture Toughness (K_{Ic}) MPa-m½	40	75	**87**	48
	Shear Modulus (G) GPa	51.7	44	**80**	**80**
	Shear Strength (τ) MPa	-	550	703	1000
Thermal Properties	CTE, linear 20°C (µm/m-°C)	-	8.6	12.8	12.2
	CTE, linear 250°C (µm/m-°C)	-	9.2	13.5	13.7
	CTE, linear 500°C (µm/m-°C)	-	9.7	14.3	14.6
	Specific Heat Capacity (J/g-°C)	0.610	0.526	0.435	0.473
	Thermal Conductivity(W/m-K)	5.8	6.7	11.4	42.7
	Melting Point (°C)	-	1604-1660	1260-1336	1370-1510
	Solidus (°C)	-	1604	1260	1370
	Liquidus (°C)	-	1660	1336	1510

High affinity of almost all tool materials to Ti6Al4V as well as elevated temperature in the tool-work-piece engagement cause the chemical reaction of materials diffusion and adhesion to the cutting tool (Zhu, Zhang et al. 2013). During the cutting process, Ti6Al4V compels the tool tip to

bear roughly 80% of the generated heat. Consequently, even at high material removal rate, the chips cannot evacuate the massive thermal loads (Konig 1978).

Moreover, at low shear angle (The angle of a plane where work material slips on, to start chip formation), the tool slides than cutting the work-piece (e.g. initial cutting cycles) because of increasing the normal force on the work-piece's surface; so, the cutting zone temperature and pressure rise (Davim 2012). Then, the scraped materials melt and adhere to the tool tip; the hot adhered particles in the vicinity of oxygen turn into fragments as TiO and V2O3 (Jin, Riahi et al. 2014). Thereafter, the particles on rubbing between the tool and work-piece scratch and furrow the tool surface (Huang and Liang 2004). Schematic view of tool wearing is illustrated in Figure 2-4.

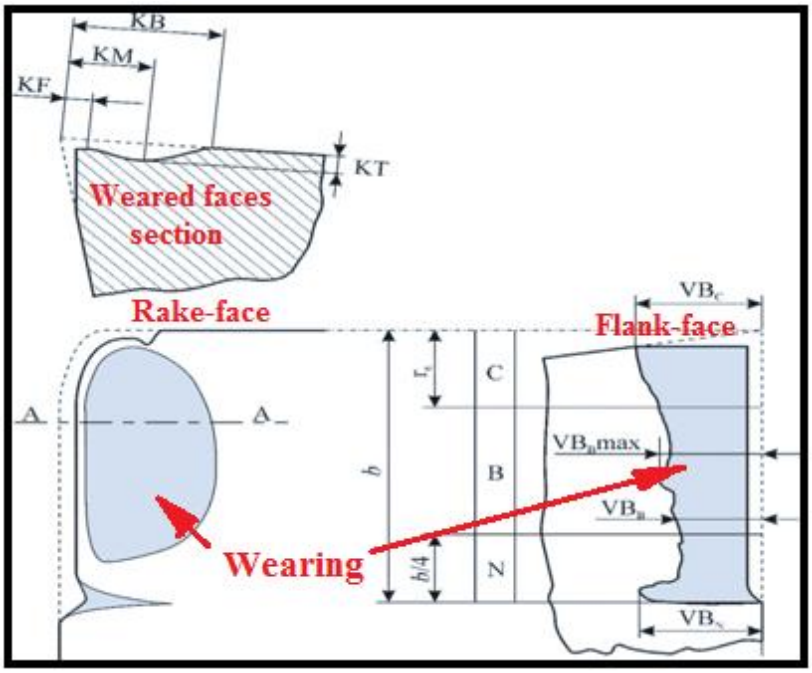

Figure 2-4: The cutting tool and its related wearing type
(Fabrication mécanique avancée, Marek Balazinski,
École Polytechnique de Montréal, Québec, Canada)

During a cutting process, large strain and high related rate dominate the chip formation. Failure of a ductile materials under high strain rate occurs through an adiabatic shear band (Shear band is a thin band with huge plastic shear strain during dynamic loading) (Zener and Hollomon 1944).

As for brittle materials, (e.g. MMCs), failure happen as nucleation, growth, and coalescence of micro-voids to form a crack (Worswick, Qiang et al. 1992). Furthermore, additional cutting speed surpasses the plastic deformation region and accomplishes to brittle fracture of the chips (Vaughn and Krueck 1960). According to (Recht 1964), machining of brittle materials at high cutting speed reduces the tool vibration and tool wear while high productivity and lower machining cost are expected.

2.3. Cutting Process

2.3.1. Heat Generation during the Cutting Process

One of the main machining phenomena is heat generation in the cutting zone (Figure 2-5). Plastic deformation of the work material as well as friction between cutting tool and work-piece and chips are essential parameters to impel the high thermal loads on a cutting process. High thermal load generally leads to tool degradation and deteriorated surface quality.

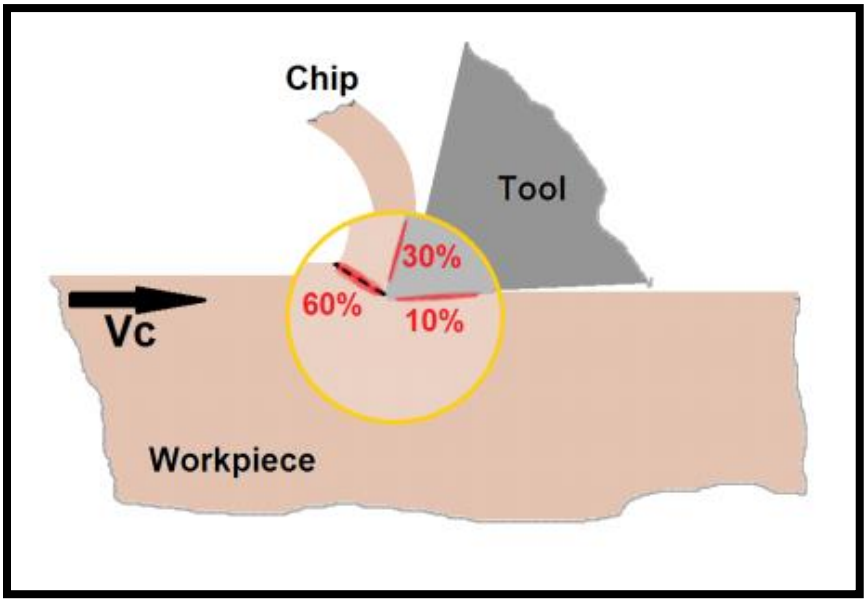

Figure 2-5: Heat distribution along the cutting process (Pramanik, Zhang et al. 2008)

At high cutting speed, the strain rate in the shear zone increases; therefore, due to elevated energy, thermal load is intensified. However, according to the work material properties, thermal

conductivity and strength, the temperature decreases after a certain level of cutting speed(Figure 2-6).Thermal conductivity of a work-piece dominates the temperature elevation rate at the tool tip (Kagnaya, Lazard et al. 2011). Friction is one other parameter to increase rapidly the temperature due to cutting speed. Thus, adding the motion friction to the material deformation increases the cutting heat transferred to the tool-work interface.

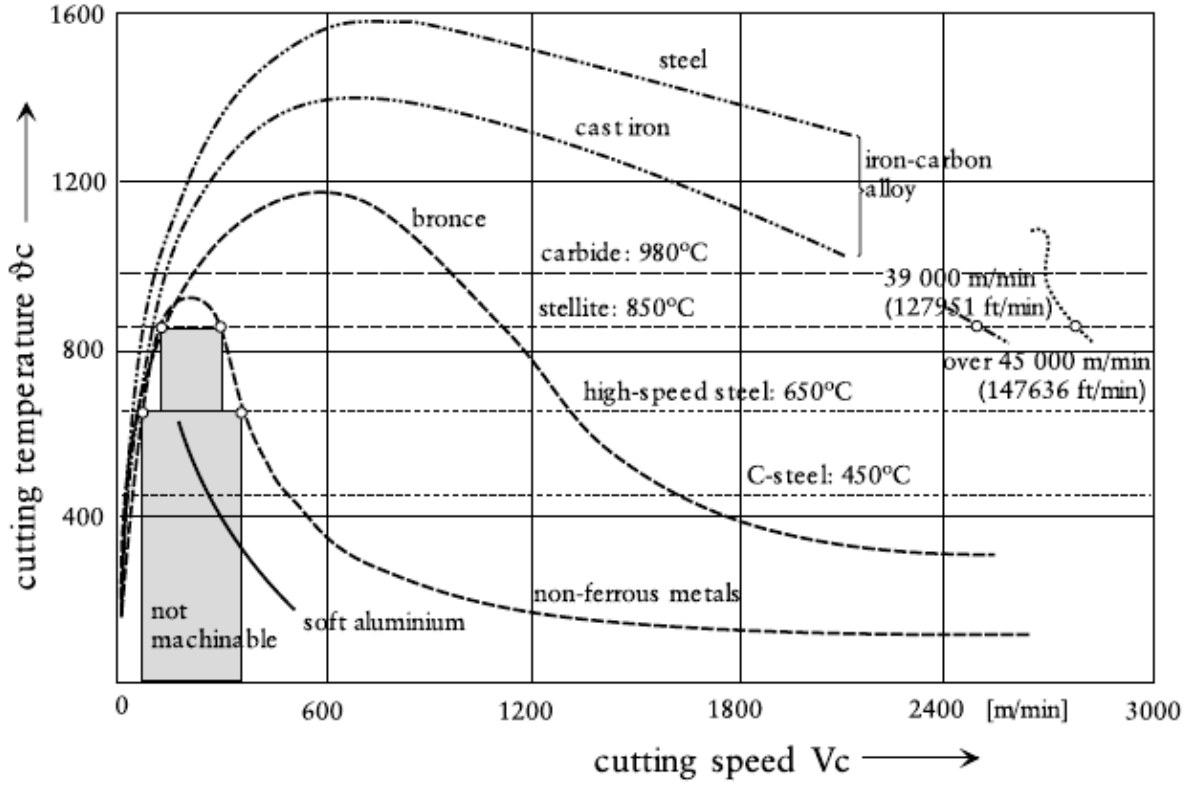

Figure 2-6: Relationship between cutting speed and cutting temperature in different materials (Schulz 1999)

High cutting speed increases the cutting zone temperature and deformation strain rate and eventually leads to change in the work-material structure (Thakur, Ramamoorthy et al. 2010). At high cutting speed, the chip dispel the temperature in the cutting zone (King 1985). Aero-engine materials (e.g. nickel and titanium alloys) maintain high toughness and hardness at high temperatures; this feature leads to their poor machinability (Ezugwu, Bonney et al. 2004). The elevated temperatures during machining the aerospace's materials harden work surfaces and cause higher tool wear and deteriorated surface finish.

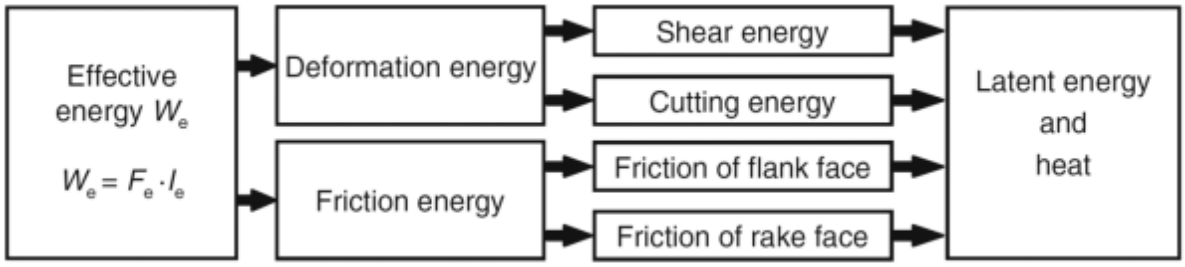

Figure 2-7: Energy cycle during cutting process (Klocke and Kuchle 2011)

Two essential phases of titanium alloys structures classified as α with hexagonal closed packed lattice (hcp) which abide up to temperature around 883.5°C and β on body centred cubic (bcc) lattice forming after α up to 1662°C. Both phases display distinctive performances of the plasticity (Kaçal and Yıldırım 2013).

Super-plasticity of Ti6Al4V is extended by growing α phase and the maximum super-plasticity at ratio of α 40% to β phase (Hsiung and Nieh 1997). At super-plasticity temperature, the β phase extends exponentially until complete phase transformation; then after forming the lattice bcc of β phase, the super-plasticity is faded.

However, titanium alloys have poor machinability according to their remarkable resistances to plastic deformation (Lee and Lin 1997). Therefore, the abrasive particle and high resistance to plastic deformation in Ti-MMC constrains high-energy load to the tool-work-piece engagement as shown in Figure 2-7. High cutting energy and temperature cause several problems in the cutting process as:

- Reducing the strength, hardness and wear resistance of the cutting tool;
- Degrading the dimensional accuracy of the work-piece;
- Thermal damage to the machined surface.

2.3.2. Chip formation

The segmented chip formation generally occurs during machining of titanium alloys. During orthogonal cutting of titanium alloy, up to a certain level of cutting speed, localized deformations occur without any segmentation, while at higher speed, localized segmentation tends to appear

(Rokicki, Spotz et al.). During cutting MMCs, reinforcement particles lead the material to resist the plastic deformation and rumpling. Therefore, cutting force may pass the ultimate strength and produces cavities around hard particles in MMC's soft matrix. The cavities are expanded until they turn into segmented chips (Huang, Zhou et al. 2012).

Lower plastic deformation appears in machining of high strength materials. During high speed milling of Ti-6AI-4V, the increased cutting speed fades the plastic deformation and induces to crack (Du, Chen et al. 2006). However, chip segmentation reduces the cutting force as that observed when having continues chip (Daymi, Boujelbene et al. 2009). In this case, the force fluctuation would appear and consequently deteriorated surface finish results.

During machining Ti-MMC, the cutting force propagates into the matrix along with the reinforcements' clusters, breaking them and their bonds toward the outer boundary of shear zone. Crack initiation at outer zone of the chip causes segmentation onward the shear zone and the saw-tooth chips formation (Bejjani, Balazinski et al. 2011). It should be noted that cutting at a certain level of ductility proposes the good machinability (Armarego and Brown 1969).

Thicker chips result at increased feed rate and decreased cutting speed and depth of cut (Daymi, Boujelbene et al. 2009). Another important parameter on the chip formation is the work material's thermal conductivity. Lower heat-transfer from cutting zone decreases the chip thickness. Moreover, the heat left in the cutting zone raises the zone temperature (Sun, Brandt et al. 2009). The ratio of α to β in the structure and the particles dislocations in the α phase have relationship with decreasing the matrix temperature and rising the superplastic deformation (Kim, Kim et al. 1999). Thus, adding the particulate reinforcements in the titanium matrix holds super-plasticity of the matrix at elevated temperature and limits the β grains growing (Lu, Qin et al. 2010).

2.3.3. Cutting force effects

The first general issue on machining MMCs corresponds to the matrix structure that intensifies the cutting force. Whereas, the reinforcement's hardness, atomic bonding and quantities increase the maximum pressure on the tooltip, friction force as well as the cutting forces fluctuation frequency. Lower levels of cutting speed and higher feed rate decrease the effect of the reinforcements on the tooltip (Gaitonde, Karnik et al. 2008).

One of the machinability criteria known as specific cutting pressure Kr has relationships with uncut chip section area as well as cutting force. Higher levels of Kr tends to degrade the tool wedges (Thakur, Ramamoorthy et al. 2010). Increased cutting speed diminishes the plastic deformation; decreases the Kr (Specific Cutting Pressure) and increases the cutting shear angle. As a result, the effective force on the cutting edge decrease (Daymi, Boujelbene et al. 2009).

During the high speed machining of Al/SiC, in addition to the cutting force, feed force also tends to decrease. Moreover, high feed rate reduces the flank wear and increases the area of heat conduction and heat generation. Higher level of depth of cut in cutting MMC increases the cutting force and flank wear on the carbide tool (Kremer, Devillez et al. 2008).

Disregarding, the matrix properties generate fluctuation of the thrust force (Smith 2008). In the S. Sikder et al study (Sikder and Kishawy 2012), cutting force changed little when strength and hardness of matrix increase from Al6061 to Al7075. However, cutting force depicts more direct relation to the percentage of reinforcements. Furthermore, friction force partakes 20% of the total force in MMC's cutting process (Das, Behera et al. 2011). If abrasive effect of hard particles in matrix reduces, thereafter, specific cutting force would be decreased by aggressive feed rates and higher cutting speeds (Kremer, Devillez et al. 2008).

2.4. Cutting Tools

The following section presents the most widely used cutting tools in machining Ti-MMCs.

2.4.1. Common conventional tools

There are four types of cutting tool materials as:

- Carbide
- Ceramic (Al2O3/Si3N4)
- Cubic Boron Nitride (CBN) high percent
- Cubic Boron Nitride (CBN) low percent
- Polycrystalline Diamond (PCD)

As shown in Table 2- 2, on one hand PCD displays the greatest hardness between all tool materials; meanwhile its relatively low toughness makes the tool vulnerable to impacts and resulted shocks during cutting force fluctuation. On the other hand, a cutting tool material such as

carbide with high toughness may withstand the impact and force effects; but by having lower hardness, the MMC's reinforcements scratch and degrade the cutting edge (Stephenson and Agapiou 2005). According to Table 2-2, PCD feature outstanding hardness and incomparable heat conductivities, while ceramic tools are out of range and PCD tools provide the best combination among other tools. Table 2-2 shows the significant toughness of the carbide tool and the highest bulk strength of high percent CBN material.

Table 2-2: The properties of the cutting tools materials(Heath 1986)

Properties	WC (k10)	Al2O3+TiC	CBN (High %)	CBN (Low %)	PCD (Syndite10)
ρ (g/cm^3).	14.7	4.28	3.12	4.28	4.12
Y (GPa.)	**4.50**	**4.50**	3.80	3.55	**7.60**
HK (GPa.)	13	17	**31.6**	**27.5**	**50**
K_{IC} (MPa.m^{½})	**10.8**	3.31	6.30	3.70	**8.80**
E (GPa.)	620	370	**680**	587	**776**
G (GPa.)	258	160	279	**284**	**363**
B (GPa.)	**375**	232	**405**	254	**301**
υ	0.22	0.22	0.22	0.15	0.07
C (10^{-6}/K.)	5.00	7.80	4.90	4.70	4.20
k (W/m K.)	100	16.7	100	44	**560**

[P (Density), **Y** (Yield Strength), ***HK*** (Knoop Hardness), **K_{Ic}** (Fracture Toughness), **E** *(*Elasticity Modulus), **G** (Shear Modulus), **B** (Bulk Modulus), **υ** (Poisson Ratio), **C** (Coefficient Thermal Expansion), ***k*** (Heat Conductivity)]

2.4.2. Cutting tools deficiencies

The friction force and hydrostatic pressure generated during cutting process deform the Ti-MMC and erodes the tool-edge. During machining the high fracture toughness materials (i.e. titanium), cutting speeds variation plays more important role than the feed rate. For instance, during machining Inconel, which has poor machinability, the ceramic tool wears exponentially by gradually increasing the cutting speed. Meanwhile, the feed rate and depth of cut have less effects on the tool degradation rate (Sikder and Kishawy 2012).

Huang et al (Huang, Zhou et al. 2012) studied milling Al-MMC using cemented and PCD tools. It was observed that cutting forces tend to rapidly increase and afterward smoothly mounted up to

flank wear (VB=0.6mm) on the carbide tools. The flank wear was propagated rapidly even at the low cutting speed. However, in the case of PCD tools, cutting forces was gradually increased with an average of about half of that observed in the carbide tool.

The wear in the PCD tool was very rapid at the beginning of the cut, and it became uniform when using v_c= 300 m/min. They claimed the reinforced particles could not make micro-cuts on the flank surface of PCD tool. In the other word, the harder tool decreases the force and consequently less tool wear results.

Titanium base components reveal high toughness during cutting process (Froes, Friedrich et al. 2004). CBN tool shows different consequences in cutting the titanium constituents, when the cutting temperature is the most important phenomena.

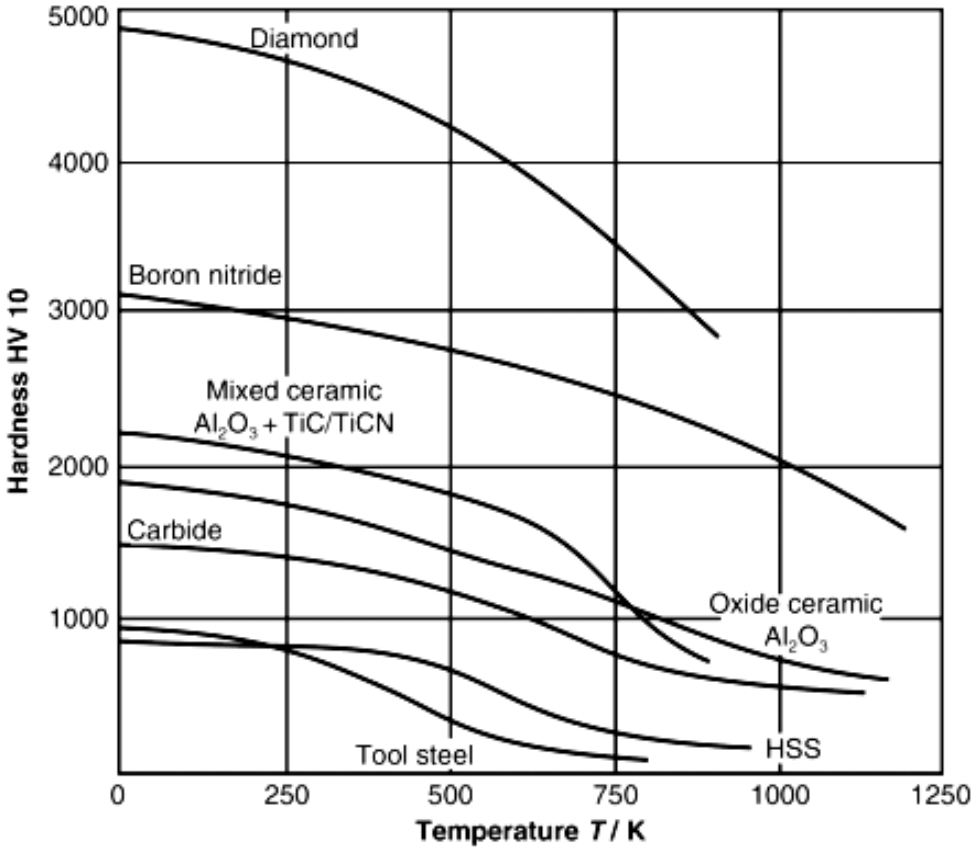

Figure 2-8: Temperature and hardness in various cutting tool materials (Source: CeramTec)

Further, the cutting speed between 185±22 [m/min] addresses the stable cutting and more appropriate work-surface quality (Zoya and Krishnamurthy 2000). Machining titanium alloys with PCD tools at cutting speed 150 m/min was optimized in (Corduan, Himbart et al. 2003). Zhang et al. (Zhang, Zhou et al. 2013) investigated the effects of vibration on the PCD tool and observed that vibration is one the critical parameters affecting the tool wear.

The cutting tool should possess sufficient strength and hardness at elevated temperatures during machining aerospace materials. Most of the cutting tools lose their hardness and strength at high temperature and experience accelerated wear (Figure 2-8). Aerospace industries utilize coated carbide, CBN, ceramics and PCD tools in machining various materials. Titanium alloys reveal high affinity to the ceramic tools, which hinders their machinability (Kertesz, Pryor et al. 1988).

2.4.3. Tools wear

During the cutting operation, the cutting tool is exposed to various axial and non-axial stresses including the hydrostatic pressure, bending, shearing, vibration and thermal loads, and consequently tool's material erosion, edge chipping and rusting on the tool wedge generally would be appeared.

Two essential categories that degrade the cutting tool are:

- The wear on the tool face due to gradual erosion that tend to increase the cutting forces.
- Because of the thermal or mechanical shocks, brutal wears generally appear on the tool. The main features depicted are deformation of the tool tip, cracking and tearing-off a portion of the cutting tool up to complete failure.

The gradual tool wear occurs with three features on the tool faces (Figure 2-9) as:

- Crater wear on the rake face
- Flank wear on the flank face
- Corner wear on the auxiliary flank face near tool nose

When a cutting tool experiences a tangential movement against a work surface, the work-piece embeds hard particles on the tool surface and offensive grooves are generated there. This tool wear mechanism is known as abrasion. Atomic bonding of the work surface's material and welding to the tool lead to adhesion wear.

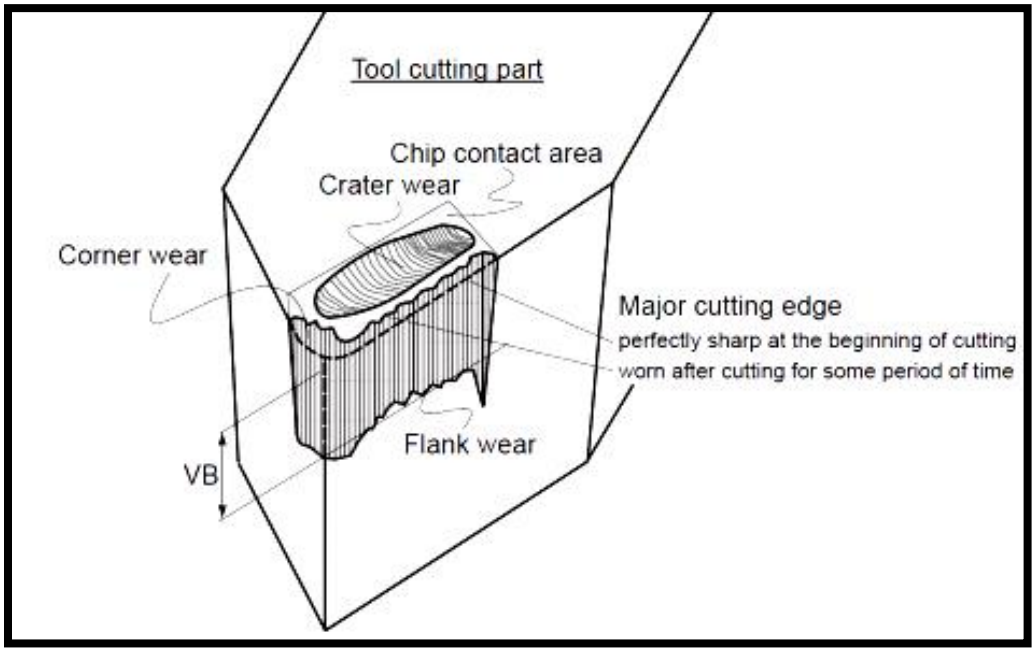

Figure 2-9: Various modes of wear on the tool's faces
("Mechanics of Machining" Lesson-3: Geometry of single point
Cutting tools, Kharagpur.Version 2 ME IIT.)

As a result of high temperature, atoms of the next surface replace and defuse, so the diffusion mechanism occurs on the tool, particularly on the tool rake face as crater wear (Figure 2-10). Vicinity to oxygen at elevated temperature induces different mechanisms which oxidize materials on the tool surface (Klocke and Kuchle 2011).

On the width of the wear ribbon (VB) presented in Figure 2-9, the cutting force elevates to a critical value and deforms or breaks the tooltip. Generally, 0.5 mm of flank wear increases by 90% the feed-force, 100% the passive force and 20% the cutting-force (Klocke and Kuchle 2011). Less machining is expected upon proper modification of productivity and cutting conditions (Kagnaya, Lazard et al. 2011).

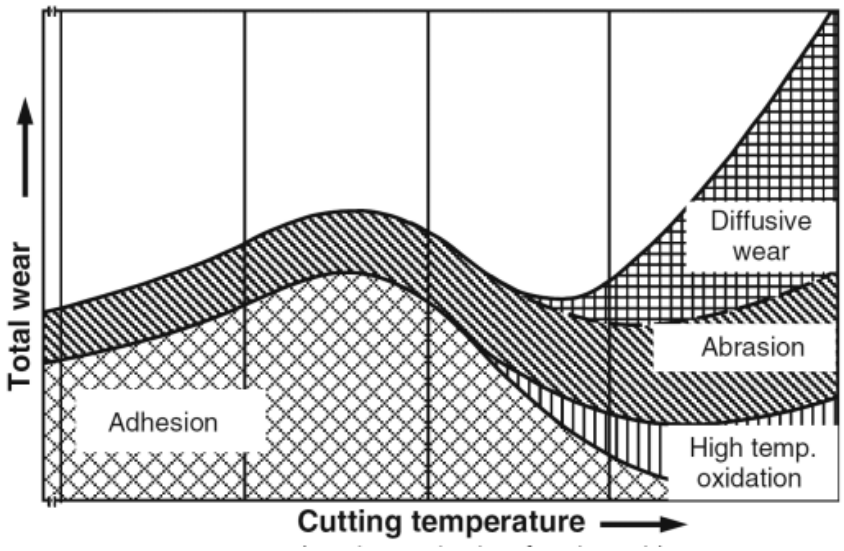

Figure 2-10: Tool wear mechanisms

Titanium based materials have poor machinability. High speed steel (HSS) and carbide tools display difficulty to cut those materials over cutting speed range of 30-60 m/min (Hosseini and Kishawy 2014). Polycrystalline diamond (PCD) and Polycrystalline boron nitride (PCBN) depict good performances at high speed machining of titanium alloys (Honghua, Peng et al. 2012).

2.4.4. Surface quality (finish) of Ti-MMC work-piece

During standard milling of Ti-6AI-4V, the average surface roughness Ra is about 6.4 µm, but in high speed milling Ra decreases to 0.8µm, because surface layers wrinkle less than that observed in low speed machining. Higher levels of cutting speed and lower levels of feed rate and depth of cut improve the surface quality and structural integrity of the work-pieces. One of the main surface integrity attributes is residual stress which seems to be generated due to mechanical (plastic deformation), thermal (plastic flow) and physical (specific volume changing) stresses. Tensile residual stress results from the thermal residual stress and plastic deformation generates compressive stress.

Based on the literature, except the work done by Bejjani et al (Bejjani, Balazinski et al. 2011), no more research study deals with surface quality of Ti-MMC machined parts. According to Bejjani et al (Bejjani, Balazinski et al. 2011), the surface roughness in Ti-MMC work-pieces is more

sensitive to variation of feed rate than cutting speed. Nevertheless, using PCD tools led to more rough work-pieces than that when carbide tools were used.

2.5. Cutting fluides

During the forming or machining process of metallic components, the tools generally experience the dynamical performances' difficulties and high temperature generation. Thus, cutting fluids are proposed to lubricate the trajectory of the tool motion and decrease the cutting temperature. Moreover, the cutting fluid carries away the chips from the cutting zone (Marinescu, Rowe et al. 2004). A good cutting fluid should maintain strong heat capacity rate [J/s˚k], wettability to the solid surfaces, as well as sufficient diffusibility to the solids contact areas. The cutting fluid protects the tools from high thermal loads, scratching and rusting, and it decreases the friction coefficient between the surfaces on relative motion. Decreased friction between the tool and work surfaces lead to improved surface quality. One of the main characteristics of the cutting fluid is transparency that allows better observation of the process. Finally, the cutting fluid should not foam and be harmful to the health (Vagnorius 2010). Three major applications of the cutting fluid (El Baradie 1996) are:

1. **Lubrication:** The tool surface can be protected from scratching and welding upon proper use of lubrication. This protection is achieved when the fluid forms a protecting layer on the tool-work contact surface and reduces the cutting force and friction between the tool and work surface. Decreased forces and stresses lead to longer tool life.
2. **Cooling:** The fluid transfers out the heat from the machining zone and controls the process temperature. The increased capacity of heat absorption in the fluid generates more stable and consistent processes.
3. **Chip evacuation:** Other important responsibility of the cutting fluid is to carry away the chips from the cutting zone.

The proper control of process temperature determines the tool life and work quality. For instance, TiAlN coated carbide tools required less cooling and allows higher temperature in the cutting zone (Dudzinski, Devillez et al. 2004). Fluctuations of the temperature in various sections of the

cutting zone impels the thermal shock on the tool and generally cause tool fracture and failure (Marinescu, Rowe et al. 2004).

Certain disadvantages of the cutting fluids are (El Baradie 1996):

- Additional machining cost;
- Health hazardous effects;
- The risk of thermal shock when using cemented carbide tools.

The cutting fluids can be generally grouped into three main categories (Çakīr, Yardimeden et al. 2007):

- **Oils**: mostly extracted from petrol derivatives;
- **Emulsified oils**: combination of water and oil. The relative ratio is varied by the severity of process;
- **Synthetic fluids (chemical):** provides adequate cooling effect on the cutting zone.

2.6. Design of the experiment

Experiment is a process which does not have any predetermined outcome and needs to be applied until a unique by formulated process with defined consequence is achieved (Kaps, Lamberson et al. 2004).

The principle elements of an experimental plan are replication, blocking and randomization (Imai, King et al. 2008). Replication is a simultaneous process of conducting several experiments as well as measurements for one effect. Blocking displays a composition of several variables in similar experimental condition. Randomization arranges the experimental variables as a package to prevent the occurrence of any bias in the test results. Bias is probability that one result occurs more than others. Randomization detects the interaction effects of uncontrollable parameters on the responses within an experimental plan (Montgomery 2008).

The best and most robust experimental results would be achieved upon adequate use of sufficient experimental tests; but a large number of runs waste experimental cost and time. Therefore, an adequate design is necessary to conduct several randomized experiments to achieve precise outcomes with the minimum cost and time (Simmons, Nelson et al. 2011). A successful design of experiment needs a sequential process (Taguchi and Yokoyama 1993) as:

1. To establish the experimental objective and research hypothesis (e.g. the effects of cutting conditions and tools materials on the work-piece surface quality);
2. To specify the experimental parameters and their levels (e.g. cutting speed, feed rate and depth of cut);
3. To recognize the response parameters (e.g. the tool wear, productivity);
4. To determine the background parameters (including material, tool, machine);
5. To determine the noise parameters (e.g. machining vibration);
6. To configure the levels of variations for each experimental parameters;
7. To define relationship between the experimental and noise parameters;
8. To evaluate the correlation between each individual experimental step;
9. To ensure the absence of hidden parameters to reduce the noise effects;
10. To blind to the conditions and decrease the bias effect.

Experimental parameters are expressed in two categories as (1) Quantitative which is specified by a point or a value; (2) Qualitative which takes a quality rank. Empirical model in the optimization studies uses quantitative values to define which effective parameters at what level have the most significant effects on the response variation (Montgomery 2008).

Furthermore, the experimental tests would be arranged randomly to avoid any bias. Those methodologies increase the precision of statistical analysis. Meanwhile, the similar conditions must be maintained for all experimental parameters and their levels. Another important element in experimental arrangement is the interaction effects between experimental parameters which appear to have significant hidden effects on the responses variation.

Proper arrangement of experimental plan is an important step in design of experiment. Furthermore, an optimized sample size is needed to reduce the cost and time; nevertheless, that should make precise results too. An experimental study should include enough replications to determine uncertainties and to reduce the noise effects on responses. Also, recognition of any difference between the experimental parameters with high noise vulnerability and/or numerous noise parameters needs a large sample size; otherwise experimental design could be arranged with short sample (Montgomery 2008).

Taguchi design method

Taguchi presents a method, which allows the runs of least number of parameters in experiment. Taguchi optimization procedure is constructed based on the robust design conception, which requires a system with minimum vulnerability to noise parameters.

A robust design proposes the lowest cost of the products by considering the client requested quality. It does not have certain mathematical model to predict the results and instead, it only can make decision about a process by conducting the experiments. Taguchi method is widely used in industrial plants to define the optimum settings of variables and materials in their experimental plans (Phadke 1989).

Within Taguchi method, the variables are divided into two groups; experimental and noise parameters. Experimental parameters are the input variables configured by the operator to set desired results. The noise parameters are undesirable variables, which are uncontrollable and cause inappropriate responses to process performance. They are grouped as outer noises (e.g. thermal and mechanical loads) and inner noises (e.g. abrasion). A robust system is capable in finding consistency after eliminating or decreasing the noise parameters (Phadke 1989).

Taguchi used an efficient arrangement to run a small amount of experimental parameters so called Orthogonal array to yield meaningful consequence (Ross 1988). There are three steps to identify the orthogonal array equation $l_A(m^n)$ (A presented the number of experiment test, mthe number of levels and the experimental parameters number) in Taguchi based design of experiment as follows:

- To calculate the total degrees of freedom; Degrees of Freedom in Taguchi Method estimate by df= (n-1) (m-1)
- To verify the total interactions and parameters
- To use interaction between columns in the related standard table for the non-matched parameters

2.7. Method of Analyze of variance (ANOVA)

The first step in identification of the manipulating parameters on an experiment can be done with the ANOVA analysis. ANOVA is a statistical and analytical tool that determines total variation

within each level of the experiment and between all the levels. In other word, ANOVA in a regression analysis calculates the impact factors of the experimental parameters on the responses (Montgomery 2008).

By achievement of the ANOVA results, further analyses can be performed to determined detail of variations during the experiment. ANOVA's procedure is performed on a response distribution as Eq. (2.1):

$$y_{ij} = \mu_i + \varepsilon_{ij} (i = 1,2,...,a; j = 1,2,...,n_i) \tag{2.1}$$

Where y_{ij}, μ_i and ε_{ij} are respectively the measured response, response distribution mean of each parameter level and response residual or deviation (Montgomery 2008).

The experiment levels responses distribution mean μ_i and the total distribution mean μ are estimated respectively from:

$$\mu_i = \frac{1}{n}\sum_{j=1}^{n} y_{ij} \tag{2.2}$$

n is the number of responses in each level

$$\mu = \frac{1}{a}\sum_{i=1}^{a} \mu_i \tag{2.3}$$

a is the number of level for each parameter

ANOVA analyses the experiment with a statistics tests named as F-test which proposes as:

$$F = \frac{MS_{Between}}{MS_{Within}} \tag{2.4}$$

Which $MS_{Between}$ is the variance mean between the experiments levels and MS_{Within} is the variance mean within the levels of experiment(Box 1953).

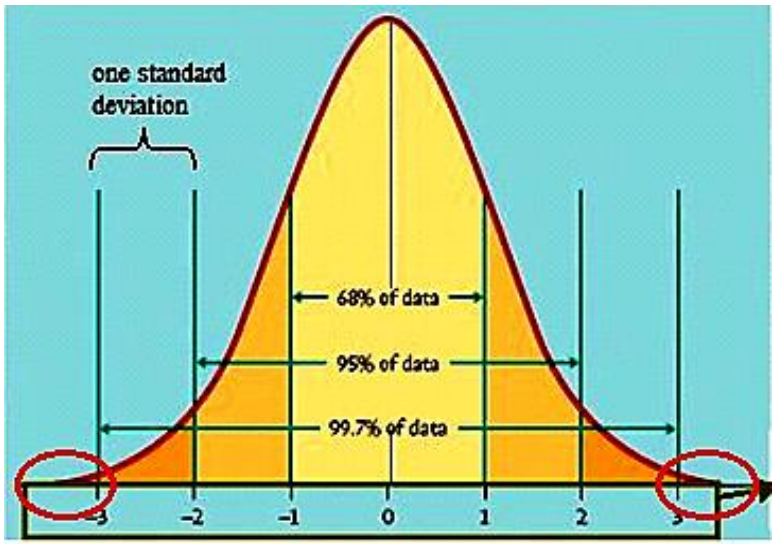

Figure 2-11: Statistical distribution of a response(Woodcock 1997)

According to Eq.2.4, ANOVA confects a value for the effectiveness of Experimental parameters (experiment's parameters) and their combination effects on the responses variations with 95% Confidence Interval (CI) (Figure 2-11).

Probability of an F-value is determined by P-value. P-value shows the smallest margin of probability of the response variation occurrence of a given parameter during the experiment. Therefore, the smaller P-value depicts effectiveness of the related experimental parameters. P-value lies between zeros to one and can be interpreted as follows:

- If P-value > 0.10, the element is not considered as a statistically significant process parameter.
- If $0.05 \leq$ P-value ≤ 0.10, the element is statistically a mildly-significant process parameter.
- If P-value < 0.05, the element is considered as a statistically significant process parameter.

Variability of the response values is identified by coefficient of determination R2 which describes the effectiveness of the experimental parameters, their levels and their interactions. The coefficient of determination indicates how a regression model is fitted to the chosen parameters.

The R^2 greater than 75% depicts the responses are sensitive to the variation of selected experimental parameters and their levels.

The mode of analysis to use depends on objective and design model. In an optimization study, the profitability of process or the minimum cost of production is of greater importance than the risk of failure (Montgomery 2008).

2.8. Optimisation methods

According to literature review, the most highly used optimization methods in academic and industrial studies are response surface methodology (RSM), desirability function and Taguchi method. A brief overview of aforementioned methods is presented in the following sections.

2.8.1. Response surface methodology (RSM)

The RSM proposes a combination of mathematical and statistical techniques to model and analyze the engineering processes and products problems (Myers, Montgomery et al. 2009). RSM is an approximated model and cannot formulate the independent variables relationship on several experimental models.

2.8.2. Desirability function

Harrington (1965) developed a model for multiple response optimization which later Derringer (1980) modified it to become the most frequently used method, so-called desirability function. Multiple responses problem can be transformed to a single response condition by the desirability function. The values between 0 and 1 specify the range of desirability for the responses proximities to the target value. The worst desirability carries out with the zero value and the best desirability is one to achieve the target response.

2.8.3. Taguchi Method

To achieve the least variability of the experimental responses of an experiment or a production process, Taguchi proposed a method to measure the process conditions' robustness of each experimental parameter to resist the effects of intervening uncontrollable factors and minimize the variation (Noise parameters). The Noise parameters vary and damage the results of an experiment and a production process. During a production process, the noise parameters are not

detectable and controllable; but we can identify the noises in an experiment and minimize their effect by optimizing the robustness of process conditions of the controllable parameters (Taguchi and Yokoyama 1993). Taguchi method (Ross 1988) propounds the most desirable parameters combination to perform optimization process. Taguchi proposed a different analytic method which has been widely used for optimization studies in manufacturing processes (Phadke 1989, Bagci and Aykut 2006, Hou, Su et al. 2007, Nalbant, Gökkaya et al. 2007, Zhang, Chen et al. 2007, Tsao 2009, Moshat, Datta et al. 2010). Taguchi method optimizes the model by minimizing the governing parameters and eliminates those parameters having poor quality and less effectiveness on response variation (Taguchi and Yokoyama 1993).

Based on Taguchi method, the highest/strongest and lowest/weakest levels indicate the critical effects of the input variables on the desired outputs. Taguchi represents the quality of the process and product as a loss function (Figure 2-12). He defined two sorts of input parameters, so called controllable parameter and noise parameter. Weaker noise parameter and more precise results are expected (Heizer and Render 1991).

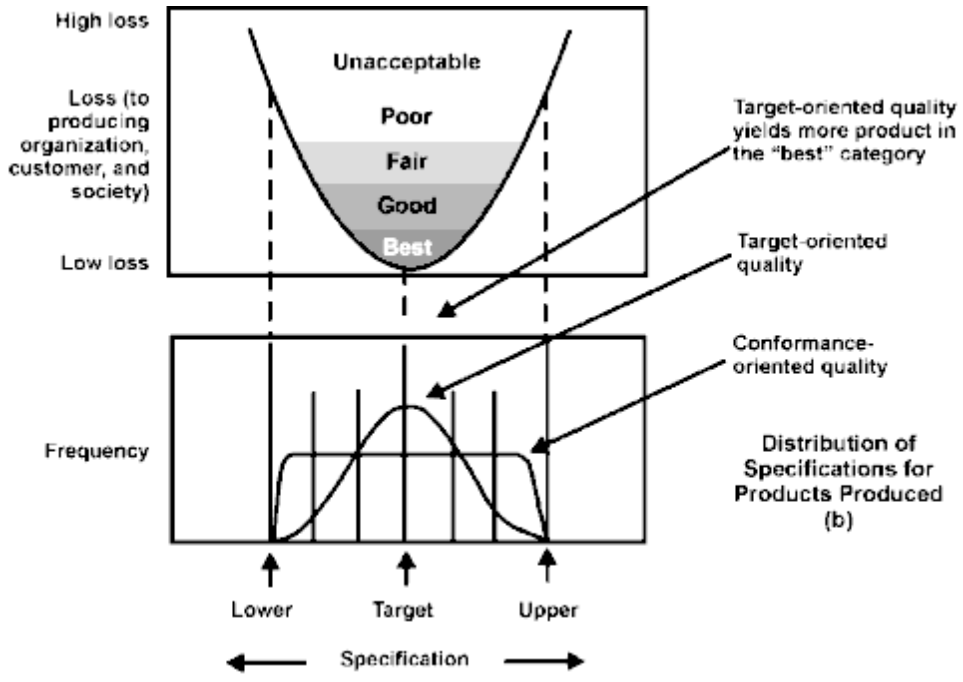

Figure 2-12: Taguchi loss function (Heizer and Render 1991)

Taguchi method has efficient tools for consolidation of a high quality system that consists of multiple processes to achieve a certain quality of products or the enhancement of a process performance (Ross 1988). Taguchi method induces in three fields such as planning, experimentation and result analysis (Taguchi and Yokoyama 1993). The loss function displays the healthiness of the system using a quality index so called signal to noise ratio (SNR). SNR represents the deviation of a variable from the target value (Dhavamani and Alwarsamy 2011). This deviation results from the noise intervention in the process (i.e. diffusion of the tool material to the work-piece chips during the machining process).

Loss function and signal to noise ratio (SNR)

The robustness of a process is determined by loss function. The loss function uses a performance index so-called signal to noise ratio (SNR). SNR represents the deviation of a response from the target value under different noise conditions (Dhavamani and Alwarsamy 2011). Two principal attitudes of SNR value are:

- Reduction the variation interval of the responses
- Decreasing the responses mean difference from the target value of the process.

Taguchi determined three quality categories corresponding to SNR values (Kilickap 2010). In this configuration, the units are converted to db, which identifies intensity of each level of the signal.

- The larger the better

$$\text{SNR}\,(\eta) = -10\log_{10}\left(\frac{1}{\text{N}}\sum_{i=1}^{N}\frac{1}{Y_i^{\,2}}\right) \tag{2.5}$$

Where N is the number of replications and Y_i is the response

- The smaller the better

$$\text{SNR}\,(\eta) = -10\log_{10}\left(\frac{1}{N}\sum_{i=1}^{N}Y_i^{-2}\right) \tag{2.6}$$

The larger-the-better has been used for higher desirability of quality aspects and the smaller-the-better for minimizing the undesirable effects.

- The nominal the better

$$\text{SNR}\ (\eta) = -10\log_{10}\left(\frac{m^2}{\sigma^2}\right) \tag{2.7}$$

Where m is mean of responses, and σ is standard deviation of responses

This signal ratio displays the aspect position on a normal distribution of variables and states that the optimum result is obtained at the mean of the results. In this case, the objective is to decrease the response variation; meanwhile the mean of the response can be enhanced. Deficiencies of the Taguchi method are (Kilickap 2010):

1. Distinguishing a good signal between the noises when interactions between the variables are powerful.
2. SNR has not a good logical definition.

The strategies of smaller-the-better or larger-the-better are not only used to achieve the controlled level and the condition of the optimum result, but also to gain the most desirable process. In an experiment plan, the number of the levels is correlated to parameters variation. However, the worst and the best conditions should be considered at the noise parameters definition (Kaps, Lamberson et al. 2004). When two or more parameters make different actions on the experiment, avoiding interactions between their levels cause failure in the model (Figure 2-13).

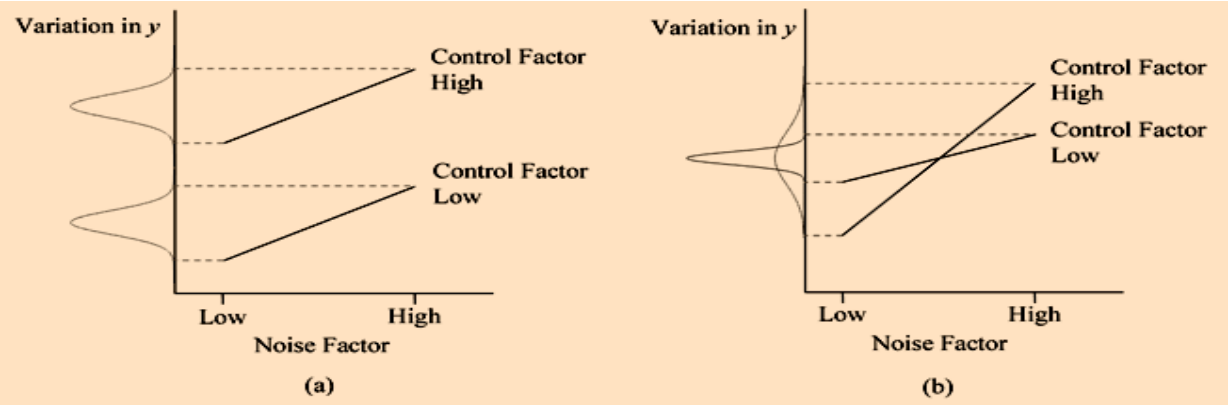

Figure 2-13: Two kinds of interaction amongst the controllable parameters (experimental parameters) and the noise parameters on the experiment results; a) without interaction, b) with interaction (http://reliawiki.org/index.php/Robust_Parameter_Design)

2.8.4. Conclusion of literature review and refining of problematic

- No research work was reported yet on high speed cutting of Ti-MMCs.
- The mechanism and severity of the tool wear largely depends on the tool and work-piece material, machine as well as the cutting conditions used.
- The low thermal conductivity and modulus of elasticity, high chemical affinity to the tools materials as well as abrasive hard particles are the main parameters governing the poor machinability of Ti-MMCs.
- Friction force plays an essential role in the adhesion wear. Abrasive forces also play an essential role in the adhesion.
- Due to heterogeneity of the work-piece structure, the material yields through a tiny layer of the material in front of cutting tool.
- High resistance of the work-piece during plastic deformation increases the hydrostatic pressure on the cutting edge; thus the adjacent tool faces are affected by chipping.
- Cutting ductile materials as titanium components consumes higher deformation energy and experiences higher cutting temperature while vibration the tools appear as the consequences of machining brittle materials. Accordingly, appropriate setting levels of process parameters should be defined to eliminate both undesired effects.
- Due to high strength and elasticity in the matrix of Ti-6AI-4V, slower plastic deformation appears in the tool/work-piece engagement. This leads to spring back effects and consequently, the fracture-work decreases by abating the plastic deformation.
- Increased depth of cut and cutting speed (up to 60 m/min) increase the cutting force. Higher levels of cutting speed seem to generate the segmented chips.
- It was observed that abrasion and low thermal conductivity of Ti-MMC are the primary parameters of tool failure.
- High manufacturing cost and poor machinability prevent the industries to widely employ Ti-MMC in their products. To encourage individual clients and industrial sectors, precise strategies should be defined to eliminate or at least minimize the effects of both undesired phenomena. To that end, the use of adequate optimization tools to select the appropriate setting levels of process parameters, are strongly recommended.

- Based on the prominent features of Taguchi method, this optimization technique is an ideal tool for optimization. By knowing the tool types and geometries as well as the relationship between machining results and the cutting conditions, Taguchi method can be used to optimize the process by maintaining and high productivity, superior work-piece surface quality as well as adequate tool life.

CHAPTER 3 METHODOLOGY

3.1. Introduction

It is important to define the experimental plan, optimization tool and method of analysis before conducting any experimental study. To that end, these elements are comprehensively investigated and outcomes are presented in the following sections.

3.2. Experimental plan

In this experimental study, it is not necessary to identify all noise parameters and only those with higher and stronger effects need to be defined. Upon configuring the parameters, the levels of experimental parameters are determined with desired variations. If the experimental parameters' levels are so proximate, it is possible to hide the real effects of parameters; therefore the model would fails. Whereas, if output slightly changes; a wider range of variation must be arranged.

The key elements of the proposed experimental studies in this research are:

- **Objective:** The performance of each cutting tool material (PCD, CBN, and Carbide) and inserts during turning and milling Ti-MMC is investigated. This includes comprehensive studies on the effects of tools materials and cutting conditions on the tool wear rate and work-piece surface roughness.
- **Hypothesis:** Tool flank wear is the main aspect of tool wear rate. Average value of surface roughness specifies the quality of the work-piece surface finish. Wet machining is strongly recommended for precise machining of Ti-MMC.
- **Experimental parameters:** Cutting tool, cutting speed v_c (m/min), feed rate *fr* (mm/rev) and depth of cut a_p (mm).
- **Response or depended parameter:** The material removal rate *MRR* (mm^3/min), Maximum Wear of the Straight part of Cutting Edge VB_{Bmax}(µm) and the average surface roughness *Ra* (µm)
- **Constant parameters:** Machine tool, cutting tool, tool holder, work material, coolant and cutting volume defined for each test are considered as the constant parameters.

- Operational Definition: The cutting process parameters are completely defined.

Table 3-1: Experimental parameters in machining Ti-MMCs

List	Experimental parameters	Noise parameters
1	Cutting speed	Abrasion particles
2	Cutting feed	Low thermal conductivity
3	Depth of cut	Vibration

As shown in Table 3-1, with respect to each cutting tool/insert used in milling and turning operations, six experimental variables are also used in experimental study. The experimental plans are arranged as multi-level full factorial design of experiment and orthogonal array. A complete overview of experimental studies is presented in the chapter 4-5.

In the designing of experimental plan of this study, the degree of freedom is df = (3-1) (3-1) =6. The smallest plan near to this situation is $L_9(3^4)$ which has 8 degrees of freedom.

3.3. Method of analysis

The effects of the manipulating parameters in this study are analyzed with the ANOVA analysis to determine which of the cutting parameters has the maximum effect on the cutting experiments (the cutting speed v_c, feed rate f_r and depth of cut a_p).

3.4. Optimization method

In this study, the loss function convex as depicted in Figure 3-1 is the lowest tool wear and surface roughness. The noises can act with different characteristics on the signal to achieve a desired work surface quality and less tool wear.

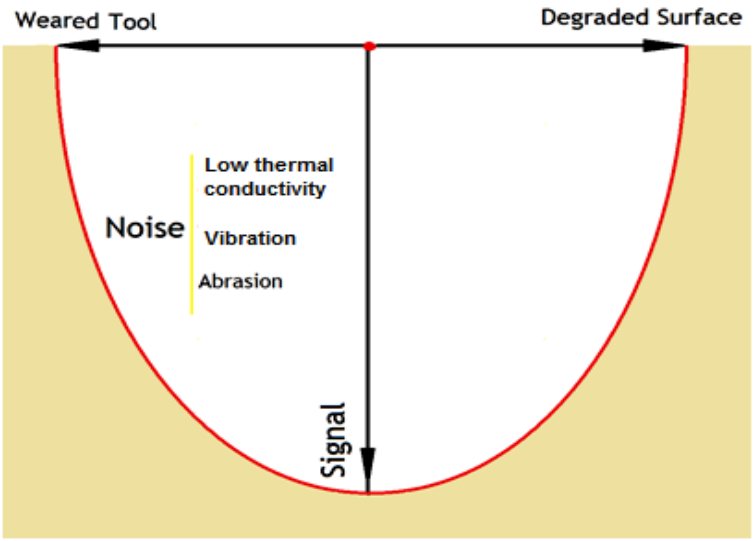

Figure 3-1: The curvature of the noises and their effects on the tool wear and work surface quality (Derivation from http://reliawiki.org/index.php/Robust_Parameter_Design)

In this study, the effects of three experimental parameters at three levels are constructed by the combination of the responses as depicted in Table 3-2. According to Table 3-2, y is the response value and the index number determines the experiment's run number. As mentioned earlier, "smaller-the-better" is well related to research objectives which are reduced tool wear and surface roughness in Ti-MMC work-pieces. The SNR values of each level of experimental parameters are presented in Table 3-3.

Table 3-2: Effects of individual levels of experimental parameters

Cutting Speed (m/min)	Cutting Feed (mm/rev)	Depth Of Cut (mm)
$V_{C1}^2 = \frac{y_1^2+y_2^2+y_3^2}{3}$	$f_{r1}^2 = \frac{y_1^2+y_4^2+y_7^2}{3}$	$a_{P1}^2 = \frac{y_1^2+y_5^2+y_9^2}{3}$
$V_{C2}^2 = \frac{y_4^2+y_5^2+y_6^2}{3}$	$f_{r2}^2 = \frac{y_2^2+y_5^2+y_8^2}{3}$	$a_{P2}^2 = \frac{y_2^2+y_6^2+y_7^2}{3}$
$V_{C3}^2 = \frac{y_7^2+y_8^2+y_9^2}{3}$	$f_{r3}^2 = \frac{y_3^2+y_6^2+y_9^2}{3}$	$a_{P3}^2 = \frac{y_3^2+y_4^2+y_8^2}{3}$

Table 3-3: SNR within each level of the experimental parameters

Cutting Speed (db)	Cutting Feed (db)	Depth Of Cut (db)
$SNR\ (V_{C1}) = -10\log V_{C1}^2$ 10	$SNR\ (f_{r1}) = -10\log f_{r1}^2$ 1 10	$SNR\ (a_{P1}) = -10\log a_{P1}^2$ 10
$SNR\ (V_{C2}) = -10\log V_{C2}^2$ 10	$SNR\ (f_{r2}) = -10\log f_{r2}^2$ 2 10	$SNR\ (a_{P2}) = -10\log a_{P2}^2$ 10
$SNR\ (V_{C3}) = -10\log V_{C3}^2$ 10	$SNR\ (f_{r3}) = -10\log f_{r3}^2$ 3 10	$SNR\ (a_{P3}) = -10\log a_{P3}^2$ 10

Finally, as showed in Table 3-4 the level of the maximum power of each parameter and their RSD for the tool wear and surface roughness were estimated. Following that, the optimum cutting conditions were calculated which depicts the lowest deviation from both strongest signals.

Table 3-4 reveals the relative standard deviation (RSD) between power of each level of signal and the strongest signal. Relative Standard Deviation RSD is the precise measurement in a data analysis. RSD measures the dispersion of a signal distribution around the mean value (here it assumed as the best and most powerful SNR). RSD is determined by percentage of the standard deviation of signals from the strongest signal dividing to the strongest signal.

According Table 3-4 the level of the maximum power of each parameter and their RSD for the tool wear and surface roughness were estimated. Following that, the optimum cutting conditions were calculated which depicts the lowest deviation from both strongest signals.

Table 3-4: Relative Standard Deviation of each Level Signal Power from the Strongest Signal

Cutting Speed %	Cutting Feed %	Depth Of Cut %
$RSD_{SN}(V_{C1}) = \frac{SNR(\max) - SNR(V_{C1})}{SNR(\max)} \times 100\%$	$RSD_{SN}(f_{r1}) = \frac{SNR(.max) - SNR(f_{r1})}{SNR(.max)} \times 100.\%$	$RSD_{SN}(a_{P1}) = \frac{SNR(max) - SNR(a_{P1})}{SNR(max)} \times 100.\%$
$RSD_{SN}(.V_{C2}) = \frac{SNR(.\max) - SNR(.V_{C2})}{SNR(\max)} \times 100.\%$	$RSD_{SN}(f_{r2}) = \frac{SNR.(max) - SNR(f_{r2})}{SNR.(max)} \times 100.\%$	$RSD_{SN}(a_{P2}) = \frac{SNR\ (max) - SNR\ (a_{P2})}{SNR\ (max)} \times 100.\%$
$RSD_{SN}(V_{C3}) = \frac{SNR..(max) - SNR..(V_{C3})}{.SNR..(max)} \times 100.\%$	$RSD_{SN}(f_{r3}) = \frac{SNR(max) - SNR(f_{r3})}{SNR(max)} \times 100.\%$	$RSD_{SN}(a_{P3}) = \frac{SNR\ (max) - SNR(a_{P3})}{SNR\ (max)} \times 100.\%$

3.5. Cutting tools

3.5.1. Turning tool holder

Similar cutting tool (Figure 3-2) was used in turning operations and only inserts were changed with respect to each experimental plan.

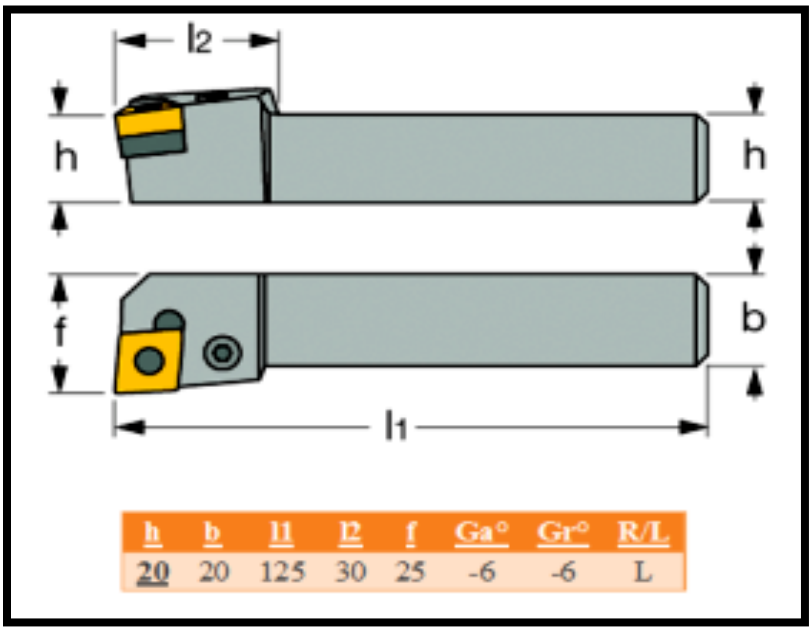

Figure 3-2: Turning tool holder used in the experiment (BECKER Diamantwerkzeuge GmbH)

3.5.2. Milling cutter

The carbide inserts (X-500 (Figure 3-3) and X-400 (Figure 3-4)) were used on Kennametal milling tools. Furthermore, indexable milling tool (Figure 3-5) was used with PCD inserts. There were not CBN inserts match with our cutter types, so only carbide and PCD insets were used in milling tests.

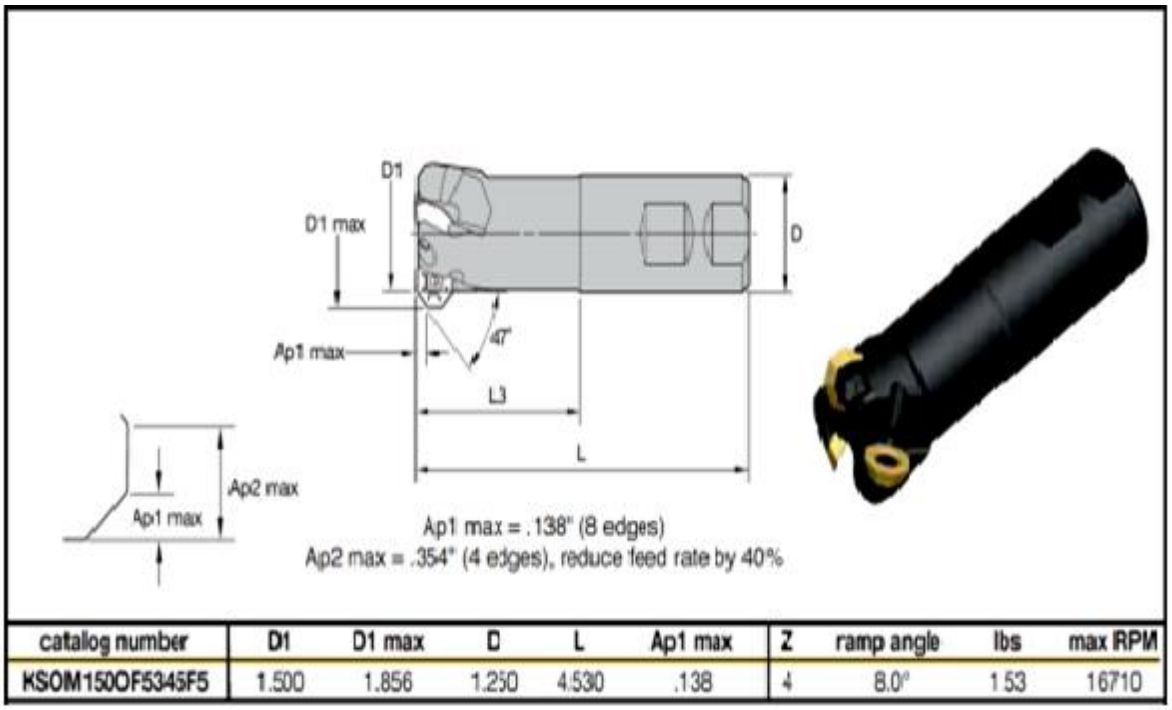

catalog number	D1	D1 max	D	L	Ap1 max	Z	ramp angle	lbs	max RPM
KSOM150OF5345F5	1.500	1.856	1.250	4.530	.138	4	8.0°	1.53	16710

Figure 3-3: Milling tool and carbide insert X500 (Kennametal)

Product		Dimensions (mm)					
EDP	Item Description	D	L/H	l_1	d_1	a_e max plunging	No. of Teeth
7791VS09 Modular Head							
031405	7791VS09SA032Z3R43	32	43	M16	17	8	3

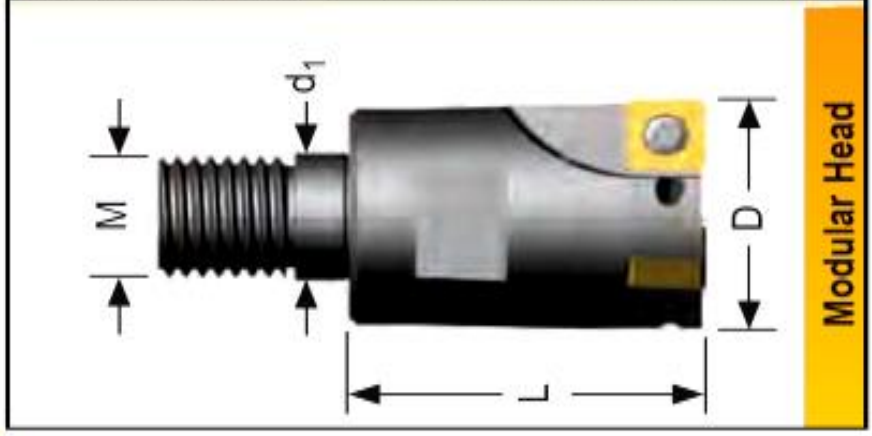

Figure 3-4: Milling tool and carbide insert X400 (Kennametal)
[This tool actually is used for plunging but the geometry of the related insert X-400 is highly robust]

Figure 3-5: Milling cutter with PCD inserts (BECKER)

3.6. Inserts

3.6.1. Turning carbide inserts

After a comprehensive investigation on commercial cutting tools proposed by various world leading manufacturers (e.g. ISCAR, NTK, Mitsubishi, Ingersoll, SECO, SANDVIK), the SECO insert tool was selected for turning tests (the reasons are mentioned below) (Table 3-5).

Table 3-5: Characteristics of the coated carbide insert for turning tests (SECO)

Item	Grade	d	r	l	s	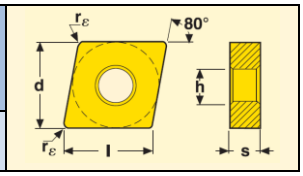
CNMG 120404-MF1	TH1000	12.7	0.4	12.9	4.76	

TH1000 is a coated carbide insert of WC sintered strut with a Nano-laminate PVD-coat of TiSiN-TiAlN. SECO Inc. proposes the inserts of TH1000 in turning of materials which have high toughness and hard surface components. The grade has anti-chipping and high edge fracture toughness. Further, TH1000 is recommended for finishing to semi-finishing processes of super alloys. The enhanced smooth coating allows the tool to operate at

1.5- 2 times higher speeds than that offered by other grades. A hard deposited laminate on the tool surface prevent scratching and grooving the strut by the work material abrasion. These characteristics are achieved by lamination of a polycrystalline nano-composite of alternating TiAlN and TiSiN (Each layer thickness 0.5 to 10 ηm).

3.6.2. Milling carbide inserts

Two types of carbides inserts (X400 and X500) were used in milling tests. The carbide insert X500 contains multilayers coats of TiN—TiC—TiN which are laminated by CVD technique. X500 is widely used to cut ductile iron, nickel and titanium alloys. The carbide insert X400 is coated with single layer of PVD. Both inserts are comprised of tungsten carbides particles and cobalt (Co) as the base binder and ruthenium (Ru) as the key feature of the binder. At least 3% of weight of the binder is made of Ru to improve the tool performances. Ru depicts high hardness and melts roughly at 2,500° C. This additional substance is used to enhances the thermal resistance of the tool and diminishes the crack propagation on the tool edge into the substrate when cutting super alloys or materials embedded hard particles (Festeau, Fang et al. 2007). Smooth surface displays the difficulty of formation on the carbide inserts with the binders of Co + Ru combination. The smoothness of the surface can be improved by using CVD coating.

Table 3-6: The composition of the carbide inserts (Kennametal)

Item	Chemical composition of substrate (wt. %)						Average Grain Size (µm)	Rupture Strength (N/µm^2)	Density (g/cm^3)
	WC	TiC	TaC	NbC	Co	Ru			
X500	90.8	0	0	0	8.0	1.20	<1	3500	14.55
X400	67.2	10	7	2	12	1.8	1-2	2300	11.70

Table 3-7: Characteristics of the coated carbide insets (Kennametal)

Item Description	Grade	d	r	l	s		
ODMT-0404-APEN-41	**X500**	12.7	Facet	4.00	4.76	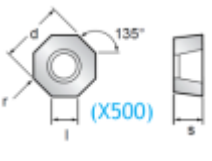	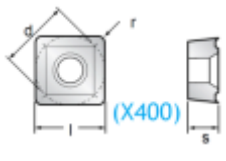
SCCT-12M5-ACTR	**X400**	12.7	Facet	12.7	5.00		

Due to strong toughness and wear resistance, X400 can be used in continuous and interrupted cuts with high material removal rate. PVD coating on Ru-featured CW tool forms a hard, smooth and rock-hard structure (Festeau, Fang et al. 2007).

3.6.3. Cubic boron nitride (CBN) & Polycrystalline diamond (PCD) inserts

Cubic Boron Nitride (CBN) is the base material in CBN tools with a binder of ceramic or metal. CBN is generally used for cutting various work materials. Experimental studies with cutting tools encompassing different contents of CBN, Diniz et al. (Diniz and Ferreira 2003) revealed that tool wear in flank and crater sides are the main tool wear phenomenon on those tools while chipping is generally occur in the tools having low contents of CBN.

Cutting tools with high contents of CBN perform better at low frequency; but those tools with higher ratio of CBN have low sensitivity to interrupted frequency variation. Chou et al (Chou and Evans 1999) observed that the centered levels of cutting speed are optimum in machining tests with CBN tools. In fact, rapid tool wear and low life in CBN tools are observed at high levels cutting speeds. Decreased surface roughness was observed during interrupted cuttings, whereas, increased roughness was noticed during continuous cuttings (Pavel, Marinescu et al. 2005).

Two types of binder are used in the CBN tools. One is the ceramic which executed to preserve the grades up to 70% weight of CBN grains. Those depict the more wear resistant CBN grades. The other binder type is metallic which hold the grains between 80-95% weights. That enhances toughness of the CBN cutting tool (Lahiff, Gordon et al. 2007).

Over 800°C, CBN depicts more strong than PCD. It is known the cutting process of the materials such as nickel alloys and titanium alloys settle on high temperatures. The problems of CBN tool are diffusion and adhesion over 800 °C(Honghua, Peng et al. 2012).

Polycrystalline diamond (PCD) is a synthetic material which seems to be the hardest material be used in the cutting tools (Davim 2002). High thermal conductivity of PCD makes tool protective to the adhesion mechanism and increases the heat dispersion rate from tool edge and cutting zone. PCD tool is more appropriate than CBN for cutting MMC by more resistant to the abrasive wear, the low affinity to adhesion, the constant and low roughness (around 0.5 μm) at all speed (Ding, Liew et al. 2005). Impurities in the PCD composition create the graphitic layers in the PCD structure which induce micro cracks and degrade the tool above 600˚C (Morgan 2005).

Despite CBN materials, PCD in vicinity to the oxygen transforms to the carbide-dioxide over 600°C (Heath 1986). The crystal of diamond while has strongest covalent bonds, on its surface has one free electron on each bond. So the diamond acts as a reactive material to adjacency the metals objects. Paired electrons at the surface of crystals prevent the CBN atoms of bonding with the neighbors materials (Kobashi 2010).

Amongst commercial tools offered by several companies, the chosen CBN and PCD tools in our study were manufactured by BECKER Diamantwerkzeuge GmbH (Table 3-8 and Table 3-9).

Table 3-8: Characteristics of PCBN and PCD inserts used in turning (Becker)

Item	Grade	d	d1	s	l	r	l1		
CNMA- 432 -MC	PBC-10	12.7	5.1	4.8	12.9	0.8	2.8	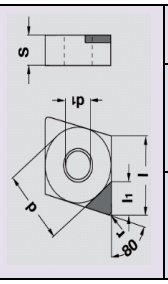	Uncoated standard CBN, with neutral geometry.
CNGA-432-MW	PDC	12.7	5.1	4.8	12,9	0.8	2.8		Polycrystalline diamond carbide (fine size grains).

Table 3-9: Characteristics of PCD inserts used in milling (BECKER)

Item Description	Grade	l	l1	r	
BFPL280508	PDC-CU-S	22.6	3.5	0.8	100% diamond, Without Carbide reinforcement, Coarse grains, Solid Polycrystalline

3.7. Work-piece Material

Dynamet Technology Inc. supplied a plate of Ti-MMC in 184.125×87.5×31.25 mm3 for milling experiments and a cylindrical work-piece with 75mm in diameter and 400mm in length for turning operations. The work-piece comprised of 10-12% TiC particles dissipated in the Ti6Al4V matrix.

3.8. CNC machines

Two CNC machines were used in this work for milling and turning operations. Their specifications are presented in the next section. The experimental works were all completed at laboratoire de recherché en fabrication virtuelle (LRFV) at École Polytechnique de Montréal.

3.8.1. Turning machine (Lathe)

The turning experiments were completed using a MAZAK Nexus 200 CNC turning center (Figure 3-8). The specification of this machine is presented in Table 3-12.

Table 3-10: Specification of MAZAK Nexus 200 (https://www.mazakusa.com)

SPECIFICATION	
Maximum Speed	5000 rpm
Motor Output (30 minute rating)	35.0 hp / 26 kw

Figure 3-6: The CNC turning center MAZAK Nexus 200

3.8.2. Milling machine

The milling tests were conducted on a 5-axis CNC (MITSUI SEIKI 5-Axis- Model HU40T) as presented in Figure 3-7.

Table 3-11: MITSUI SEIKI 5-AxisModel HU40T (http://www.mitsuiseiki.com)

Working Capacity	
X, Y and Z axes	36,000 mm/min (1417 IPM)
X, Y and Z axes	0.1~20,000 mm/min. (0.004~787 IPM)

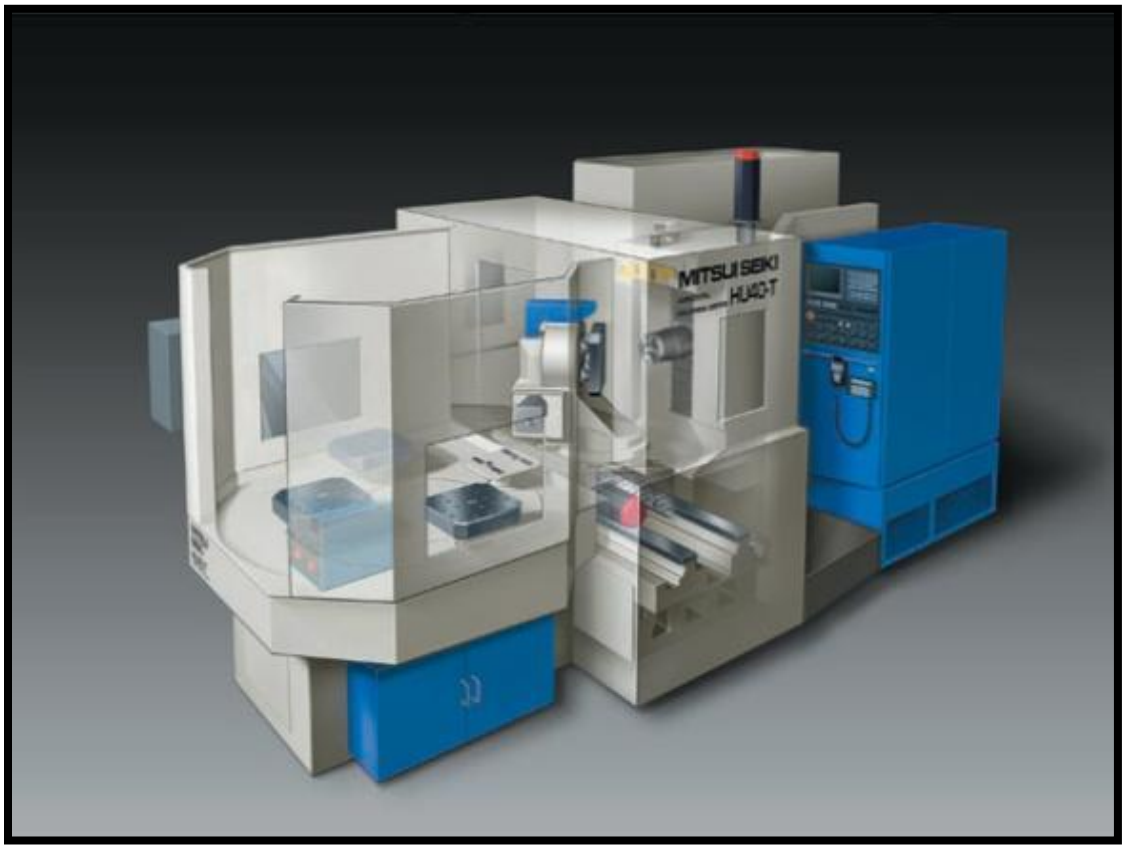

Figure 3-7: MITSUI SEIKI 5-Axis- Model HU40T (http://www.mitsuiseiki.com)

3.9. Supporting tools and strategy

3.9.1. Dynamometer

During milling and turning tests, the cutting forces were measured using Kistler dynamometers. Kistler dynamometer for turning (Model 9121;

Figure 3-8) has the following components:

- Revolver adaptor (Model 9155A) used for clamping system DIN 69880 (VDI 3425);
- Dynamometer (Model 9121) with mounted quartz sensors;
- Tool holder (Model 9153A) used for the outside diameter of turning tool.

As shown in Figure 3-8, there are four force sensors placed between the base plate and the top plate; each constructed of three paired sensors of quartz plates. Those are connected together with the connecting cable 1689B5. The dynamometer also needs three charge amplifiers to convert force signals to proportional voltages. The specifications of the dynamometer used are presented in Table 3- 14.

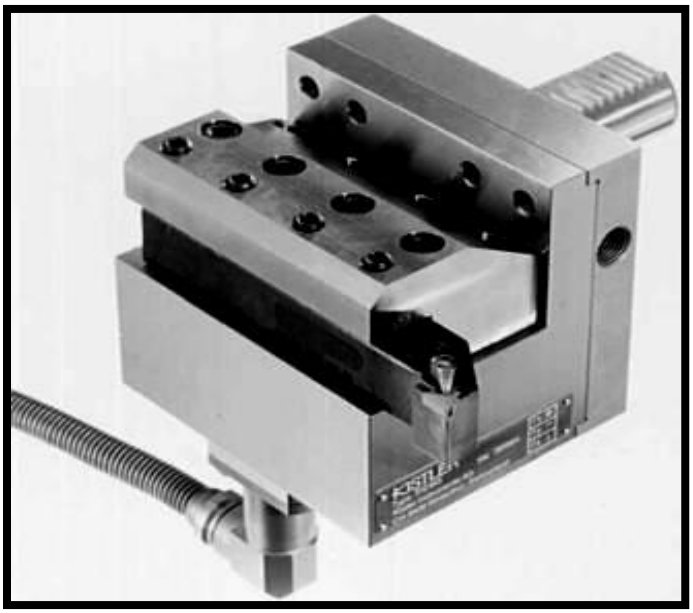

Figure 3-8: Kistler dynamometer for Turning

Table 3-12: Specification of the Kistler dynamometer used

Technical Data		
Range	Fx, Fy (kN)	Fz (kN)
Within force application range I (for turning the outside diameter)	3	6
Within force application range II (for turning the inside diameter)	2	4
Calibrated partial range	0…3	0…6
Overload 20%		

Kistler dynamometer for milling (Type 9255C; Figure 3-9) was Multi-Component Dynamometer up to 60 kN, very robust dynamometer with the largest force range of all the dynamometers and high stiffness, 360 x 300 mm. Particularly suitable for heavy machining, Easy mounting with lateral flanges. The specifications of the dynamometer used are presented in Table 3-13.

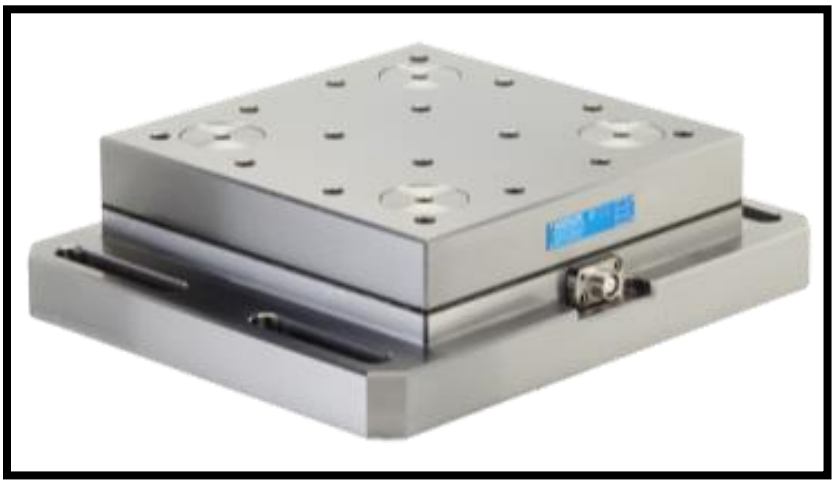

Figure 3-9: Kistler dynamometer for milling

Table 3-13: Specification of the Kistler dynamometer used

Technical Data		
Range	Fx, Fy (kN)	Fz (kN)
Force application within and max. 100 mm above top surface	30	10…60
Calibrated partial range	0…30	0…60
Overload 20%		

3.9.2. Profilometer

The work-pieces surface quality was quantified using a profilometer Mitutoyo SV-C4000. The specifications of the profilometer used are shown in Table 3-14.

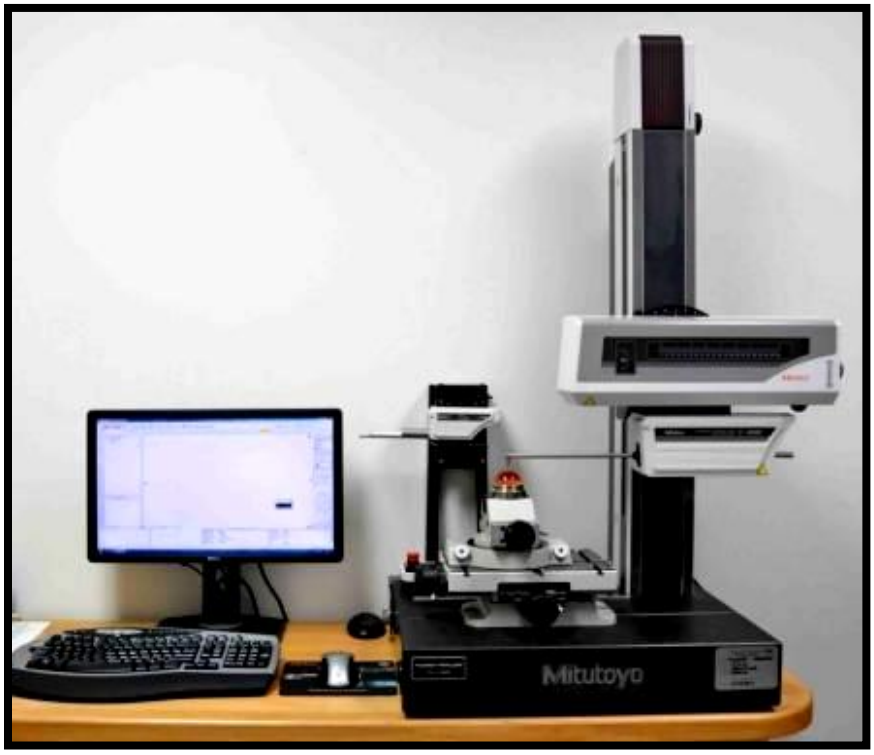

Figure 3-10: Profilometer Mitutoyo SV-C4000

Table 3-14: Specifications of the profilometer (Mitutoyo SV-C4000) used

C4000		
Measuring range/	X-axis (horizontal direction)	200mm/0.05µm
Resolution	Z-axis (vertical direction)	5mm/0.08µm
		0.5mm/0.008µm
		0.05mm/0.0008µm
Accuracy (20°C)	X-axis (horizontal direction)	±(1+2L/100)µm L: measuring length (mm)
	Z-axis (vertical direction)	±3µm/5mm

3.9.3. Microscope

The maximum flank wear (VB_{Bmax}) of the cutting tools were measured using an Olympus SZ-X12 high-resolution microscope.

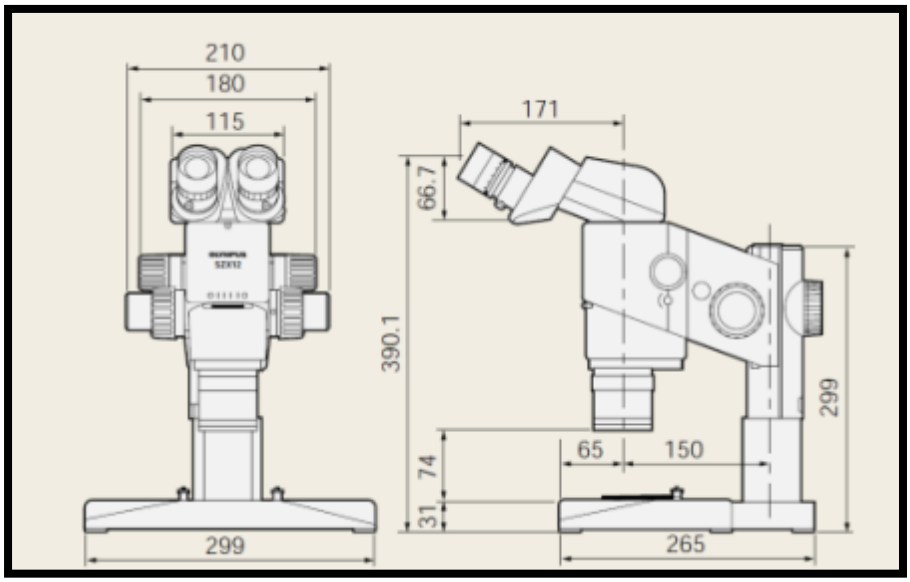

Figure 3-11: Optic Microscope (Olympus SZ-X12)
(http://www.olympusmicro.com/)

3.9.4. High resolution camera

High resolutions images captured from the tool tips and chips by a Canon EOS 6.3MP Digital Rebel Camera with Microphotography Lens with Features: 6.3-megapixel resolution including Canon's EF-S 18-55mm, f3.5-5.6 zoom lens, 1.8-inch LCD screen for zooming on images in preview; 2.5 frames/second continuous shooting speed with 4-shot burst mode as well as store images on Compact Flash type 1 or 2 memory cards, powered by a rechargeable lithium-ion battery pack (included with charger). This in fact required adequate light with proper intensity and contrast. Therefore, to that end, sensible ISO, deep aperture and deliberated shutter speed should be used in the proposed optical set up.

To capture images from small objects, the light flux emitted to the camera needs to increase the ISO sensibility. To extend the depth of field and provide more clear view of all aspects of the

object, the diaphragm of the camera should been closed by highest available aperture f-number. To cover a deep field for a small object, strong lightening is necessary. Increased light's volume may cause reflection and shadows as well as blurring leas to non-clear and non-identical images. The similar problem has been occurred when capturing the images from the worn tools. The use of two arms LCD lightening and a ring flash light were proposed to overcome these difficulties. According to Figure 3-13, the camera needed to be adjusted on the manual and the images can be captured by 3-5 times enlargement (3-5 X zoom).

After adjusting the camera and the object position, to prepare the lightening, under the object and on the lights were covered by diffuser papers. The three lights positioned with 120° angles related together. One of the light arms is fixed parallel and close to the object and the exposed surface for decreasing the reflection effect and increasing the sharpness of the sides. The other arm focused on the top of object to increase the surface brightness and the ring light illuminated the object surrounding (Figure 3-14).

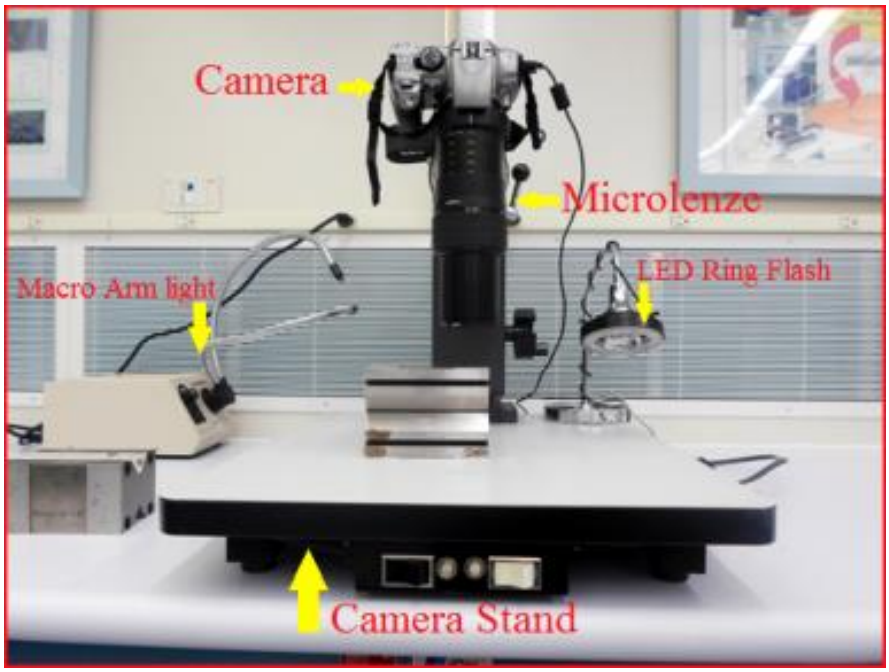

Figure 3-12: Camera setup

Figure 3-13: First adjustment of the camera

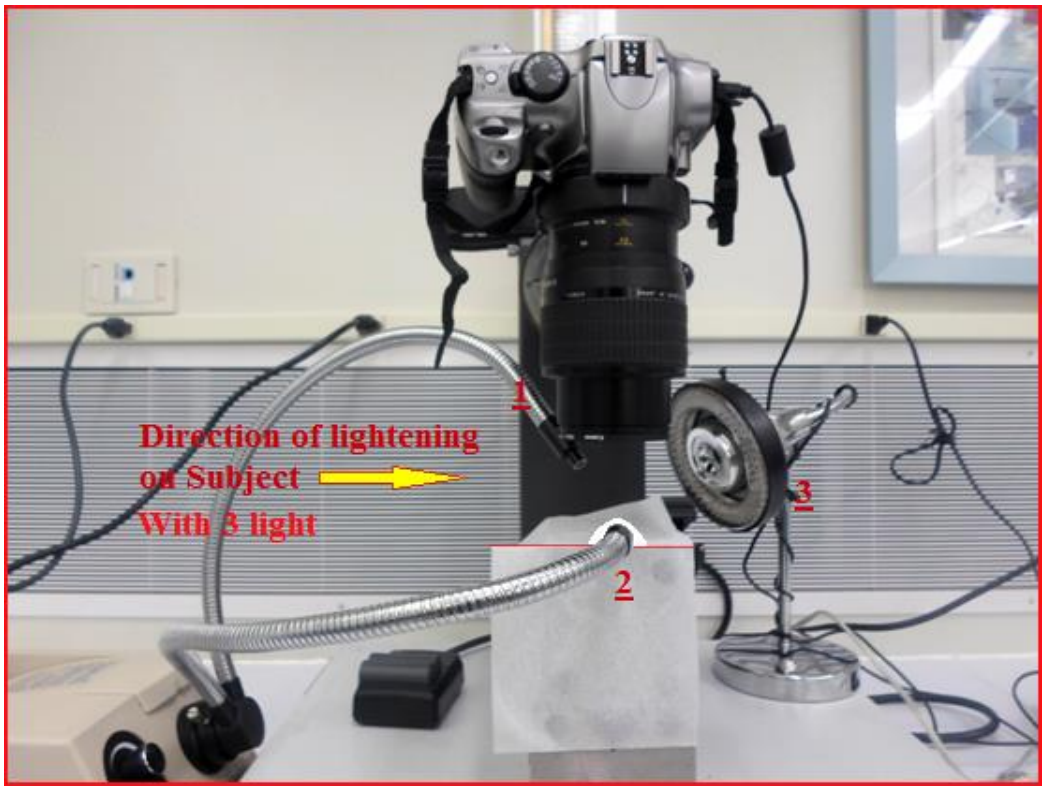

Figure 3-14: Alignment of the lights: (1) and (2) are the LCD lightening arms, and (3) is the lightening ring

CHAPTER 4 TURNING EXPERIMENTS AND RESULTS

4.1. Experimental plan

As noted earlier in chapter 3, the cutting conditions used in the turning tests were selected according to tools manufacturer's recommendations as well as the previous research studies reported in the literature. Dry turning tests were performed with the carbide inserts, while the experimental works with other inserts (CBN and PCD) were conducted in wet condition using high volume of emulsified cutting fluid. In order to achieve the research objective, a proper experimental plan is needed using following propositions (Nian, Yang et al. 1999):

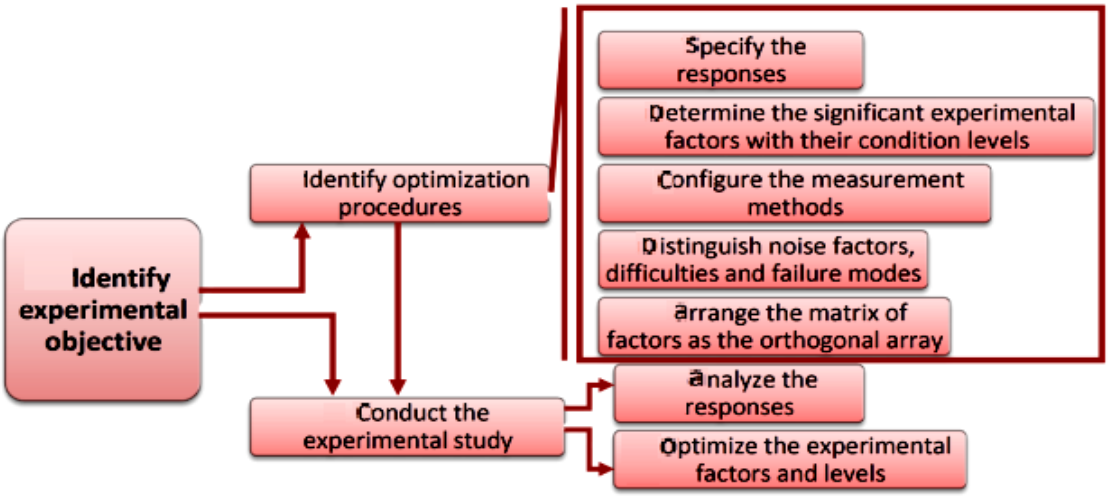

Figure 4-1: Experimental plan flowchart

4.2. Turning Experiments

With respect to each type of insert, the turning experimental studies were designed as Taguchi plan. The cutting forces were recorded by Kistler dynamometer (model 9121). After each cutting test, the individual insert were inspected and the flank wear were measured with the optical microscope (Table 3-13) and high resolution camera (Figure **3-12**). The surface finishs of work-pieces were measured by profilometer (Figure 3-10). A full description and discussion on experimental results is presented in the following sections.

4.2.1. Turning tests with Carbide inserts

The experimental tests were arranged as orthogonal array $L_{27}(3^{13})$ (Table 4-1). The experimental parameters and their levels are shown in Table 4-2, No specific failure, including tool breakage and chatter vibration was observed in the cutting tools and cutting process.

Table 4-1: Orthogonal array $L_{27}(3^{13})$

Test No.	v_c (m/min)	f_r(mm/ rev)	a_p(mm)
1	1	1	1
2	1	1	2
3	1	1	3
4	1	2	1
5	1	2	2
6	1	2	3
7	1	3	1
8	1	3	2
9	1	3	3
10	2	1	1
11	2	1	2
12	2	1	3
13	2	2	1
14	2	2	2
15	2	2	3
16	2	3	1
17	2	3	2
18	2	3	3
19	3	1	1
20	3	1	2
21	3	1	3
22	3	2	1
23	3	2	2
24	3	2	3
25	3	3	1
26	3	3	2
27	3	3	3

Table 4-2: Cutting conditions used in turning with carbide inserts

Level No.	**Experimental parameters**		
	v_c(m/min)	**f_r (mm/ rev)**	**a_p (mm)**
1	40	0.15	0.1
2	60	0.25	0.15
3	80	0.35	0.2

4.2.2. Turning tests with CBN inserts

The experimental plan was arranged as orthogonal array $L_9(3^4)$ Table 4-3. The cutting conditions used for turning tests with CBN inserts along with responses are presented in Table 4-4. High temperature and sparks were observed in the cutting zone. To further reduce their effects on functionality of the work-piece and precision of surface quality, appropriate coolant was used during cutting operations.

Table 4-3: Orthogonal array $L_9(3^4)$

Test No	v_c (m/min)	f_r(mm/ rev)	a_p(mm)
1	1	1	1
2	1	2	2
3	1	3	3
4	2	1	2
5	2	2	3
6	2	3	1
7	3	1	3
8	3	2	1
9	3	3	2

Table 4-4: Cutting conditions and responses in turning with CBN inserts

No.	**Experimental parameters**		
	v_c(m/min)	**f_r (mm/ rev)**	**a_p (mm)**
1	150	0.3	0.1
2	175	0.45	0.15
3	200	0.6	0.2

4.2.3. Turning tests with PCD inserts

The third set of tests with PCD inserts was arranged in orthogonal array $L_9(3^4)$. The experimental parameters and their levels are presented in Table 4-5. Results and discussion are presented in the next section.

Table 4-5: Cutting conditions in turning with PCD inserts

Level No.	Experimental parameters		
	v_c(m/min)	f_r (mm/ rev)	a_p (mm)
1	400	0.3	0.1
2	450	0.4	0.15
3	500	0.5	0.2

4.3. Results and discussion

This section discusses the effects of various process parameters on surface roughness and tool wear rate with respect to each individual insert used. To that end, ANOVA and the statistical parameters including R^2, P value and F ratio were used for statistical analysis. Optimization was conducted using Taguchi method. Finally, the wear morphology in all inserts was evaluated. The details of optimization based Taguchi method are presented in appendix-1.

4.3.1. Turning with carbide inserts

The ANOVA table of surface roughness and tool wear rate is displayed in the Table 4-6. According to Table 4-7, the P-values depict the cutting speed is the only statistically significant parameter on tool wear rate, while it is not considered as an effective parameter on the surface roughness. In the other side, all three parameters have had strong effects on the surface roughness of work-piece; although, the feed rate displays the most strong effect. These observations are in agreement to what has been reported in the literature on turning titanium alloys and MMCs (Hartung, Kramer et al. 1982, Komanduri and Reed 1983, Karakaş, Acır et al. 2006, Übeylı, Acir et al. 2008, Bejjani, Balazinski et al. 2011, Sadat 2012, Hosseini and Kishawy 2014).

However, R^2=0.57 states that totally the tool wear rate cannot be statistically controlled by process parameters used. But R^2 =0.718 shows the surface roughness of work-piece is sensitive to the involved parameters.

Table 4-6: ANOVA table of results recorded in turning by carbide inserts

Parameter	Tool wear rate		Surface roughness	
	F	P	F	P
(1) v_c	10.411	0.0008	8.788	0.0018
(2) f_r	1.957	0.1674	9.476	0.0013
(3) a_p	0.987	0.3902	7.208	0.0044
	R^2 =0.572		R^2 =**0.718**	

Table 4-7: Surface roughness and tool wear rate values of turning with carbide inserts

Test No.	MRR (mm^3/min)	Ra (µm)	$\dot{\widehat{VB}}max\times10^{-2}$ ($\mu m/mm^3$)
1	600	1.2	1.3
2	900	1.1	0.8
3	1200	1.6	0.6
4	1000	1.7	0.9
5	1500	1.4	1.1
6	2000	2.5	0.8
7	1400	1.9	1.1
8	2100	2.1	0.9
9	2800	3.0	1.2
10	900	0.9	1.8
11	1350	1.1	1.6
12	1800	1.5	1.8
13	1500	2.0	1.3
14	2250	1.1	0.8
15	3000	1.3	0.7
16	2100	1.6	0.6
17	3150	1.3	0.9
18	4200	1.5	1.6
19	1200	0.7	1.6
20	1800	0.3	1.5
21	2400	0.8	2.0
22	2000	0.4	1.5
23	3000	0.9	1.3
24	4000	1.5	1.8
25	2800	1.8	1.5
26	4200	0.7	1.7
27	5600	2.5	2.1
∑	60750	38.4	34.7

Where MRR, $\dot{\widehat{VB}}_{Bmax}$ and *Ra* are respectively Material Removal Rate, The Rate of Maximum Wear of the Straight part of Cutting Edge and Average Surface Roughness

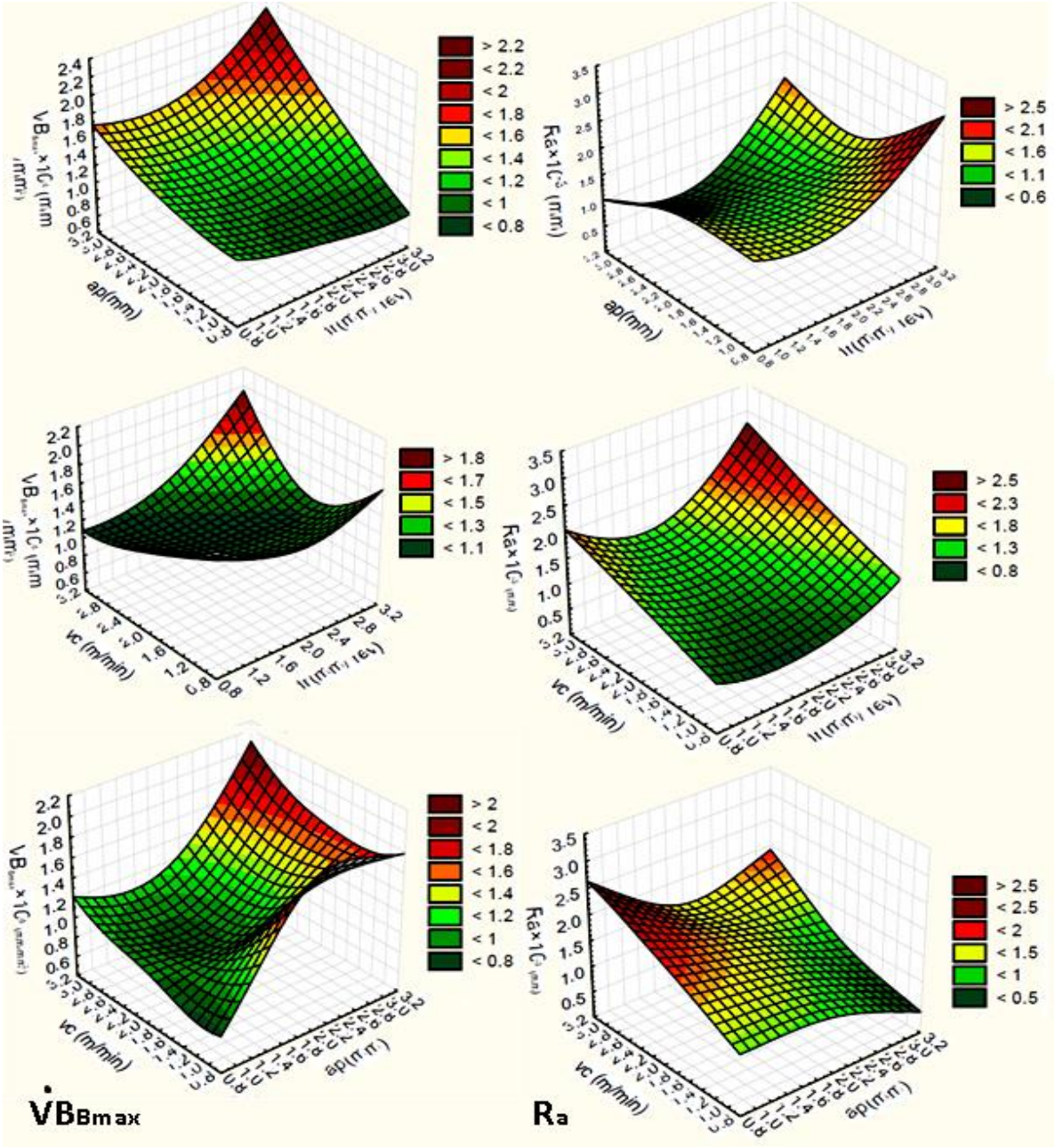

Figure 4-2: Work surface roughness & Tool wear rate
vs. cutting conditions for Carbide inserts

The total results of the tool wear rate, surface roughness were illustrated in Table 4-7. As shown in Table 4-7, the worst surface quality is observed in the tests 6 and 9 (low cutting speeds and

high feed rates); while the stable trend with acceptable surface quality was achieved in the tests 19- 23 (high cutting speeds and low feed rates). Similarly, cutting speed has higher effect on the tool wear rate than other two machining parameters.

Figure 4-2 shows a moderate cutting speed, a higher feed rate, and a smaller depth of cut induce to the low wear rate. Further, a higher cutting speed, and a moderate depth of cut decrease the surface roughness of work-piece.

Table 4-8 depicts the highest mean value is resulted in radial force than cutting and feed forces. This phenomenon underlines that the force direction was pointed towards the work-piece surface than cutting direction. Furthermore, a lower feed rate, and a moderate depth of cut decrease the cutting force. The test No. 7 (v_c= 40m/min; fr=0.35 mm/rev; a_p =0.1mm) and 13 (v_c= 60m/min, f_r=0.25mm/rev, a_p =0.1mm) display very low cutting forces.

In this experiment, Figure 4-3, for a given depth of cut, a moderate cutting speed and a moderate feed rate induce to lower radial force; a moderate depth of cut and a moderate cutting speed decrease the lower feed force.

As Table 4-7, the lowest tool wear was achieved when the lowest radial forces were recorded in the tests 2 and 3. This reveals the significant effect of radial force on tool performance. In fact, the radial force is highly affected by the intrinsic quality of the work material and the tool geometry (Hartung, Kramer et al. 1982,Komanduri and Reed 1983,Antonialli, Diniz et al. 2010) which both have great influence on the tool performance.

The cutting parameters used in test 21 (v_c=80m/min; f_r=0.15mm/rev and a_p= 0.2mm) drastically elevated the radial force, almost four times higher than mean value of feed force and three times higher than other force components. Further, in this condition, the most deteriorated insert was observed (Table 4-7).

Table 4-8: Cutting force results for turning with carbide inserts

Test No.	Radial Force Fx (N)	Feed Force Fy (N)	Cutting Force Fz (N)
1	322	84	124
2	144	38	88
3	181	83	185
4	324	50	186
5	173	74	150
6	192	54	136
7	135	35	10
8	189	79	220
9	145	41	129
10	130	38	104
11	220	88	130
12	150	65	77
13	135	35	10
14	176	46	212
15	201	34	143
16	179	64	46
17	166	64	151
18	131	37	110
19	181	36	51
20	163	153	214
21	867	184	278
22	163	30	77
23	133	37	64
24	387	77	211
25	168	29	109
26	199	80	231
27	118	17	87
∑	5672	1652	3533
M	210.07	61.19	130.85

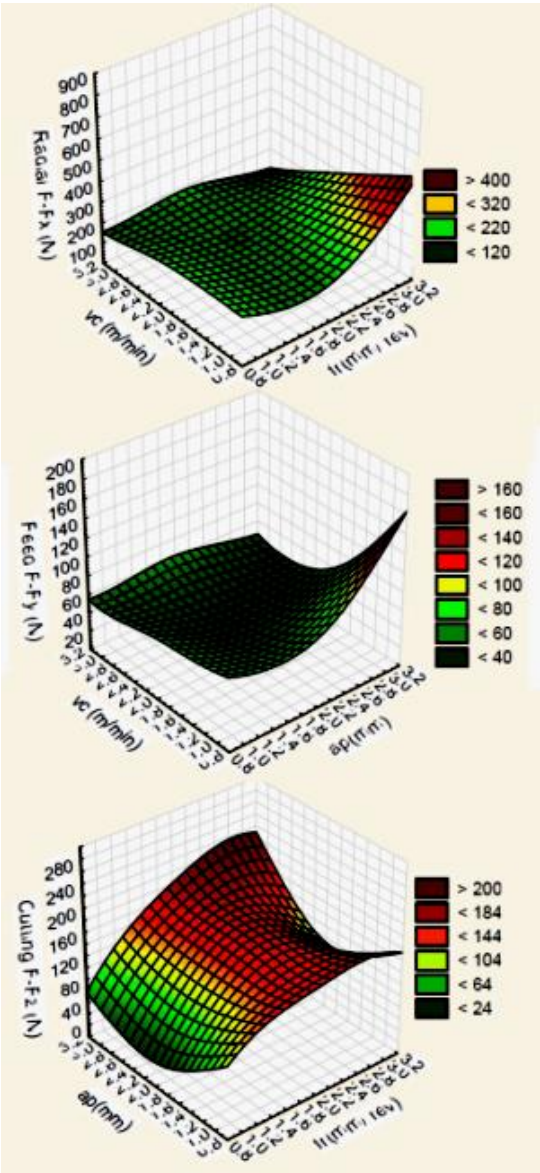

Figure 4-3: Cutting forces vs. cutting conditions for turning with carbide inserts

According to Figure 4-5, the strongest signals for surface finishes are depicted from third level of cutting speed, first level of feed rate and second level of depth of cut. Turning test with higher

level of depth of cut at lower level of cutting speed led to deteriorated insert. Changing the depth of cut from middle to high level affects the work hardening thickness and effectively more noise parameters are generated.

The strongest signal for tool life was achieved from first level of cutting speed, second level of feed rate and also second level of depth of cut. By increasing the cutting speed more noises such as the cutting thermal load affect the tool condition and high depth of cut increases the mechanical load as well as vibration on the tool. But moderate feed rate can decrease the effect of the thermal and mechanical load together on the tool.

Based on Figure 4-4 except radial force, signals of the other forces are weakened dramatically by increasing the depth of cut. Furthermore, the strongest signals for all forces have direct proportion to highest level of feed rate. In addition, it can be concluded that a moderate cutting speed produces lowest noise on the forces signals when using carbide inserts.

As Figure 4-6, the optimum cutting conditions for the best surface finish and tool life were estimated respectively with 2.5% and 2.5% RSD from the strongest signals for both (v_c=60m/min; f_r=0.25m/rev; a_p=0.15mm). The productivity of this condition is 2,250mm^3/min. The summary of the results are shown in Table 4-9.

In summary, the cutting condition that led to optimum tool life and surface roughness is not similar as that observed for optimum cutting force. This exhibits that the effective parameters on cutting forces are different than those affecting tool wear rate and surface roughness. Amongst cutting parameters, the grade, chemical composition and mechanical behavior of insert seem to be the governing parameters.

The experimental results reveal that cutting Ti-MMC with higher levels of feed rate is recommended. To reduce the radial forces, the geometry of the cutting tools and inserts need to be revised carefully.

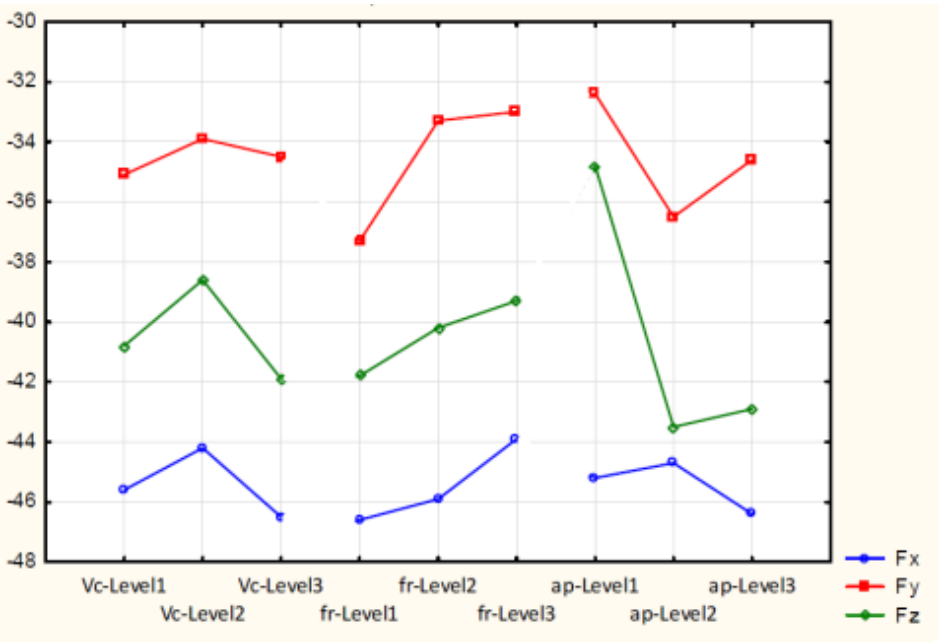

Figure 4-4: SNRs of cutting related forces (Fx, Fy, Fz)

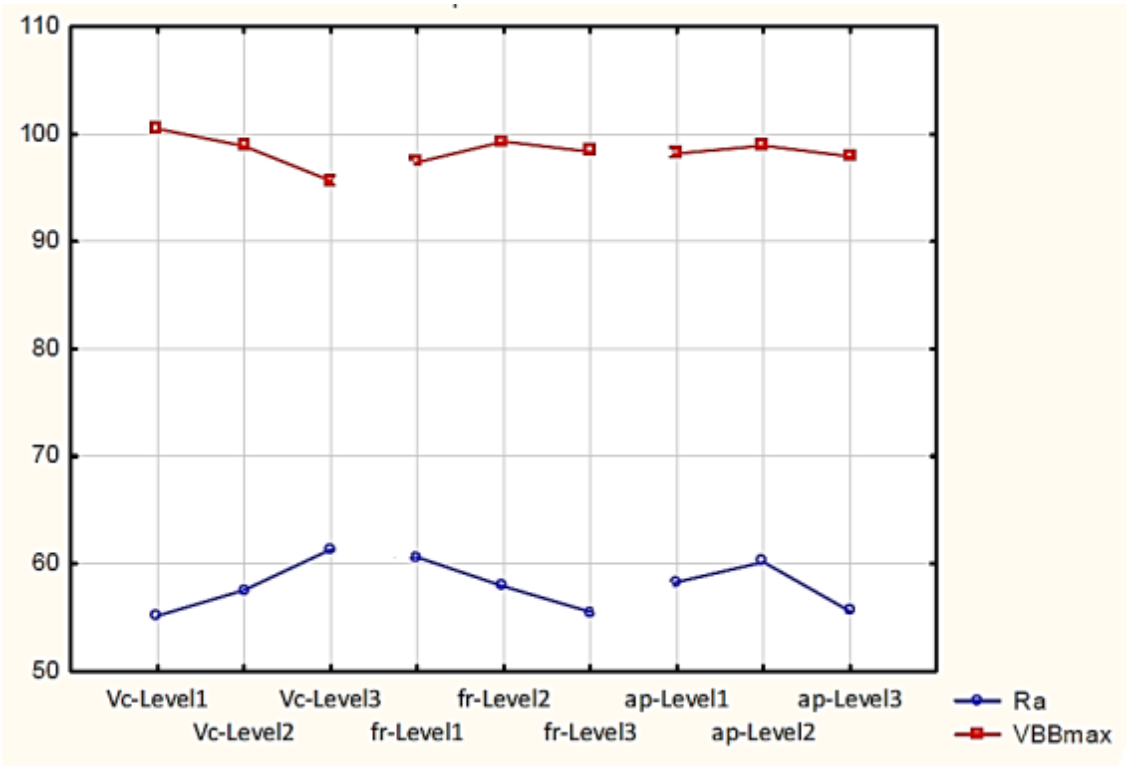

Figure 4-5: SNRs of tool wear rate and work surface roughness

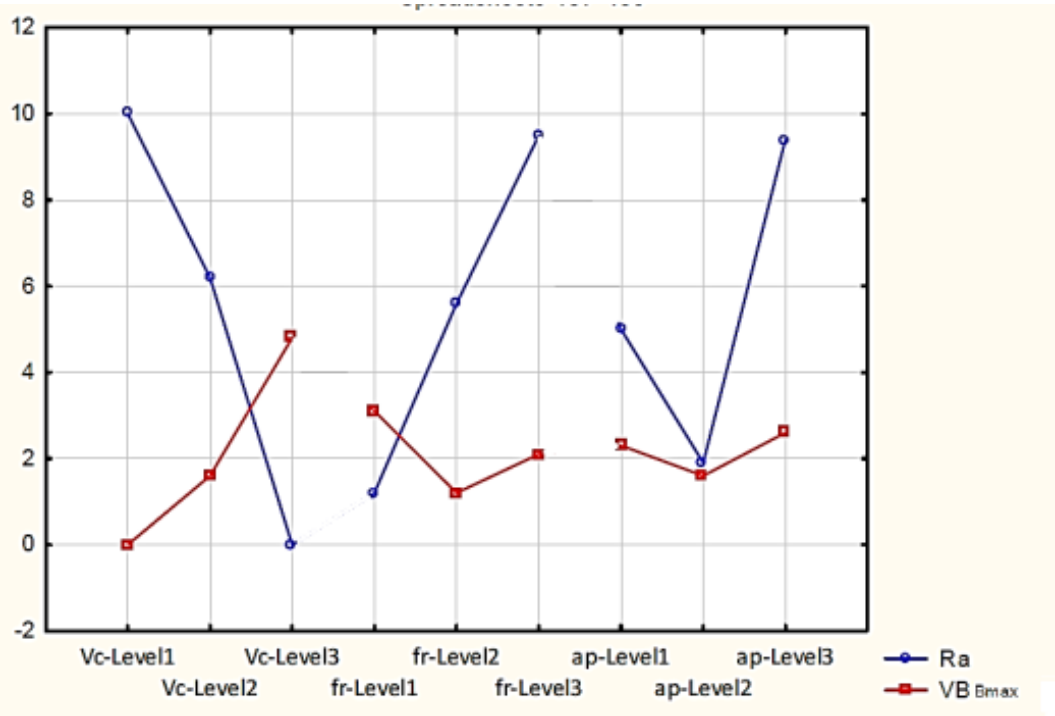

Figure 4-6: RSDs of tool wears and surface roughness signal to noise

Table 4-9: Final results of optimized cutting conditions for the turning carbide inserts

	v_c(m/min)	f_r (mm/rev)	a_p (mm)	MRR (mm^3/min)
Optimum conditions for the work surface finish	80	0.15	0.15	1800
Optimum conditions for the tool life	40	0.25	0.15	1500
Total optimized conditions for the tool life and work surface finish	**60**	**0.15**	**0.15**	**2250**
Optimum conditions for minimum cutting applied forces	**60**	**0.35**	**0.1**	**2100**

4.3.2. Turning with CBN inserts

ANOVA results of the work surface roughness and tool wear rate during the turning of Ti-MMC by CBN insert are displayed in Table 4-10. It is to underline that variation of tool wear rate is highly effected by cutting speed and depth of cut. This is in agreement with the findings in literature (Zoya and Krishnamurthy 2000, Froes, Friedrich et al. 2004, Honghua, Peng et al. 2012). Cutting speed is the only mildly significant parameter on the work surface roughness.

A high R^2 is reported for the tool wear rates and surface roughness values (Table 4-10) and this confirms that the variation of surface roughness is mostly controlled by interaction effects between cutting parameters, which is not however desirable for process control, modeling and optimization

Table 4-10: ANOVA table of results recorded in turning by CBN inserts

Parameter	Tool wear rate		Surface roughness	
	F	P	F	P
(1) v_c	29.131	**0.033**	11.295	0.081
(2) f_r	8.044	0.110	2.484	0.287
(3) a_p	62.178	**0.015**	3.161	0.240
	R^2 =**0.99**		R^2 =**0.94**	

Table 4-11 displays the Surface roughness and tool wear rate values of turning with CBN inserts. Highest surface roughness is happened at highest material removal rate (MRR); although the mot tool wear is depicted in test 7. However, the lowest tool wear rate and work surface roughness are achieved at lowest.

Table 4-11: Surface roughness and tool wear rate values of turning with CBN inserts

TestNo.	MRR (mm^3/min)	Ra (µm)	$\dot{\widehat{VB}}$max$\times10^{-2}$ (µm/mm^3)
1	4495	1.03	1.05
2	6743	1.00	1.14
3	9005	1.56	1.93
4	5268	2.10	1.07
5	15811	1.75	3.10
6	21071	1.42	1.16
7	12005	4.78	3.72
8	17956	1.79	2.36
9	24185	5.16	1.61
∑	116539	20.60	17.10
Mean	12949	2.29	1.90

Figure 4-7 shows a lower cutting speed, a moderate feed rate, and a smaller depth of cut induce to the lower tool wear rate and work surface roughness.

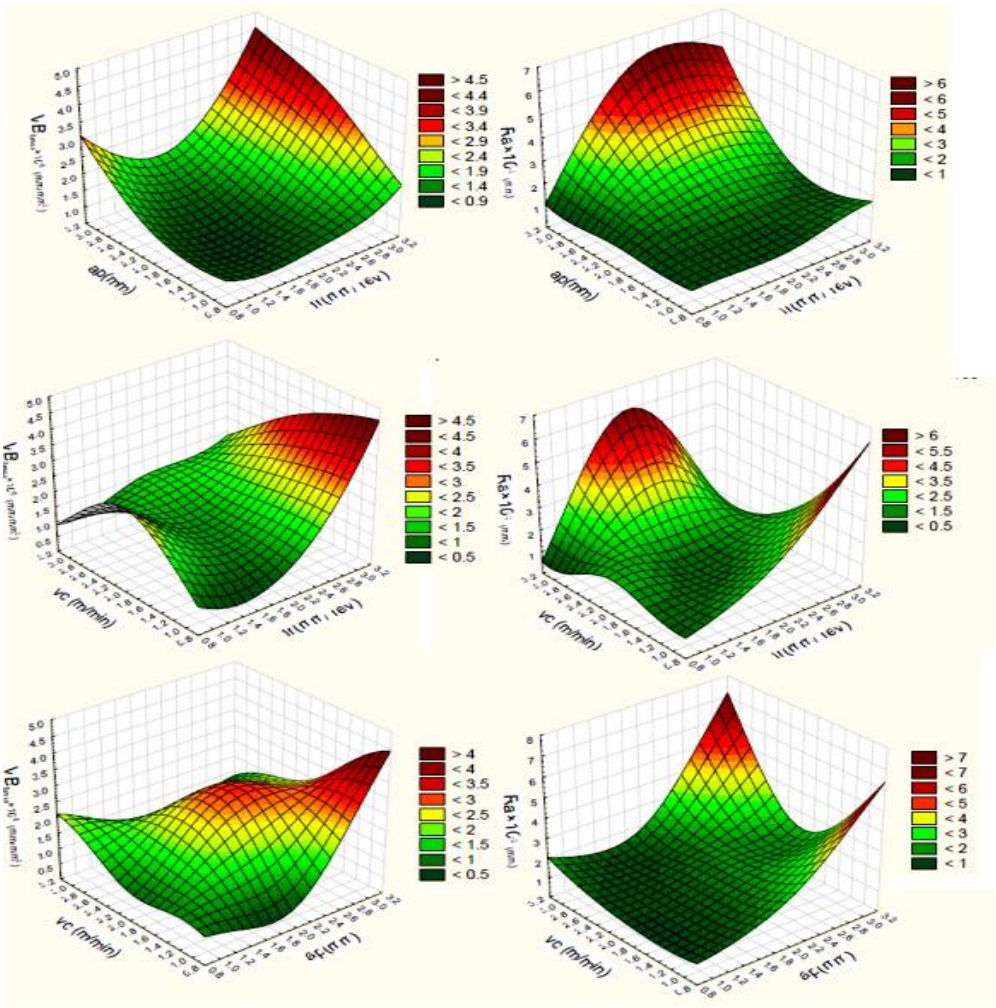

Figure 4-7: Work surface roughness & Tool wear rate vs. cutting conditions for CBN

Turning with CBN inserts led to more rough work-pieces that observed with carbide inserts (Table 4-12). The average value of tool wear rate and surface roughness when using CBN insert is approximately 150% more than that observed in carbide (Table 4-12); although, the productivity mean of the CBN with tested condition is 500% higher than carbide insert.

Table 4-12: Comparing mean of results and productivities

Cutting insert used	Ra (μm)	$\dot{\widehat{VB}}$**max**(μm/mm^3)	**MRR (mm^3/min)**
Carbide	1.42	0.013	2,100
CBN	2.29	0.019	12,002

As shown in Figure 4-8, the stronger signal to noise ratio (SNR) for work surface finish is observed in the first levels of cutting speed (150m/min) and depth of cut (0.1mm). Maximum degradation in work surface quality appeared when cutting speed and depth of cut were changed from 175m/min to 200m/min and 0.1 to 0.15mm, respectively. The middle level of feed rates (f_r =0.45mm/rev) seems to have the strongest SNR among the levels of feed rate used. Moreover, as Figure 4-8 the strongest SNR for tool life was achieved at v_c=150m/min, f_r=0.6m/rev and a_p=0.15mm. Regardless of the insert (CBN and carbide) used, the lowest level of cutting speed produced the strongest SNR. It exhibits that in the case of machining titanium alloys, the optimum selection of cutting speed is riskier than other cutting parameters.

According to Figure 4-9, when CBN insert was used, the optimum cutting conditions for the best surface finish and tool life were achieved at v_c=150m/min, f_r=0.45m/rev and a_p=0.15mm by 4.6% and1.6 %RSDs from the strongest signals to noise (Figure 4-9). The productivity under this condition was 5,945mm^3/min. Summary of the results is shown in Table 4-13.

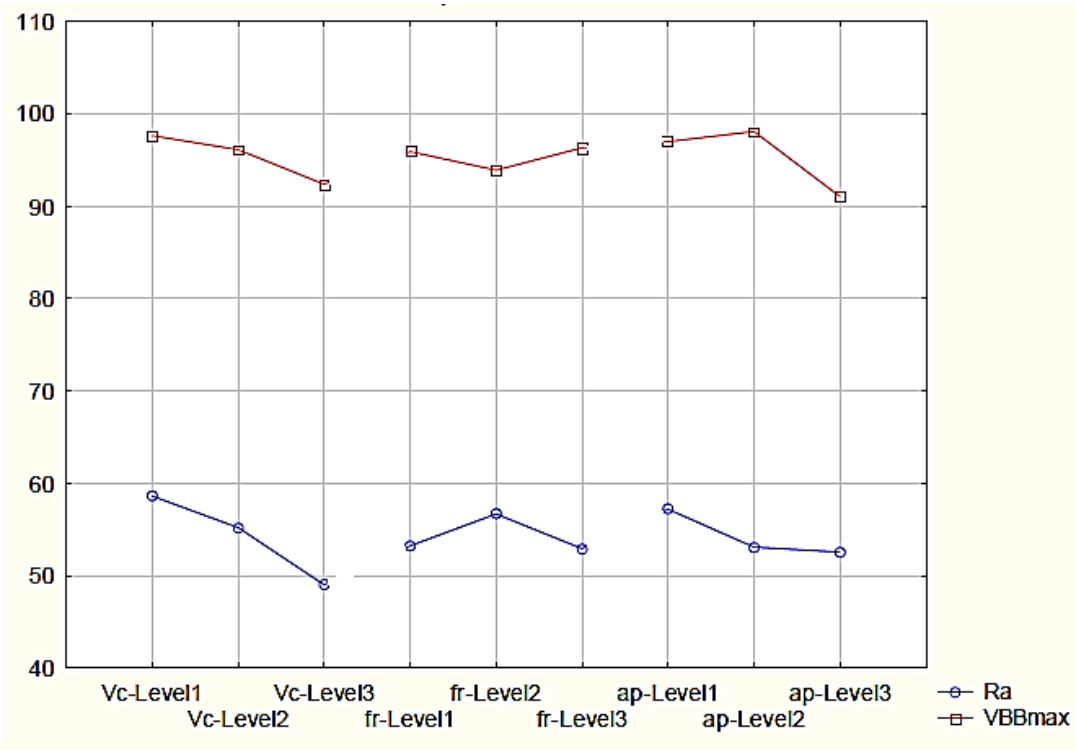

Figure 4-8: SNRs of tool wear rate and work surface roughness

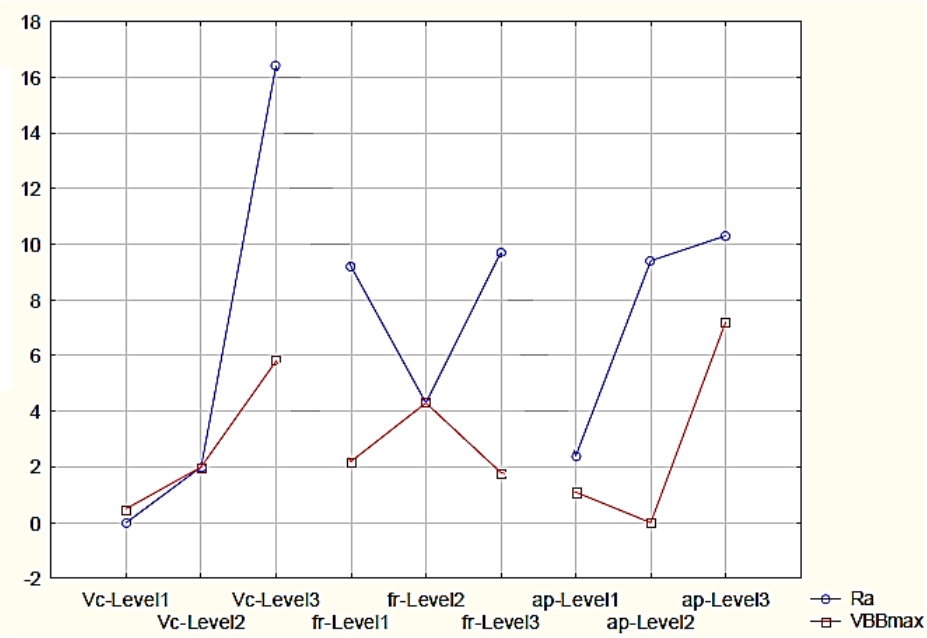

Figure 4-9: RSDs of tool wears and surface roughness signal to noise

Table 4-13: Final results of optimized cutting conditions for the turning CBN

	v_c(m/min)	f_r (mm/rev)	a_p (mm)	MRR (mm^3/min)
Optimum conditions for the work surface finish	150	0.45	0.1	4495
Optimum conditions for the tool life	150	0.60	0.15	6753
Total optimized conditions for the tool life and work surface finish	**150**	**0.45**	**0.15**	**6743**

4.3.3. Turning with PCD inserts

This section presents the results of turning tests with PCD inserts and clarifies the effects of high speed machining on tool insert performance. Those tests with elevated insert wear are highlighted (Table 4-14). Based on Table 4-14, except few tests that are set with lower levels of cutting parameters, other tests led to failure in the PCD inserts. As shown in Table 4-14, even under lubricated condition, high levels of cutting and depth of cut have catastrophic effects on PCD inserts. Those inserts with high wear rate are not generally permitted to be used in further tests in real industrial environment and they are considered as the failed inserts. This leads to massive

non-desirable expenses. Although extremely high wear rate was observed in the inserts; no significant problem occurred on the work surface during cutting.

Table 4-14: Turning tests with PCD inserts having elevated tool wear

Test No.	v_c(m/min)	f_r(mm/ rev)	a_p (mm)	MRR (mm^3/min)	$\dot{VB}$max$\times10^{-2}$ ($\mu m/mm^3$)
1	400	0.3	0.1	11,987	4.93
2	400	0.4	0.15	23,954	15.30
3	400	0.5	0.2	39,891	9.07
4	450	0.3	0.15	20,211	2.40
5	450	0.4	0.2	35,900	12.27
6	450	0.5	0.1	22,474	1.60
7	500	0.3	0.2	29,916	10.80
8	500	0.4	0.1	19,977	5.20
9	500	0.5	0.15	37,425	19.73

4.4. Analyzing the tools wear during the experiments

This section presents the tools performances. Various wear mechanisms are presented and discussed. According to following pictures, the adhesion seems to be the dominant wear mechanism on CBN and carbide inserts. Tooltip can be more protected against the abrasion due to smooth layer of adhered material. Further, despite of layers of adhered materials exist on the insert edge and the shapes of the CBN insert edges were not deformed. However, in the case of low adhesion (Figure 4-14 (Right)), abrasion caused scratching and eroding the flank surface. Figure 4-14 (Left) depicts a very smooth carbonized layer on the flank face which preserves the insert edge. The depicted images confirm the strangeness of cutting edges under all cutting conditions used. Adhesion was appeared on the carbide inserts (Figure 4-15 (right)) as well as diffusion between the tool and work material (Figure 4-10).

Contrary, chipping is the dominant failure mode appeared on the PCD insert. The high heat conductivity of PCD inserts may prevent the adhering process. Thus, due to close encountering between the work material and the insert surfaces as well as brittleness of the insert, it becomes vulnerable to chipping phenomenon. In Figure 4-11, the insert edge is chipped and delaminating

of the rake surface is occurred. As shown in Figure 4-12, no adhesion and diffusion are observed on the PCD inserts; and as described earlier, chipping is the main reason of insert failure.

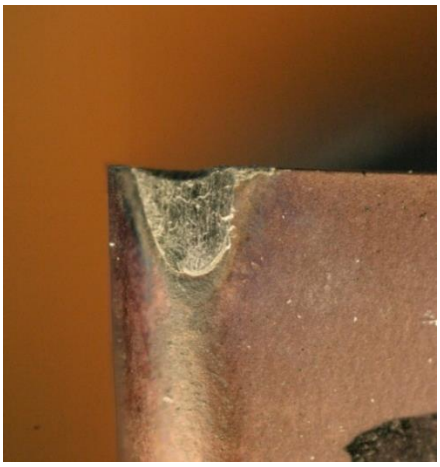

Figure 4-10: Carbide insert after turning Ti-MMC under following cutting conditions Cutting volume 9,000mm^3, v_c=80m/min; f_r= 0.25mm/rev; a_p= 0.2mm

Figure 4-11: Chipping on the PCD insert under following cutting conditions Cutting volume 7,500mm^3; v_c =500m/min, f_r= 0.4mm/rev;a_p= 0.1mm

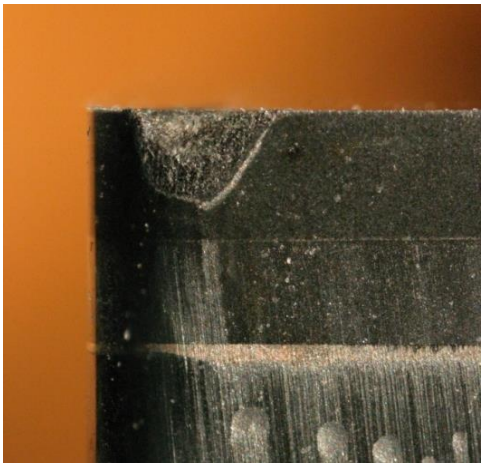

Figure 4-12: Flank wear of PCD inserts under following cutting conditions v_c =400m/min; f_r= 0.4mm/rev; a_p= 0.15mm

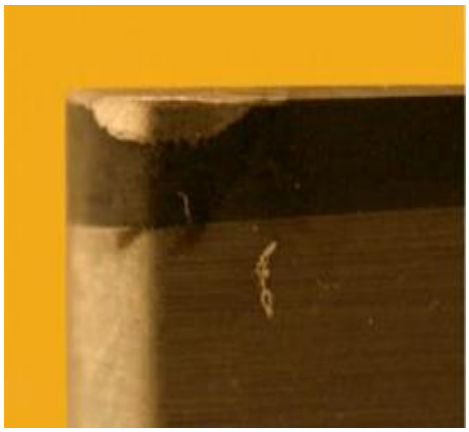

Figure 4-13: Flank wear of CBN insert under following cutting conditions Cutting volume 15,973mm^3v_c =150m/min; f_r= 0.3mm/rev; a_p= 0.1mm

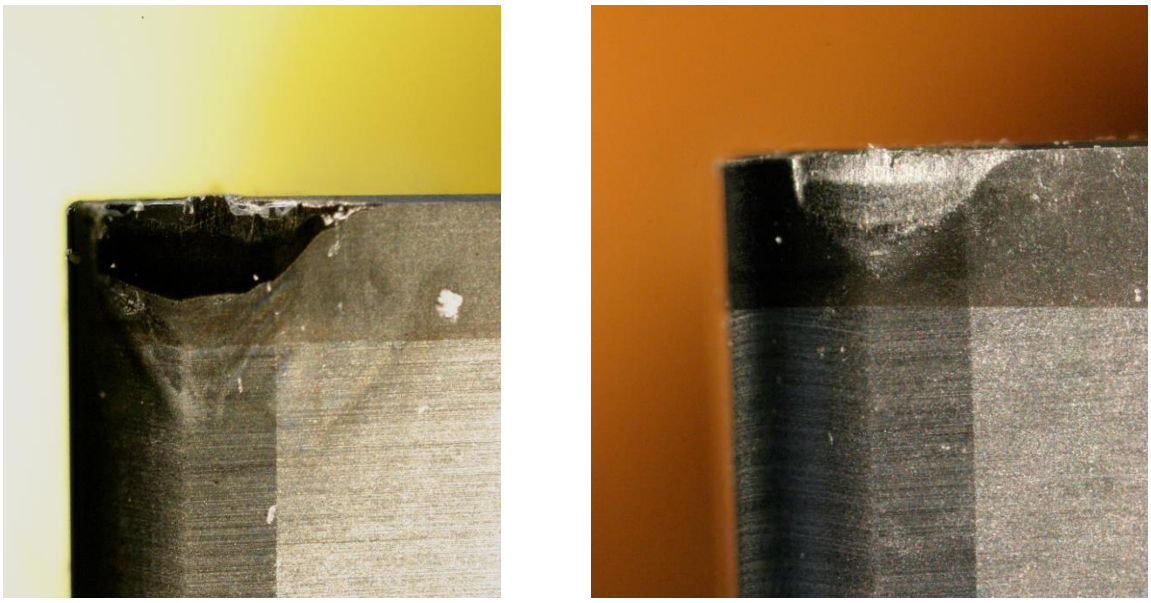

Figure 4-14: Flank wear of CBN insert under following condition;
(Left) v_c=200m/min; f_r= 0.45mm/rev; a_p= 0.1mm ; cutting volume 15,567mm^3
(Right) v_c =150m/min; f_r= 0.45mm/rev; a_p= 0.15mm; cutting volume 15,559mm^3

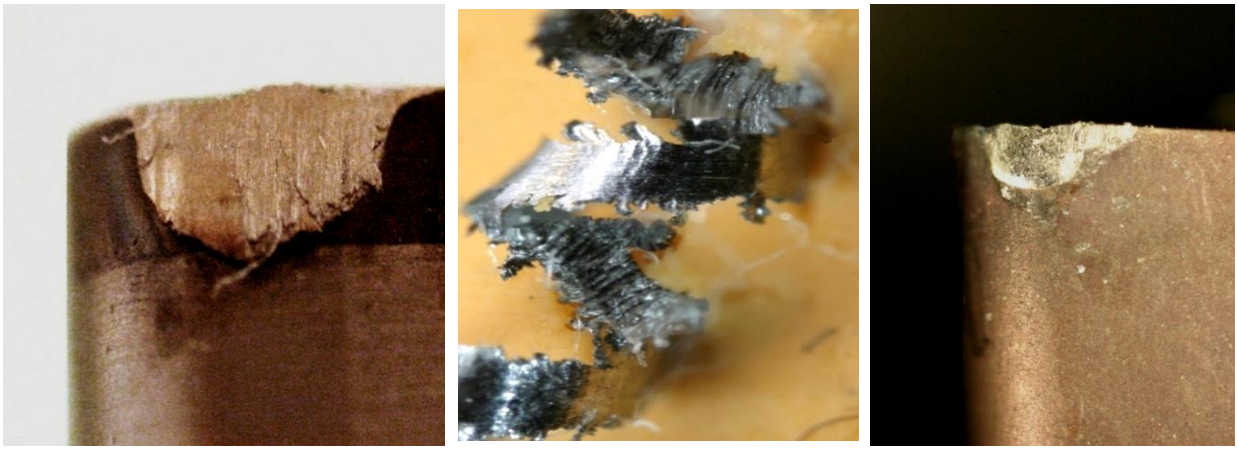

Figure 4-15: (Left) CBN insert and related chip; (Right) Carbide insert with adhered material

CHAPTER 5 MILLING EXPERIMENTS AND RESULTS

5.1. Experimental plan

As similar as turning tests, the cutting conditions used in milling tests were selected according to tools manufacturer's recommendations as well as previous research studies reported in the literature. All milling tests were conducted under lubricated condition.

5.2. Milling Experiments

Milling experiments were completed with carbide and PCD inserts. As noted in chapter 3, carbide inserts X-400 and X-500 and PCD insert PDC-CU-S (#BFPL280508) were used in face-milling tests. The trajectory of tool path as shown in Figure 5-1 was executed to decrease the tool impact on the work quality. The work-piece surface roughness and insert flank wear were measured after each test.

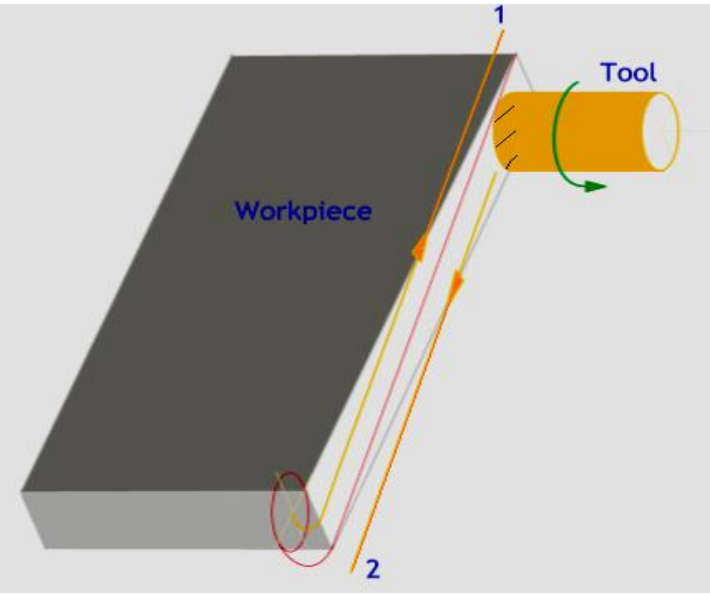

Figure 5-1: Trajectory of milling tool (Cutter) on the milling

5.2.1. Milling tests with the carbide inserts

5.2.1.1. Face milling tests with carbide insert X400

The cutting tests with the carbide insert X400 were arranged in array L_9 (3^3) as presented in Table 4-3. The cutting conditions used are presented in Table 5-1. The mean value of material removal rate in each test was 5,638 mm^3. Experimental works were conducted under lubricated condition (Figure 5-2). Because of the tool characteristic, after test-3 elevated tool vibrations were observed; so the experiment was stopped after test-5. Nevertheless, acceptable tool wear was observed in the done tests. The tool wear rate and surface roughness results are illustrated in the next section.

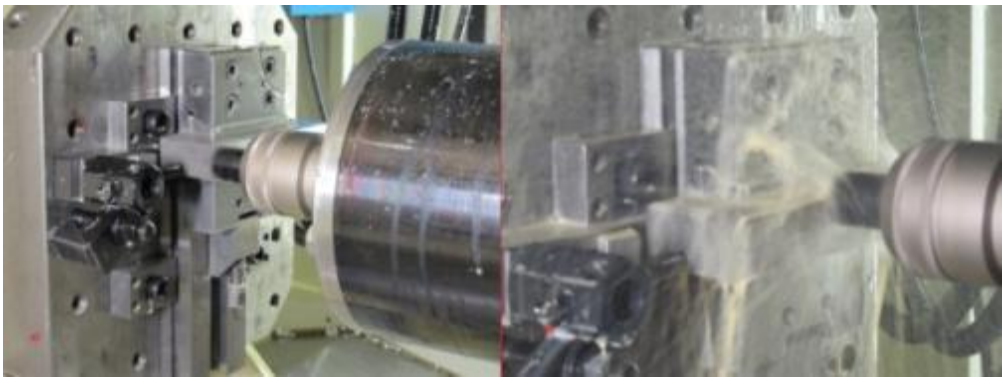

Figure 5-2: Lubricated face milling with carbide inserts

Table 5-1: The cutting conditions used in face milling with X400 inserts

Level No.	Experimental parameters		
	v_c (m/min)	f_r(mm/rev)	a_p (mm)
1	70	0.2	0.1
2	100	0.35	0.15
3	130	0.5	0.2

5.2.1.2. Face milling tests with carbide X500

The face milling tests with carbide insert X500 were arranged as orthogonal arrayL18 (21×37) (Table 5-2). Based on the recommendations received from the tool manufacturer, the cutting

conditions were selected (Table **5-3**). A cutting volume of 4,800 mm3 was followed for each cut and with respect to each cutting test performed; the productivity was measured (Table 5-6). No specific problem (i.e. tool breakage, chatter vibration) was observed in the cutting tests with carbide insert X500. The tool wear and surface roughness were measured for optimization purposes. The optimization results are presented in the next section.

Table 5-2: Milling experimental plan arranged in orthogonal array L_{18}

Test No.	v_c (m/min)	f_r(mm/rev)	a_p (mm)
1	1	1	1
2	1	2	1
3	1	3	1
4	2	1	1
5	2	2	1
6	2	3	1
7	3	1	1
8	3	2	1
9	3	3	1
10	1	1	2
11	1	2	2
12	1	3	2
13	2	1	2
14	2	2	2
15	2	3	2
16	3	1	2
17	3	2	2
18	3	3	2

Table 5-3: Cutting parameters in milling with X500 insert

Level No.	Experimental parameters		
	v_c(m/min)	f_r (mm/rev)	a_p (mm)
1	45	0,1	0.11
2	70	0.2	0.16
3	95	0.3	

5.2.2. Milling tests with PCD inserts

The last set of milling experiments were conducted using PCD inserts. As similar as other milling tests, the experimental plan was arranged as orthogonal array $L_9(3^4)$. Due to limited information available in the literature, the cutting parameters listed in Table 5-4 were selected based on industrial recommendations. Fortunately, no specific problem (i.e. tool breakage, chatter vibration) was observed in the cutting tests with PCD inserts. The tool wear and surface roughness were recorded for optimization studies that are presented in the next section.

Table 5-4: Cutting parameters and the responses in milling with PCD inserts

Level No.	Experimental parameters		
	v_c (m/min)	f_r(mm/ rev)	a_p(mm)
1	150	0.1	0.1
2	175	0.17	0.15
3	200	0.24	0.2

5.3. Results and discussion

5.3.1. Statistical analysis

To define the statistically significant parameters, the experimental results were initially analyzed using ANOVA. To that end, the statistical parameters including R^2, P value and F ratio were employed. The significant parameters are then presented in red colour in each individual table. Following that, the SNR values of surface roughness and wear rate with respect to each insert used were calculated for optimization purposes and the optimum conditions were defined. Those experiments with problems/stoppage were underlined and further descriptions in regard to these tests are presented.

5.3.2. Milling Ti-MMC with carbide (X-500) tools

Table 5-5 presents the ANOVA table of the surface roughness and tool wear rate. It reveals that feed rate is the only significant parameter on the surface roughness, which could be related to chip load which directly effects on quality of the work-piece surface. Contrary, cutting speed and

depth of cut have the most significant influence on the tool wear rate, while feed rate is considered as a non-significant parameter.

Table 5-5: ANOVA of the surface roughness and tool wear rate with carbide (X-500) inserts during milling

Parameter	Tool wear rate		Surface roughness	
	F	P	F	P
(1) v_c	17.80	**0.0002**	0.62	0.5507
(2) f_r	2.28	0.1447	6.15	**0.0145**
(3) a_p	5.56	**0.0361**	0.03	0.8599
	R^2 =0.79		**R^2 =0.531**	

Periodic changes of the colour in the surface roughness (Table 5-6) exhibits the dominant effect of feed rate on the variation of the surface roughness values. Moreover, high wear rates are exhibited between test-4 and test-9.

Table 5-6: Surface roughness and tool wear rate values of carbide X-500 inserts during milling

Test No.	MRR (mm^3/min)	Ra (µm)	$\dot{VB}$max ×10^2 (µm/mm^3)
1	118	0.75	1.20
2	236	1.66	1.32
3	355	1.65	1.24
4	184	0.87	1.99
5	368	2.20	2.10
6	552	1.68	1.99
7	250	1.15	1.68
8	499	1.37	1.79
9	749	2.61	1.96
10	172	0.69	1.29
11	344	1.74	0.84
12	516	1.36	1.15
13	268	1.15	1.24
14	535	1.85	1.53
15	803	2.39	2.05
16	363	0.90	1.62
17	726	0.24	1.52
18	1089	3.17	1.99
∑	8127	27.43	28.49
Mean	452	1.52	1.58

Figure 5-3 reveals a lower cutting speed and feed rate depict lower tool wearing and work surface roughness. The work surface roughness is not sensitive to variation of depth of cuts in this experiment. The tool wear rates variation shows low sensitivity to this feed rates range in Figure 5-3. Furthermore, the significant effects of cutting speed on the tool wear rate and work surface roughness can be clearly distinguished.

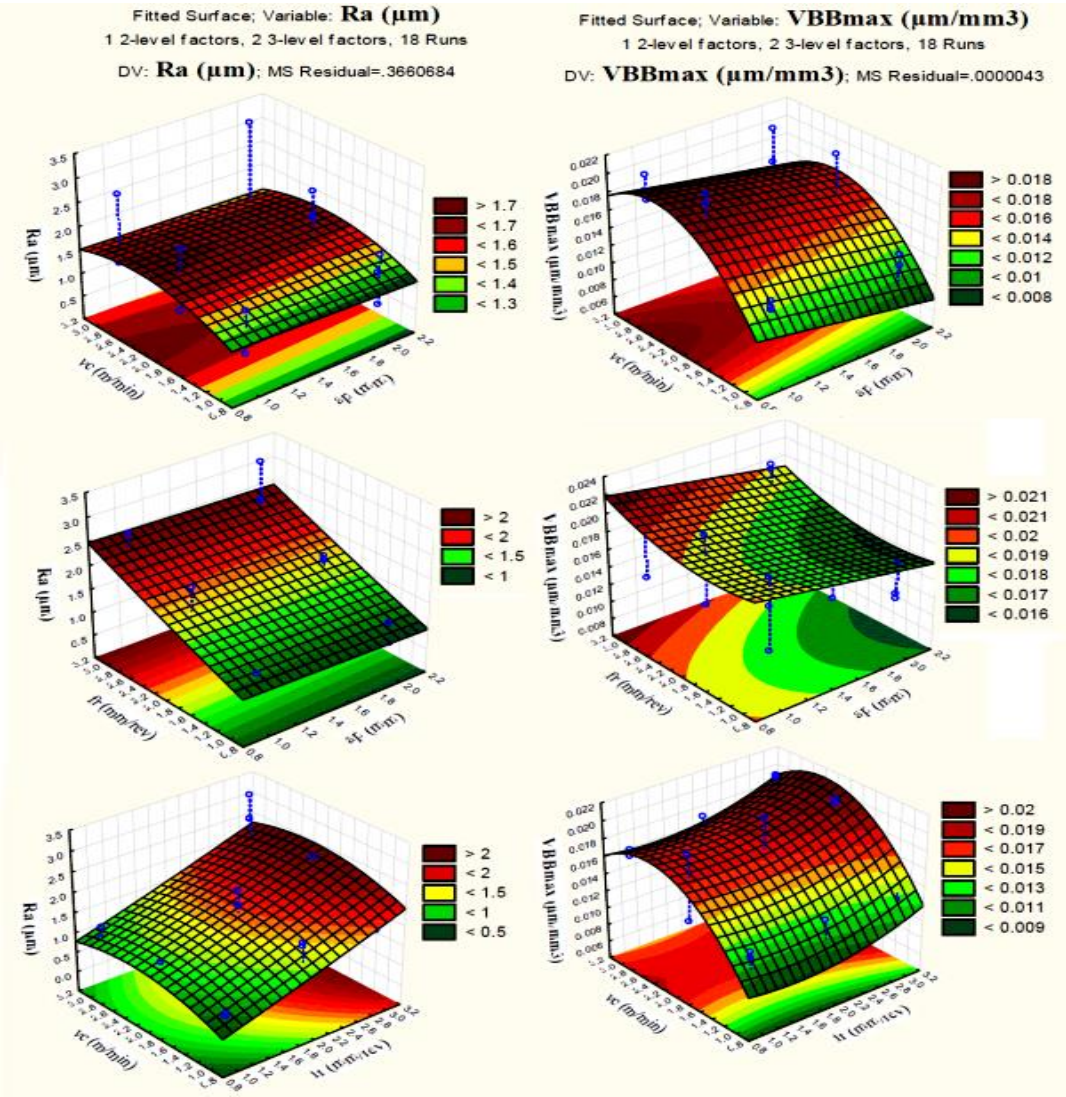

Figure 5-3: Work surface roughness & Tool wear rate vs. cutting conditions for carbide X-500 inserts

As shown in Figure 5-4, the strongest signals for surface finishes are depicted from first level of cutting speed, first level of feed rate and first level of depth of cut. Milling test with lower level of depth of cut at higher level of cutting speed led to deteriorated insert. Changing the feed rates from middle to high level affects highly the work surface roughness and effectively more noise parameters are generated. The strongest signal for tool life was achieved from first level of cutting speed, second level of feed rate and also second level of depth of cut. It could be due to intervention of the vibration noise that in fact increases the surface roughness at higher levels of cutting speed. But same as turning experiment, a moderate feed rate can decrease the effect of the thermal load and also vibration together on the tool.

The optimum cutting conditions with lowest surface roughness and tool wear rate is achieved at v_c= 45 m/min, f_r= 0.2 mm/rev and a_p= 0.16 mm with RSD equal to 6.0% and 3.2% respectively from the strongest SNR. The optimum productivity in his condition is 344mm^3/min (Figure **5-5**). The summary of results is come in Table **5-7**.

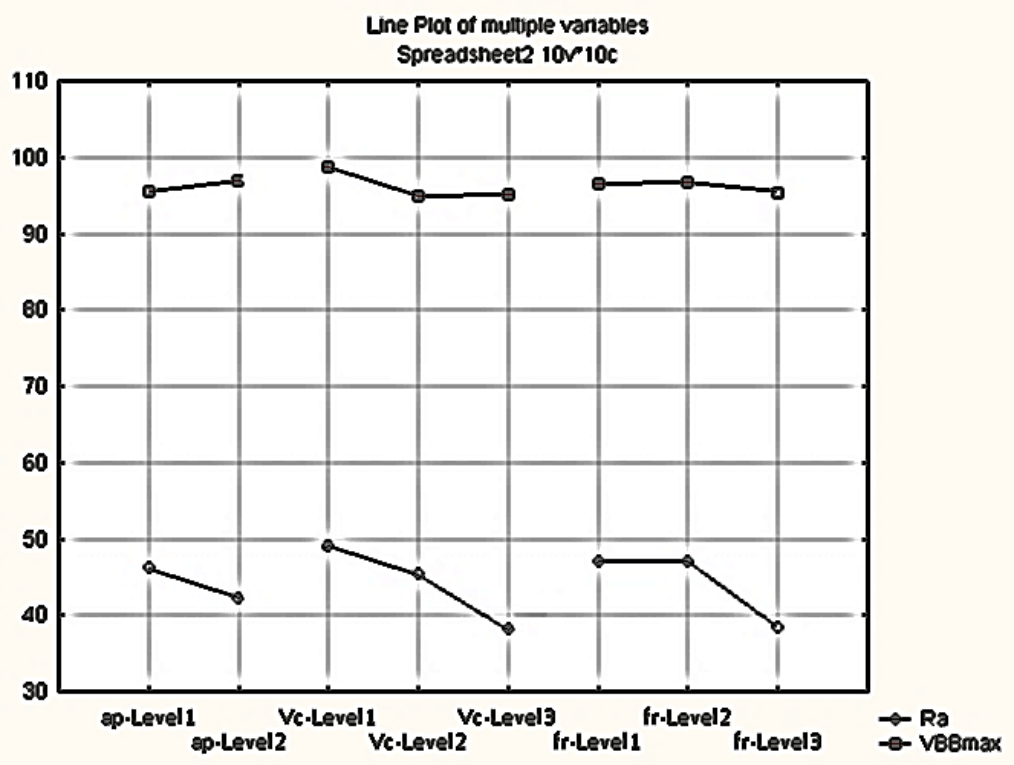

Figure 5-4: SNRs of tool wear rate and work surface roughness for X-500

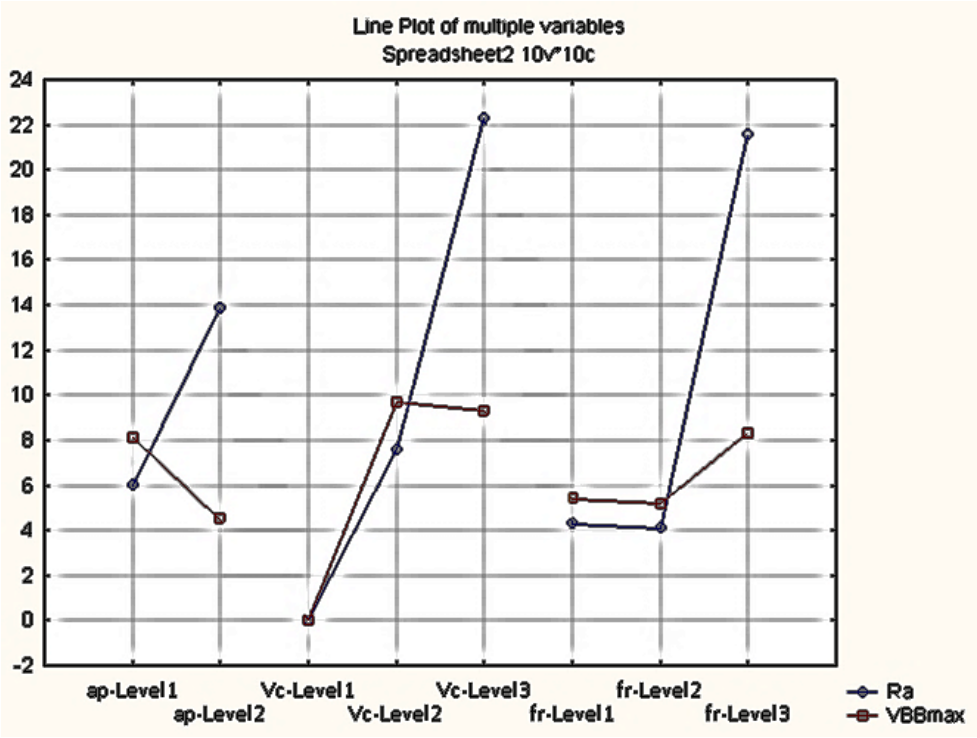

Figure 5-5: RSDs of tool wears and surface roughness signal to noise for X-500 inserts

Table 5-7: Final results of optimized cutting conditions for the milling by X-500 inserts

	v_c(m/min)	f_r (mm/rev)	a_p (mm)	MRR (mm^3/min)
Optimum conditions for the work surface finish	45	0.2	0.1	172
Optimum conditions for the tool life	45	0.2	0.16	344
Total optimized conditions for the tool life and work surface finish	**45**	**0.2**	**0.16**	**344**

5.3.3. Milling Ti-MMC with PCD inserts

The ANOVA table of surface roughness and tool wear rate when using PCD inserts is shown in Table 5-8. The total observation results are illustrated in Table 5-9 and Figure 5-6. The Taguchi based optimization results are also presented in Figure **5-7** and Figure 5-8. As shown in Table 5-8, despite of high value of R^2, none of cutting parameters are statistically significant parameters on the variation of surface roughness. It denotes that the variation of surface roughness in milling with PCD inserts are highly controlled with interaction effects between

cutting parameters. This is however a non-desirable phenomenon in process control and optimization studies. Similar observations were made on the turning tests with CBN inserts. Table 5-8 exhibits that the cutting speed has the highest effect on the tool wear which followed by depth of cut. Moreover, the high value of R^2 indicates that unlike surface roughness, tool wear rate is highly controlled by variation of process parameters, mainly cutting speed.

Table 5-8: ANOVA of the tool wear and the surface roughness of the work-pieces machined with PCD inserts

Parameter	Tool wear rate		Surface roughness	
	F	P	F	P
(1) v_c	94.428	**0.0104**	5.7552	0.1480
(2) f_r	13.857	0.0673	3.2327	0.2362
(3) a_p	25.000	**0.0384**	1.9165	0.3428
	R^2 =0.99255		**R^2 =**0.916	

Based on Table 5-9**,** the smooth variation of the input parameters is observable in the column of the surface roughness. Slight variation is only visible for the cutting speed.

Figure 5-6 shows a lower cutting speed and depth of cut have direct relation with lower tool wearing and lower depth of cut decreases the work surface roughness. The work surface roughness is low sensitive to variation of cutting speeds by these conditions. The tool wear rates variation shows low sensitivity to this feed rates range in Figure 5-6 reveals the significant effects of depth of cut on the tool wear rate. The results totally had low sensitivity to feed rates variation.

Table 5-9: Results of the surface roughness and wear rate for PCD inserts during milling

Test No	MRR (mm^3/min)	Ra(μm)	$\dot{VB}$max ×10^2 (μm/mm^3)
1	443	0.19	3.99
2	1131	0.17	4.75
3	2128	0.23	11.31
4	894	0.25	1.94
5	2035	0.25	4.74
6	1427	0.24	3.94
7	1648	0.34	16.22
8	1910	0.30	9.34
9	1800	0.32	15.1
∑	13416	2.29	7.133
Mean	1491	0.25	0.793

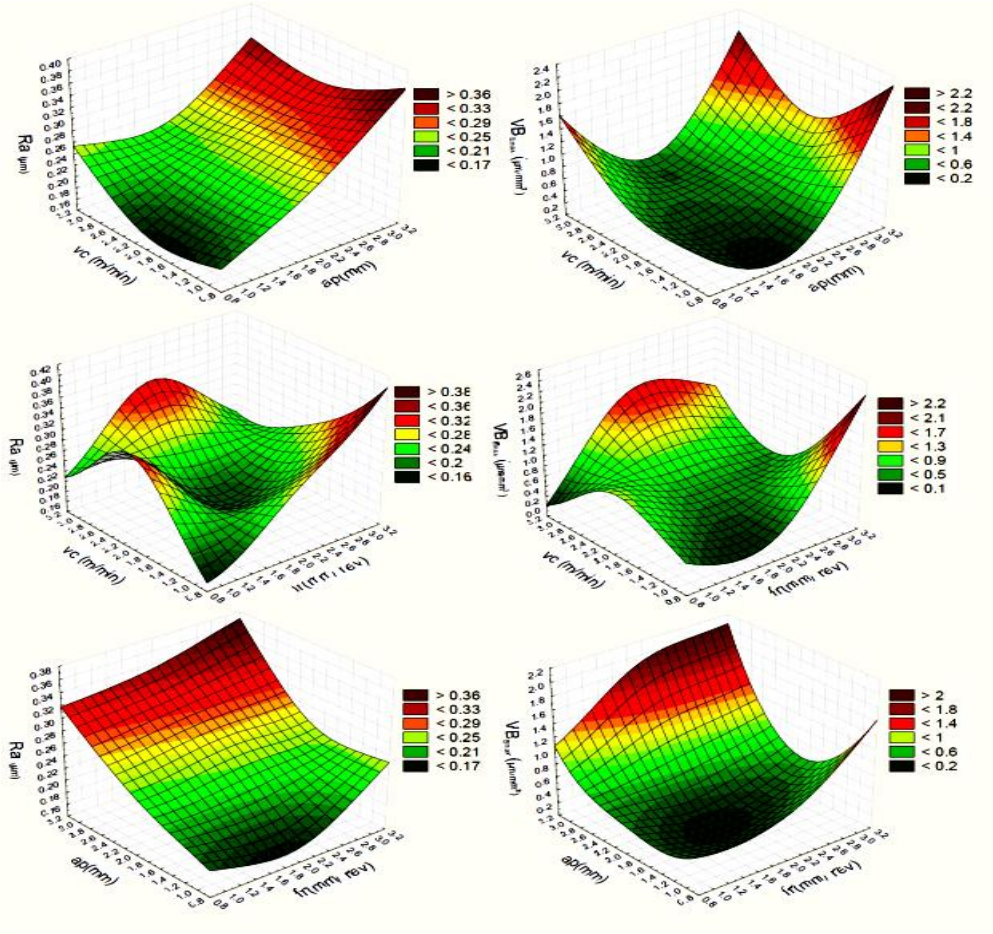

Figure 5-6: Work surface roughness & Tool wear rate vs. cutting conditions for PCD inserts

Based on Figure **5-7** the strongest signal through surface roughness noises passes by vc= 175m/min, fr=0.1mm/rev, and ac= 0.1mm. However, the lowest level of cutting speed (150m/min) emit strongest signal through the tool wearing noises. The similar signals to tool wear rate is achieved at feed rates 0.17 mm/rev at v_c=150m/min for lowest tool wearing.

Figure 5-8 shows that in this experiment the optimum cutting condition was obtained at v_c=150m/min, f_r=0.17mm/rev, and a_c= 0.1mm with 7.1% and 7.8% RSDs from the strongest levels respectively for surface finish and tool life. The productivity of this condition is 754mm^3/min. The summary of the results is presented in Table **5-10**.

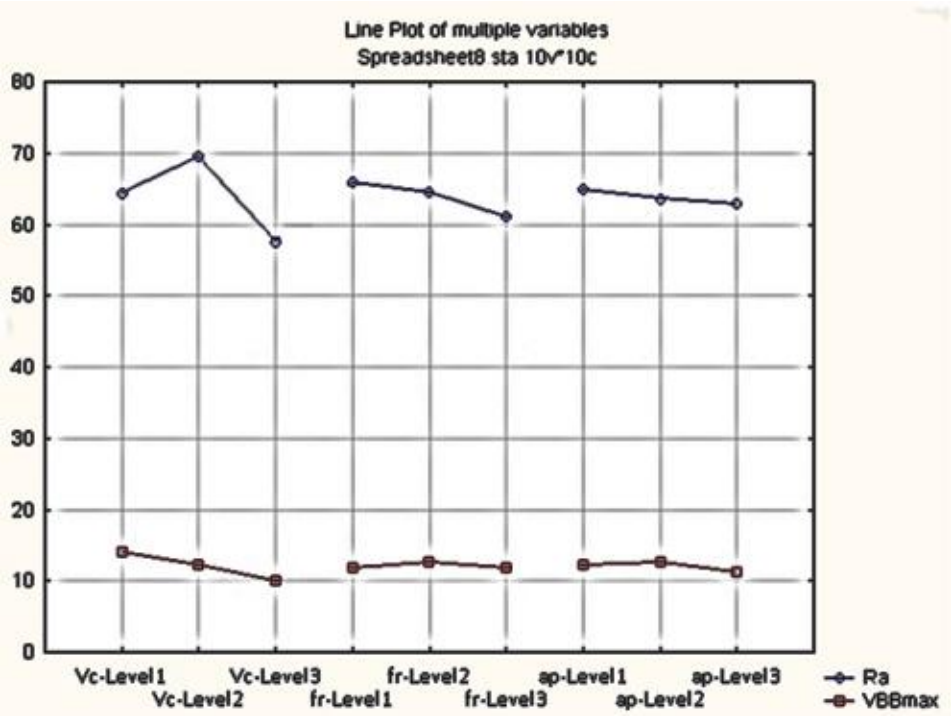

Figure 5-7: SNRs of tool wear rate and work surface roughness for PCD

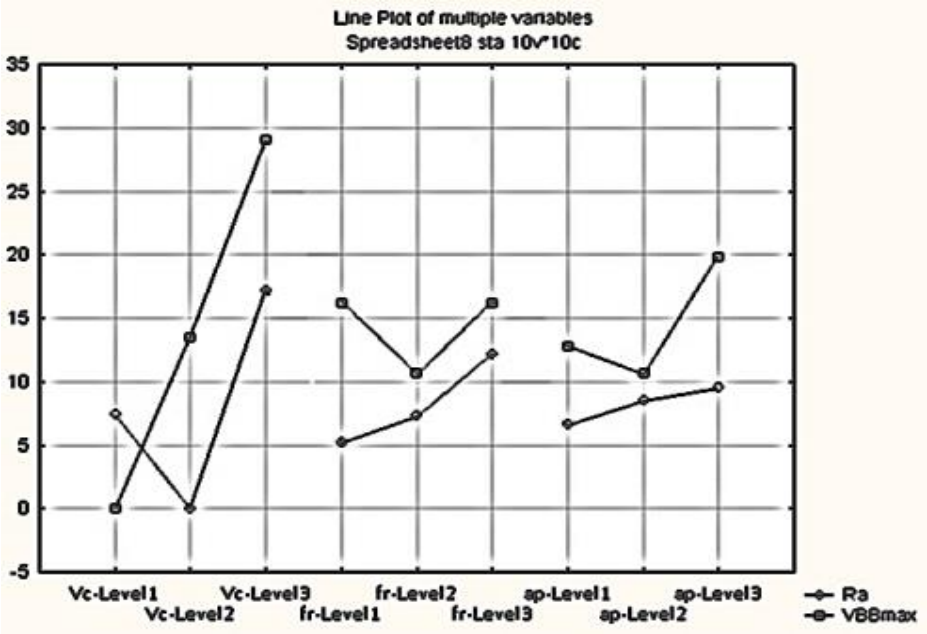

Figure 5-8: RSDs of tool wears and surface roughness signal to noise for PCD

Table 5-10: Final results of optimized cutting conditions for the milling by PCD inserts

	v_c (m/min)	f_r (mm/rev)	a_p (mm)	MRR (mm^3/min)
Optimum conditions for the work surface finish	175	0.1	0.1	443
Optimum conditions for the tool life	150	0.17	0.15	1131
Total optimized conditions for the tool life and work surface finish	**150**	**0.17**	**0.1**	**754**

5.3.4. Tools wear and failure analysis

This section present those milling tests that led to complete stoppage, tool/insert breakage or catastrophic insert wear.

Tools failure and damage

The milling cutter used with insert X400 was a plunging approach angle cutter that induces to a sensible vibration face milling tests. Table 5-11 reveals that promising tool wear rate were recorded under low levels of cutting speed and high levels of cutting feed. Moreover, at a certain level of cutting speed and feed rate, the best conditions were obtained with acceptable productivity and cutting volume. As shown in Table 5-11, despite of the chatter vibration occurred in the tests, high wear rate was only observed in two tests. The overview of tool wear profile is shown in next section.

Table 5-11: The wear on the carbide insert X400when used in milling

Test No.	Experimental parameters				Responses		
	v_c (m/min)	f_r (mm/rev)	a_p (mm)	n (rev/min)	tc (Sec.)	MRR (mm^3/min)	$\dot{\widehat{VB}}$max× 10^2 (µm/mm^3)
1	70	0.2	0.1	697	264.3	627	4.0
2	70	0.35	0.15	697	105.7	1646	3.4
3	70	0.5	0.2	697	52.9	3135	5.7
4	100	0.2	0.15	995	129.5	1343	3.6
5	100	0.35	0.2	995	52.9	3135	5.3
6	100	0.5	0.1	995	74	2239	**Stopped**
7	130	0.2	0.2	1294	71.2	2329	
8	130	0.35	0.1	1294	81.3	2038	
9	130	0.5	0.15	1294	39.9	4367	

Table 5-12 presents the cutting parameters used as well as experimental responses for PCD milling inserts. There is no systematic database about allowable levels of cutting parameters, for milling Ti-MMC with PCD inserts. As depicted in Table 5-12, milling tests with PCD inserts at high levels of cutting speed (350-600 m/min) led to insert failure. Therefore, lower levels of cutting speed were then used in the rest of the cutting tests.

Table 5-12 reveals that at very low level of depth of cut and high level of cutting feed, acceptable tool wear rate can be observed. Moreover, at a certain level of cutting speed under uniform level of depth of cut 0.05 mm, the optimum values of cutting volume and productivity were achieved.

Table 5-12: The results of milling tests with PCD inserts

	Experimental parameters				Responses		
Test No.	**v_c (m/min)**	**f_r (mm/ rev)**	**a_p (mm)**	**n (rpm)**	**t_c (Sec)**	**MRR (mm^3/min)**	**$\dot{\widehat{VB}}max\times10^2$ (µm/mm^3)**
1	600	0.1	0.1	6018	9.2	3815	-
2	450	0.3	0.1	4514	8.2	4280	-
3	350	0.2	0.1	3511	10.5	3343	-
4	350	0.3	0.07	3511	209.7	2305	-
5	300	0.5	0.07	3009	146.9	3291	3.4
6	250	0.6	0.07	2508	146.9	3291	2.7
7	250	0.9	0.07	2508	4.9	4935	-
8	250	0.7	0.05	2508	220.1	2745	**1.2**
9	250	0.85	0.05	2508	145.1	3332	**1.9**

Tools wear

Adhesion is the dominant wear mechanism appears on the edge of the carbide inserts (Figure 5-9, Figure 5-10). In Figure 5-9 (a), the oxidation on the edge of carbide X500 is clearly visible. It indicates a high temperature-cutting zone that causes oxidation and diffusion of the work material to the tool edge. Despite of chatter vibration observed in the tests with carbide insert X400, the insert cutting edge depicted acceptable performance and stability (Figure 5-10).

As similar as turning, the edge chipping seems to be the main reason of degradation the PCD inserts in the milling of T-MMC (Figure 5-11, Figure 5-12). High heat conductivity of PCD decreases the temperature in the cutting process. As presented in the Figure 5-11, not only, edge chipping is observed in the cutting zone; but also it appears to happen in areas out of cutting zone. Figure 5-12 displays a large cavity on the rake face by the edge chipping and there is no effect of adhesion.

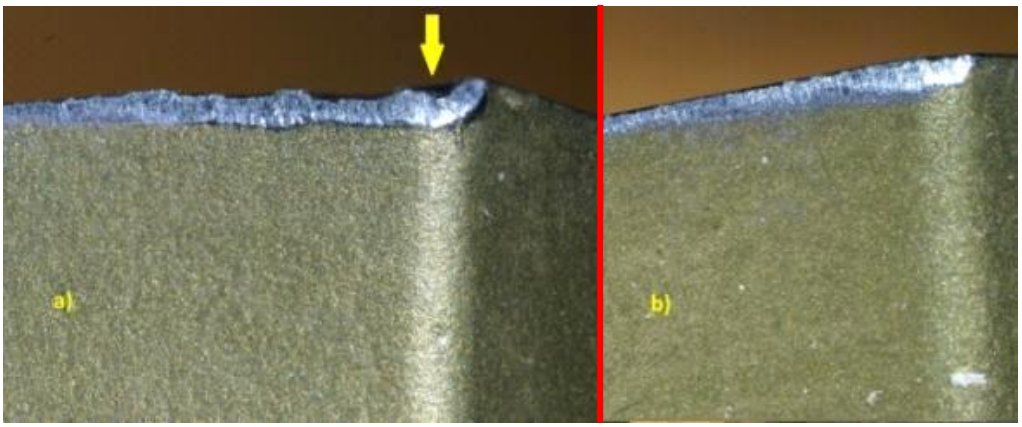

Figure 5-9: Milling Ti-MMC with carbide insert X500under following conditions
(a) cutting volume= 4,680mm^3; v_c= 95m/min; f_r=0.1mm/rev; a_p=0.16mm
(b) cutting volume= 4,860mm^3; v_c= 45m/min; f_r=0.1 mm/rev; a_p=0.16mm

Figure 5-10: Milling with carbide insert X400 under following cutting conditions;
(a) Cutting volume5,525mm^3;v_c=100m/min; f_r=0.35mm/rev; a_p=0.2mm
(b)Cutting volume5,525mm^3;v_c=75m/min; f_r=0.35mm/rev; a_p=0.15mm

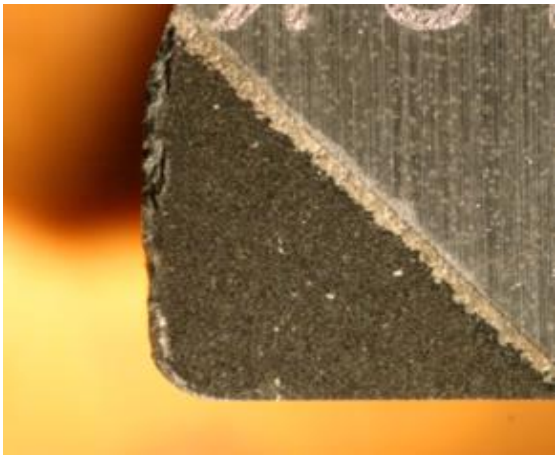

Figure 5-11: Edge chipping of the PCD at v_c= 200m/min, f_r=0.17mm/rev and a_p= 0.1mm

Figure 5-12: Wear in the PCD tool at v_c=450m/min, f_r=0.3 mm/rev and a_p= 0.1mm

CHAPTER 6 CONCLUSION AND RECOMMENDATIONS

Experimental works were conducted on (1) Turning and (2) Milling of Ti-MMCs using three prevalent inserts (coated carbide, PCD and CBN). Cutting conditions were selected according to recommendations made by the tools suppliers, research studies reported in the literature and industry recommendation.

Based on experimental results, high abrasive and strong mechanical properties of Ti-MMC degrade all inserts within the first few seconds of cutting operations. This reveals that the cutting tools and inserts require adequate hardness and toughness to resist the reinforced particles. Likewise, the inserts need enough toughness to tolerate the force fluctuation, spring back and impacts due to the matrix toughness, elasticity and heterogeneity.

To increase the tool life when machining Ti-MMCs, the highest possible level of feed rate should be chosen according to the tool strengths and resistances.

Flank wear is the main wear component in cutting Ti-MMC. Cutting speed is the dominant cutting parameter to improve the flank wear; unlikely, increasing feed rate diminishes the flank wear rate.

During discontinuous cuts with high levels of depth of cut, Ti-MMC performs as a high toughness material; while at steady state processes under low level of depth of cut, Ti-MMC depicts the abrasive properties, but still better performance is observed. This reveals that the use of high levels of depth of cut is not recommended for machining Ti-MMC.

As mentioned for carbide insert, cutting speed and feed rate are the governing cutting parameters on the tool wear rate during turning and milling Ti-MMCs. Similar parameters were the governing parameters on the surface roughness in both milling and turning processes; the dominant parameter was the feed rate. Depth of cut is the main parameter governing tool wear rate during turning Ti-MMC with PCD inserts. The next effective cutting parameter is cutting speed. However, in milling with PCD inserts, cutting speed and depth of cut are the most effective parameters on the tool wear rate.

In the course of adequate selection of optimum or near to optimum cutting parameters in machining Ti-MMCs, the appropriate levels of cutting parameters should be chosen when machining Ti-MMC. The following observations are noted:

- Despite the insert used, moderate to high levels of cutting feed should be chosen. Moreover, to confirm the observations made in the previous studies, the depth of cut must not exceed 0.16 mm.
- The optimum values of responses in cutting with CBN and carbide inserts were achieved at lowest levels of cutting speed (150 and 40 m/min). Moderate levels of feed rate (0.45 and 0.25mm/rev). Depth of cut 0.15 mm appeared to be ideal for the both inserts
- Optimum cutting conditions in milling by carbide and PCD inserts have been achieved by the minimum cutting speed. Center levels of depth of the cut for carbide and lowest level of depth of cut for the PCD insert are the proposed cutting conditions. Center levels of cutting feeds for both inserts are seemed to be optimum parameters in cutting Ti-MMC.
- During milling operations with PCD inserts, some considerable results were achieved with low wear rates at high levels of cutting speeds and feed rates at uniform depth of cut 0.05 mm. This phenomenon needs to be further studied in wider scopes.
- CBN inserts revealed good performance in machining Ti-MMC. Due to high strength of CBN insert, relatively uniform surface roughness was observed in all cutting conditions used. This exhibits that the effects of cutting parameters, particularly depth of cut and cutting speed on CBN insert are not clearly defined yet. Therefore, further studies in this regard are still demanded.
- Experimental studies confirmed that insert grade X400 is a high toughness and strong grade. The use of this grade with a modified approach angle in face milling of Ti-MMC is strongly recommended.

BIBLIOGRAPHY

AB, A. "Ti6Al4V Titanium Alloy." ArcamAB(KrokslättsFabriker).

Abkowitz, S., S. M. Abkowitz, H. Fisher and P. J. Schwartz (2004). "CermeTi® discontinuously reinforced Ti-matrix composites: Manufacturing, properties, and applications." Jom56(5): 37-41.

Antonialli, A. I. S., A. E. Diniz and R. Pederiva (2010). "Vibration analysis of cutting force in titanium alloy milling." International Journal of Machine Tools and Manufacture50(1): 65-74.

Armarego, E. and R. H. Brown (1969)."The machining of metals." PRENTICE-HALL INC, ENGLEWOOD CLIFFS, N. J., 1969, 437 P.

Bagci, E. and Ş. Aykut (2006). "A study of Taguchi optimization method for identifying optimum surface roughness in CNC face milling of cobalt-based alloy (stellite 6)." The International Journal of Advanced Manufacturing Technology29(9): 940-947.

Bejjani, R., M. Balazinski, B. Shi, H. Attia and H. Kishawy (2011).Machinability and Chip Formation of Titanium Metal Matrix Composites, IJAMS- International Journal Advanced Manufacturing systems.

Box, G. E. (1953)."Non-normality and tests on variances."Biometrika: 318-335.

Çakīr, O., A. Yardimeden, T. Ozben and E. Kilickap (2007)."Selection of cutting fluids in machining processes." Journal of Achievements in materials and Manufacturing engineering25(2): 99-102.

Chou, Y. K. and C. J. Evans (1999). "Cubic boron nitride tool wear in interrupted hard cutting." Wear225: 234-245.

Ciftci, I. (2009). "Cutting tool wear mechanism when machining particulate reinforced MMCs." Technology12(4): 275-282.

Corduan, N., T. Himbart, G. Poulachon, M. Dessoly, M. Lambertin, J. Vigneau and B. Payoux (2003). "Wear mechanisms of new tool materials for Ti-6AI-4V high performance machining." CIRP Annals-Manufacturing Technology52(1): 73-76.

Das, S., R. Behera, G. Majumdar, B. Oraon and G. Sutradhar (2011). "An experimental investigation on the machinability of powder formed silicon carbide particle reinforced

aluminium metal matrix composites." International Journal of Scientific & Engineering Research2(7): 1.

Davim, J. P. (2002). "Diamond tool performance in machining metal–matrix composites." Journal of materials processing technology128(1): 100-105.

Davim, J. P. (2012). Tribology in Manufacturing Technology, Springer.

Daymi, A., M. Boujelbene, S. B. Salem, B. H. Sassi and S. Torbaty (2009)."Effect of the cutting speed on the chip morphology and the cutting forces." Archives of Computational Materials Science and Surface Engineering1(2): 77-83.

Derringer, G. (1980)."Simultaneous optimization of several response variables." J. Quality Technol.12(4): 214-219.

Dhavamani, C. and T. Alwarsamy (2011). "Review on optimization of machining operation." Int J Acad Res3: 476-485.

Ding, X., W. Liew and X. Liu (2005). "Evaluation of machining performance of MMC with PCBN and PCD tools."Wear259(7): 1225-1234.

Diniz, A. and J. Ferreira (2003). "Influence of refrigeration/lubrication condition on SAE 52100 hardened steel turning at several cutting speeds." International Journal of Machine Tools and Manufacture43(3): 317-326.

Du, Q., X. Chen and K. Zhang (2006). Study on high speed cutting machinability of medical titanium alloy Ti-6Al-4V. Technology and Innovation Conference, 2006.ITIC 2006. International, IET.

Dudzinski, D., A. Devillez, A. Moufki, D. Larrouquere, V. Zerrouki and J. Vigneau (2004)."A review of developments towards dry and high speed machining of Inconel 718 alloy." International Journal of Machine Tools and Manufacture44(4): 439-456.

El Baradie, M. (1996)."Cutting fluids: Part I. characterisation." Journal of materials processing technology56(1): 786-797.

El Baradie, M. (1996). "Cutting fluids: Part II. Recycling and clean machining." Journal of materials processing technology56(1): 798-806.

Esslinger, J. (1960). "Titanium in Aero Engines."MTU Aero Engines, Munich, Germany.

Ezugwu, E. O., J. Bonney, R. B. da Silva and A. Machado (2004). "Evaluation of the performance of different nano-ceramic tool grades when machining nickel-base, inconel 718, alloy." Journal of the brazilian Society of Mechanical Sciences and Engineering26(1): 12-16.

Festeau, G., X. D. Fang and D. J. Wills (2007). PVD coated ruthenium featured cutting tools, Google Patents.

Froes, F., H. Friedrich, J. Kiese and D. Bergoint (2004). "Titanium in the family automobile: the cost challenge." Jom56(2): 40-44.

Gaitonde, V., S. Karnik and J. P. Davim (2008). "Some studies in metal matrix composites machining using response surface methodology." Journal of reinforced plastics and composites.

Ganguly, P., W. Poole and D. Lloyd (2001). "Deformation and fracture characteristics of AA6061-Al 2 O 3 particle reinforced metal matrix composites at elevated temperatures." Scriptamaterialia44(7): 1099-1105.

Harrington, E. (1965). "The desirability function." Industrial quality control21(10): 494-498.

Hartung, P. D., B. Kramer and B. Von Turkovich (1982). "Tool wear in titanium machining." CIRP Annals-Manufacturing Technology31(1): 75-80.

Heath, P. J. (1986). "Properties and uses of amborite[polycrystalline cBN]." Industrial diamond review46(514): 120-127.

Heizer, J. and B. Render (1991). Production and operations management: strategies and tactics, Allyn& Bacon.

Honghua, S., L. Peng, F. Yucan and X. Jiuhua (2012). "Tool life and surface integrity in high-speed milling of titanium alloy TA15 with PCD/PCBN tools." Chinese Journal of Aeronautics25(5): 784-790.

Hosseini, A. and H. A. Kishawy (2014).Cutting Tool Materials and Tool Wear.Machining of Titanium Alloys, Springer: 31-56.

Hou, T. H., C. H. Su and W. L. Liu (2007). "Parameters optimization of a nano-particle wet milling process using the Taguchi method, response surface method and genetic algorithm." Powder Technology173(3): 153-162.

Hsiung, L. and T. Nieh (1997). "Substructure in a creep deformed lamellar TiAl alloy." Scriptamaterialia36(3): 323-330.

Huang, S., L. Zhou, X. Yu and Y. Cui (2012)."Experimental study of high-speed milling of SiCp/Al composites with PCD tools." The International Journal of Advanced Manufacturing Technology62(5-8): 487-493.

Huang, Y. and S. Y. Liang (2004). "Modeling of CBN tool flank wear progression in finish hard turning." Journal of manufacturing science and engineering126(1): 98-106.

Hunt, W. (1997). "Metal Matrix Composites." Mechanical Engineering -New York and Basel-Marcel -Deker: 293-300.

Hurless, B. E. and F. H. Froes (2002)."Lowering theCost of Titanium." The AMPTIAC Quarterly 6(2): 3–9.

Hurlich, A. (1968). Low temperature metals.Proc.

Imai, K., G. King and E. A. Stuart (2008)."Misunderstandings between experimentalists and observationalists about causal inference." Journal of the royal statistical society: series A (statistics in society)171(2): 481-502.

Irfan, M. and V. Prakash (2000). "Dynamic deformation and fracture behavior of novel damage tolerant discontinuously reinforced aluminum composites." International Journal of Solids and Structures37(33): 4477-4507.

Jin, L., A. Riahi, K. Farokhzadeh and A. Edrisy (2014)."Investigation on interfacial adhesion of Ti–6Al–4V/nitride coatings." Surface and Coatings Technology260: 155-167.

Kaçal, A. and F. Yıldırım (2013)."High Speed Hard Turning of AISI S1 (60WCrV8) Cold Work Tool Steel."ActaPolytechnicaHungarica10(8).

Kagnaya, T., M. Lazard, L. Lambert, C. BOHER and T. Cutard (2011). "Temperature evolution in a WC-6% Co cutting tool during turning machining: experiment and finite element simulations." WSEAS Trans. Heat Mass Transf6: 71-80.

Kainer, K. U. (2006). Metal matrix composites: custom-made materials for automotive and aerospace engineering, John Wiley & Sons.

Kaps, M., W. Lamberson and W. Lamberson (2004). "Concepts of experimental design." Biostatistics for animal science: 263-271.

Karakaş, M. S., A. Acır, M. Übeyli and B. Ögel (2006). "Effect of cutting speed on tool performance in milling of B 4 C p reinforced aluminum metal matrix composites." Journal of materials processing technology178(1): 241-246.

Kertesz, J., R. Pryor, D. W. Richerson and R. Cutler (1988). "Machining titanium alloys with ceramic tools." JOM Journal of the Minerals, Metals and Materials Society40(5): 50-51.

Kilickap, E. (2010). "Modeling and optimization of burr height in drilling of Al-7075 using Taguchi method and response surface methodology." The International Journal of Advanced Manufacturing Technology49(9): 911-923.

Kim, J., J. Kim, Y. Lee, C. Park and C. Lee (1999). "Microstructural analysis on boundary sliding and its accommodation mode during superplastic deformation of Ti–6Al–4V alloy." Materials Science and Engineering: A263(2): 272-280.

King, R. I. (1985). "Handbook of high speed machining technology." Chapman and Hall, 29 West 35 th Street, New York, New York 10001, USA, 1985.

Klocke, F. and A. Kuchle (2011). Manufacturing processes 1: cutting, Springer Science & Business Media.

Kobashi, K. (2010). Diamond films: chemical vapor deposition for oriented and heteroepitaxial growth, Elsevier.

Komanduri, R. and W. Reed (1983). "Evaluation of carbide grades and a new cutting geometry for machining titanium alloys." Wear92(1): 113-123.

Konig, W. (1978).Applied research on the machinability of titanium and its alloys. Proc. AGARD Conf. Advanced Fabrication Processes, Florence, Italy.

Kremer, A., A. Devillez, S. Dominiak, D. Dudzinski and M. El Mansori (2008)."MACHINABILITY OF AI/SiC PARTICULATE METAL-MATRIX COMPOSITES UNDER DRY CONDITIONS WITH CVD DIAMOND-COATED CARBIDE TOOLS." Machining Science and Technology12(2): 214-233.

Lahiff, C., S. Gordon and P. Phelan (2007). "PCBN tool wear modes and mechanisms in finish hard turning." Robotics and Computer-Integrated Manufacturing23(6): 638-644.

Lee, W. and C. Lin (1997). "Adiabatic shear fracture of titanium alloy subjected to high strain rate and high temperature loadings." Le Journal de Physique IV7(C3): C3-855-C853-860.

Leyens, C. and M. Peters (2003). Titanium and titanium alloys, Wiley Online Library.

Lu, J., J. Qin, Y. Chen, Z. Zhang, W. Lu and D. Zhang (2010)."Superplasticity of coarse-grained (TiB+ TiC)/Ti–6Al–4V composite." Journal of Alloys and Compounds490(1): 118-123.

Marinescu, I. D., W. B. Rowe, B. Dimitrov and I. Inaski (2004). Tribology of abrasive machining processes, Elsevier.

Montgomery, D. C. (2008).Design and analysis of experiments, John Wiley & Sons.

Morgan, P. (2005). Carbon fibers and their composites, CRC press.

Moshat, S., S. Datta, A. Bandyopadhyay and P. Pal (2010). "Optimization of CNC end milling process parameters using PCA-based Taguchi method." International Journal of Engineering, Science and Technology2(1): 95-102.

Muthukrishnan, N. and J. P. Davim (2011). "An investigation of the effect of work piece reinforcing percentage on the machinability of Al-SiC metal matrix composites." Journal of Mechanical E.

Myers, R. H., D. C. Montgomery and C. M. Anderson-Cook (2009). Response surface methodology: process and product optimization using designed experiments, John Wiley & Sons.

Nalbant, M., H. Gökkaya and G. Sur (2007)."Application of Taguchi method in the optimization of cutting parameters for surface roughness in turning." Materials &design28(4): 1379-1385.

Nian, C., W. Yang and Y. Tarng (1999)."Optimization of turning operations with multiple performance characteristics." Journal of Materials Processing Technology95(1): 90-96.

Niknam, S. A., R. Khettabi and V. Songmene (2014). Machinability and Machining of Titanium Alloys: A Review. Machining of Titanium Alloys, Springer: 1-30.

Njuguna, M. J., D. Gao and Z. Hao (2013). "Tool Wear, Surface Integrity and Dimensional Accuracy in Turning Al2124SiCp (45% wt) Metal Matrix Composite using CBN and PCD Tools."

Pavel, R., I. Marinescu, M. Deis and J. Pillar (2005). "Effect of tool wear on surface finish for a case of continuous and interrupted hard turning." Journal of Materials Processing Technology170(1): 341-349.

Phadke, M. S. (1989). Quality engineering using robust design, Prentice Hall Englewood Cliffs, NJ.

Phadke, M. S. (1989). "Quality Engineering Using Robust Design, PTR Prentice-Hall."Inc., Englewood Cliffs, NJ.

Poletti, C., A. Merstallinger, T. Schubert, W. Marketz and H.-P.Degischer (2004). "Wear and Friction Coefficient of Particle Reinforced Ti- Alloys." Materialwissenschaft und Werkstofftechnik35(10- 11): 741-749.

Pramanik, A., L. Zhang and J. Arsecularatne (2008). "Machining of metal matrix composites: Effect of ceramic particles on residual stress, surface roughness and chip formation." International Journal of Machine Tools and Manufacture48(15): 1613-1625.

Recht, R. (1964). "Catastrophic thermoplastic shear." Journal of Applied Mechanics31(2): 189-193.

Rokicki, P., Z. Spotz, L. Fusova, K. Saksl, C. Siemers and B. ZAHRAB "CHIP FORMATION PROCESS OF Ti-15V-3Al-3Sn-3Cr ALLOY."

Ross, P. J. (1988). "Taguchi techniques for quality engineering: loss function, orthogonal experiments, parameter and tolerance design."

Sadat, A. B. (2012). Surface integrity when machining metal matrix composites.Machining of Metal Matrix Composites, Springer: 51-61.

Schulz, H. (1999). "The history of high-speed machining."Revista de Ciência e Tecnologia7(13): 9-18.

Sikder, S. and H. Kishawy (2012). "Analytical model for force prediction when machining metal matrix composite." International Journal of Mechanical Sciences59(1): 95-103.

Simmons, J. P., L. D. Nelson and U. Simonsohn (2011). "False-positive psychology undisclosed flexibility in data collection and analysis allows presenting anything as significant." Psychological science: 0956797611417632.

Smith, G. T. (2008). Cutting tool technology, Springer-Verlag London.

Stephenson, D. A. and J. S. Agapiou (2005). Metal cutting theory and practice, CRC press.

Sun, S., M. Brandt and M. Dargusch (2009). "Characteristics of cutting forces and chip formation in machining of titanium alloys." International Journal of Machine Tools and Manufacture49(7): 561-568.

Taguchi, G. and Y. Yokoyama (1993). Taguchi methods: design of experiments, Amer Supplier Inst.

Taylor, B. and E. Weidmann (2008). "Metallographic preparation of titanium, struers application notes." Struers. Denmark: RosendahlsBogtryk.

Thakur, D., B. Ramamoorthy and L. Vijayaraghavan (2010). "Effect of high speed cutting parameters on the surface characteristics of superalloy Inconel 718." practice1: 5.

Tsao, C. (2009). "Grey–Taguchi method to optimize the milling parameters of aluminum alloy." The International Journal of Advanced Manufacturing Technology40(1): 41-48.

Übeylı, M., A. Acir, M. SerdarKarakaş and B. Ögel (2008). "Effect of feed rate on tool wear in milling of Al-4% Cu/B4 C p composite." Materials and Manufacturing Processes23(8): 865-870.

Vagnorius, Ž. (2010). "Reliability of metal cutting tools:: Stochastic tool life modelling and optimization of tool replacement time."

Vaughn, R. and R. Krueck (1960). "Recent Developments in Ultra-High Speed Machining." Technical paper255.

Ward-Close, M., S. Godfrey and J. Robertson (2001). "Titanium metal matrix composites." Series in Materials Science and Engineering: 241.

Welsch, G., R. Boyer and E. Collings (1993). Materials properties handbook: titanium alloys, ASM international.

Woodcock, R. W. (1997). Woodcock diagnostic reading battery, Itasca, IL: Riverside.

Worswick, M., N. Qiang, P. Niessen and R. Pick (1992). "Microstructure and fracture during high-rate forming of iron and tantalum." Marcel Dekker, Inc., Shock-Wave and High-Strain-Rate Phenomena in Materials(USA), 1992: 87-95.

Zener, C. and J. Hollomon (1944). "Effect of strain rate upon plastic flow of steel." Journal of Applied physics15(1): 22-32.

Zhang, J. Z., J. C. Chen and E. D. Kirby (2007). "Surface roughness optimization in an end-milling operation using the Taguchi design method." Journal of Materials Processing Technology184(1): 233-239.

Zhang, Y., Z. Zhou, J. Wang and X. Li (2013). "Diamond tool wear in precision turning of titanium alloy." Materials and Manufacturing Processes28(10): 1061-1064.

Zhu, D., X. Zhang and H. Ding (2013). "Tool wear characteristics in machining of nickel-based superalloys." International Journal of Machine Tools and Manufacture64: 60-77.

Zoya, Z. and R. Krishnamurthy (2000). "The performance of CBN tools in the machining of titanium alloys." Journal of Materials Processing Technology100(1): 80-86.

APPENDICE

Table A- 1: Calculation of Each Parameter Level's *SN* (db) on Work-piece Surface Roughness

No	(SN) vc [db]			(SN) fr [db]			(SN) ap [db]		
	Level1	**Level2**	**Level3**	**Level1**	**Level2**	**Level3**	**Level1**	**Level2**	**Level3**
1	58.49	-	-	58.49	-	-	58.49	-	-
2	59.02	-	-	59.02	-	-	-	59.02	-
3	55.97	-	-	55.97	-	-	-	-	55.97
4	55.44	-	-	-	55.44	-	55.44	-	-
5	56.89	-	-	-	56.89	-	-	56.89	-
6	51.97	-	-	-	51.97	-	-	-	51.97
7	54.56	-	-	-	-	54.56	54.56	-	-
8	53.59	-	-	-	-	53.59	-	53.59	-
9	50.35	-	-	-	-	50.35	-	-	50.35
10	-	60.71	-	60.71	-	-	60.71	-	-
11	-	58.89	-	58.89	-	-	-	58.89	-
12	-	56.36	-	56.36	-	-	-	-	56.36
13	-	54.07	-	-	54.07	-	54.07	-	-
14	-	59.25	-	-	59.25	-	-	59.25	-
15	-	57.99	-	-	57.99	-	-	-	57.99
16	-	55.85	-	-	-	55.85	55.85	-	-
17	-	57.98	-	-	-	57.98	-	57.98	-
18	-	56.71	-	-	-	56.71	-	-	56.71
19	-	-	62.54	62.54	-	-	62.54	-	-
20	-	-	71.59	71.59	-	-	-	71.59	-
21	-	-	62.05	62.05	-	-	-	-	62.05
22	-	-	68.20	-	68.20	-	68.20	-	-
23	-	-	60.65	-	60.65	-	-	60.65	-
24	-	-	56.48	-	56.48	-	-	-	56.48
25	-	-	54.78	-	-	54.78	54.78	-	-
26	-	-	63.58	-	-	63.58	-	63.58	-
27	-	-	52.15	-	-	52.15	-	-	52.15
Sum	496.29	517.82	552.01	545.62	520.95	499.55	524.64	541.44	500.03
Parameter-Effects[db]	55.14	57.54	**61.33**	60.62	57.88	55.51	58.29	60.16	55.56
D(SN) [db]	2.39		3.80	-2.74		-2.38	1.87		**-4.6**

Table A- 2: Calculation of Each Parameter Level's SN (db) on the Tool Wear Rate

No	(SN) Vc [db]			(SN) fr [db]			(SN) a_p[db]		
	Level1	**Level2**	**Level3**	**Level1**	**Level2**	**Level3**	**Level1**	**Level2**	**Level3**
1	97.72	-	-	97.72	-	-	97.72	-	-
2	101.94	-	-	101.94	-	-	-	101.94	-
3	104.44	-	-	104.44	-	-	-	-	104.44
4	100.92	-	-	-	100.92	-	100.92	-	-
5	99.17	-	-	-	99.17	-	-	99.17	-
6	101.94	-	-	-	101.94	-	-	-	101.94
7	99.17	-	-	-	-	99.17	99.17	-	-
8	100.92	-	-	-	-	100.92	-	100.92	-
9	98.44	-	-	-	-	98.44	-	-	98.44
10	-	94.89	-	94.89	-	-	94.89	-	-
11	-	95.92	-	95.92	-	-	-	95.92	-
12	-	95.10	-	95.10	-	-	-	-	95.1
13	-	97.72	-	-	97.72	-	97.72	-	-
14	-	101.94	-	-	101.94	-	-	101.94	-
15	-	103.10	-	-	103.10	-	-	-	103.1
16	-	104.48	-	-	-	104.48	104.48	-	-
17	-	100.92	-	-	-	100.92	-	100.92	-
18	-	95.94	-	-	-	95.94	-	-	95.94
19	-	-	95.92	95.92	-	-	95.92	-	-
20	-	-	96.48	96.48	-	-	-	96.48	-
21	-	-	93.98	93.98	-	-	-	-	93.98
22	-	-	96.48	-	96.48	-	96.48	-	-
23	-	-	97.72	-	97.72	-	-	97.72	-
24	-	-	94.89	-	94.89	-	-	-	94.89
25	-	-	96.48	-	-	96.48	96.48	-	-
26	-	-	95.39	-	-	95.39	-	95.39	-
27	-	-	93.56	-	-	93.56	-	-	93.56
Sum	904.65	-89	860.89	876.38	893.88	885.28	883.78	890.39	881.39
Parameter-Effects[db]	**100.52**	98.89	95.65	97.38	99.32	98.36	98.20	98.93	97.93
D(SN) [db]	-1.63		**-3.23**	1.94		-0.96	0.73		-1.0

Table A- 3: Calculation of Each Parameter Level's SN (db) on the Radial Force

No	(SN) vc [db]			(SN) fr [db]			(SN) ap [db]		
	Level1	**Level2**	**Level3**	**Level1**	**Level2**	**Level3**	**Level1**	**Level2**	**Level3**
1	-50.16	-	-	-50.16	-	-	-50.16	-	-
2	-43.17	-	-	-43.17	-	-	-	-43.17	-
3	-45.15	-	-	-45.15	-	-	-	-	-45.15
4	-50.21	-	-	-	-50.21	-	-50.21	-	-
5	-44.76	-	-	-	-44.76	-	-	-44.76	-
6	-45.67	-	-	-	-45.67	-	-	-	-45.67
7	-42.61	-	-	-	-	-42.61	-42.61	-	-
8	-45.53	-	-	-	-	-45.53	-	-45.53	-
9	-43.23	-	-	-	-	-43.23	-	-	-43.23
10	-	-42.28	-	-42.28	-	-	-42.28	-	-
11	-	-46.85	-	-46.85	-	-	-	-46.85	-
12	-	-43.52	-	-43.52	-	-	-	-	-43.52
13	-	-42.61	-	-	-42.61	-	-42.61	-	-
14	-	-44.91	-	-	-44.91	-	-	-44.91	-
15	-	-46.06	-	-	-46.06	-	-	-	-46.06
16	-	-45.06	-	-	-	-45.06	-45.06	-	-
17	-	-44.40	-	-	-	-44.40	-	-44.40	-
18	-	-42.35	-	-	-	-42.35	-	-	-42.35
19	-	-	-45.15	-45.15	-	-	-45.15	-	-
20	-	-	-44.24	-44.24	-	-	-	-44.24	-
21	-	-	-58.76	-58.76	-	-	-	-	-58.76
22	-	-	-44.24	-	-44.24	-	-44.24	-	-
23	-	-	-42.48	-	-42.48	-	-	-42.48	-
24	-	-	-51.75	-	-51.75	-	-	-	-51.75
25	-	-	-44.51	-	-	-44.51	-44.51	-	-
26	-	-	-45.98	-	-	-45.98	-	-45.98	-
27	-	-	-41.44	-	-	-41.44	-	-	-41.44
Sum	-410.48	-398.03	-418.55	-419.28	-412.69	-395.09	-406.82	-402.32	-417.93
ParameterEffects[db]	-45.61	-44.23	-46.51	-46.59	-45.85	**-43.90**	-45.20	-44.70	-46.44
D(SN) [db]	1.38		**-2.28**	0.73		1.96	0.50		-1.74

Table A- 4: Calculation of Each Parameter Level's *SN* (db) on the Feed Force

No	(SN) vc [db]			(SN) fr [db]			(SN) ap [db]		
	Level1	**Level2**	**Level3**	**Level1**	**Level2**	**Level3**	**Level1**	**Level2**	**Level3**
1	-38.49	-	-	-38.49	-	-	-38.49	-	-
2	-31.60	-	-	-31.60	-	-	-	-31.60	-
3	-38.38	-	-	-38.38	-	-	-	-	-38.38
4	-33.98	-	-	-	-33.98	-	-33.98	-	-
5	-37.38	-	-	-	-37.38	-	-	-37.38	-
6	-34.65	-	-	-	-34.65	-	-	-	-34.65
7	-30.88	-	-	-	-	-30.88	-30.88	-	-
8	-37.95	-	-	-	-	-37.95	-	-37.95	-
9	-32.26	-	-	-	-	-32.26	-	-	-32.26
10	-	-31.60	-	-31.60	-	-	-31.60	-	-
11	-	-38.89	-	-38.89	-	-	-	-38.89	-
12	-	-36.26	-	-36.26	-	-	-	-	-36.26
13	-	-30.88	-	-	-30.88	-	-30.88	-	-
14	-	-33.26	-	-	-33.26	-	-	-33.26	-
15	-	-30.63	-	-	-30.63	-	-	-	-30.63
16	-	-36.12	-	-	-	-36.12	-36.12	-	-
17	-	-36.12	-	-	-	-36.12	-	-36.12	-
18	-	-31.36	-	-	-	-31.36	-	-	-31.36
19	-	-	-31.13	-31.13	-	-	-31.13	-	-
20	-	-	-43.69	-43.69	-	-	-	-43.69	-
21	-	-	-45.30	-45.30	-	-	-	-	-45.3
22	-	-	-29.54	-	-29.54	-	-29.54	-	-
23	-	-	-31.36	-	-31.36	-	-	-31.36	-
24	-	-	-37.73	-	-37.73	-	-	-	-37.73
25	-	-	-29.25	-	-	-29.25	-29.25	-	-
26	-	-	-38.06	-	-	-38.06	-	-38.06	-
27	-	-	-24.61	-	-	-24.61	-	-	-24.61
Sum	-315.56	-305.12	-310.67	-335.32	-299.41	-296.62	-291.86	-328.32	-311.18
Parameter-Effects[db]	-35.06	-33.90	-34.52	-37.26	**-33.27**	-32.96	-32.43	-36.48	-34.58
D(SN) [db]	1.16		-0.62	3.99		0.31	**-4.05**		1.9

Table A- 5: Calculation of each parameter level's SN (db) on the cutting force

No	(SN) vc [db]			(SN) fr [db]			(SN) ap [db]		
	Level1	**Level2**	**Level3**	**Level1**	**Level2**	**Level3**	**Level1**	**Level2**	**Level3**
1	-41.87	-	-	-41.87	-	-	-41.87	-	-
2	-38.89	-	-	-38.89	-	-	-	-38.89	-
3	-45.34	-	-	-45.34	-	-	-	-	-45.34
4	-45.39	-	-	-	-45.39	-	-45.39	-	-
5	-43.52	-	-	-	-43.52	-	-	-43.52	-
6	-42.67	-	-	-	-42.67	-	-	-	-42.67
7	-2-	-	-	-	-	-2-	-2-	-	-
8	-46.85	-	-	-	-	-46.85	-	-46.85	-
9	-42.21	-	-	-	-	-42.21	-	-	-42.21
10	-	-40.34	-	-40.34	-	-	-40.34	-	-
11	-	-42.28	-	-42.28	-	-	-	-42.28	-
12	-	-37.73	-	-37.73	-	-	-	-	-37.73
13	-	-2-	-	-	-2-	-	-2-	-	-
14	-	-46.53	-	-	-46.53	-	-	-46.53	-
15	-	-43.11	-	-	-43.11	-	-	-	-43.11
16	-	-33.26	-	-	-	-33.26	-33.26	-	-
17	-	-43.58	-	-	-	-43.58	-	-43.58	-
18	-	-40.83	-	-	-	-40.83	-	-	-40.83
19	-	-	-34.15	-34.15	-	-	-34.15	-	-
20	-	-	-46.61	-46.61	-	-	-	-46.61	-
21	-	-	-48.88	-48.88	-	-	-	-	-48.88
22	-	-	-37.73	-	-37.73	-	-37.73	-	-
23	-	-	-36.12	-	-36.12	-	-	-36.12	-
24	-	-	-46.49	-	-46.49	-	-	-	-46.49
25	-	-	-40.75	-	-	-40.75	-40.75	-	-
26	-	-	-47.27	-	-	-47.27	-	-47.27	-
27	-	-	-38.79	-	-	-38.79	-	-	-38.79
Sum	-366.74	-347.65	-376.79	-376.09	-361.56	-353.53	-313.48	-391.65	-386.05
Parameter Effects[db]	-40.75	-38.63	-41.87	-41.79	-40.17	-39.28	**-34.83**	-43.52	-42.89
D(SN) [db]	2.12		-3.24	1.62		0.89	**-8.68**		0.63

Table A- 6: Calculation of each parameter level's *SN* (db) on workpart surface roughness during turning Ti-MMC with CBN insert

No	(SN) vc [db]			(SN) fr [db]			(SN) ap [db]		
	Level1	**Level2**	**Level3**	**Level1**	**Level2**	**Level3**	**Level1**	**Level2**	**Level3**
1	59.73	-	-	59.73	-	-	59.73	-	-
2	60	-	-	-	60	-	-	60	-
3	56.12	-	-	-	-	56.12	-	-	56.12
4	-	53.56	-	53.56	-	-	-	53.56	-
5	-	55.14	-	-	55.14	-	-	-	55.14
6	-	56.94	-	-	-	56.94	56.94	-	-
7	-	-	46.42	46.42	-	-	-	-	46.42
8	-	-	54.92	-	54.92	-	54.92	-	-
9	-	-	45.74	-	-	45.74	-	45.74	-
Sum	175.85	165.64	147.08	159.71	170.06	158.8	171.59	159.3	157.68
Parameter-Effects[db]	**58.62**	55.21	49.03	53.24	56.69	52.93	57.20	53.10	52.56
D(SN) [db]	-3.40	**-6.19**		3.45	-3.75		-4.10	-0.54	

Table A- 7: Calculation of each parameter level's *SN* (db) on workpartsurface roughness during turning Ti-MMC with CBN insert

No	(SN) vc [db]			(SN) fr [db]			(SN) ap [db]		
	Level1	**Level2**	**Level3**	**Level1**	**Level2**	**Level3**	**Level1**	**Level2**	**Level3**
1	99.61	-	-	99.61	-	-	99.61	-	-
2	98.87	-	-	-	98.87	-	-	98.87	-
3	94.31	-	-	-	-	94.31	-	-	94.31
4	-	99.42	-	99.42	-	-	-	99.42	-
5	-	90.16	-	-	90.16	-	-	-	90.16
6	-	98.69	-	-	-	98.69	98.69	-	-
7	-	-	88.60	88.60	-	-	-	-	88.60
8	-	-	92.56	-	92.56	-	92.56	-	-
9	-	-	95.85	-	-	95.85	-	95.85	-
Sum	292.80	288.27	277.01	287.64	281.59	288.85	290.86	294.14	273.07
Parameter-Effects[db]	97.60	96.09	92.34	95.88	93.86	96.28	96.95	**98.05**	91.02
D(SN) [db]	-1.51	**-3.75**		-2.02	2.42		2.42	1.09	

Table A- 8: (Signal/Noise) of surface roughness in milling Ti-MMC by carbide insert

No	(SN) ap [db]		(SN) vc [db]			(SN) fr [db]		
	Level1	Level2	Level1	Level2	Level3	Level1	Level2	Level3
1	48.98	-	48.98	-	-	48.98	-	-
2	48.15	-	48.15	-	-	-	48.15	-
3	48.69	-	48.69	-	-	-	-	48.69
4	44.60	-	-	44.60	-	44.60	-	-
5	44.14	-	-	44.14	-	-	44.14	-
6	44.60	-	-	44.60	-	-	-	44.60
7	46.05	-	-	-	46.05	46.05	-	-
8	45.52	-	-	-	45.52	-	45.52	-
9	44.71	-	-	-	44.71	-	-	44.71
10	-	48.06	48.06	-	-	48.06	-	-
11	-	51.80	51.80	-	-	-	51.80	-
12	-	49.07	49.07	-	-	-	-	49.07
13	-	48.42	-	48.42	-	48.42	-	-
14	-	46.55	-	46.55	-	-	46.55	-
15	-	44.03	-	44.03	-	-	-	44.03
16	-	46.05	-	-	46.05	46.05	-	-
17	-	46.62	-	-	46.62	-	46.62	-
18	-	44.25	-	-	44.25	-	-	44.25
Sum	415.43	380.60	294.74	272.33	228.97	282.16	282.78	231.10
Parameter-Effects [db]	46.16	42.29	**49.12**	45.39	38.16	47.03	47.13	38.52
D(SN) [db]	-3.87		-3.74		-7.23	0.10		**-8.61**

Table A- 9: (Signal/Noise) by input parameters in milling Ti-MMC with carbide insert

No	(SN) ap [db]		(SN) vc [db]			(SN) fr [db]		
	Level1	Level2	Level1	Level2	Level3	Level1	Level2	Level3
1	38.40	-	38.40	-	-	38.40	-	-
2	37.57	-	37.57	-	-	-	37.57	-
3	38.12	-	38.12	-	-	-	-	38.12
4	34.02	-	-	34.02	-	34.02	-	-
5	33.57	-	-	33.57	-	-	33.57	-
6	34.02	-	-	34.02	-	-	-	34.02
7	35.48	-	-	-	35.48	35.48	-	-
8	34.95	-	-	-	34.95	-	34.95	-
9	34.14	-	-	-	34.14	-	-	34.14
10	-	37.82	37.82	-	-	37.82	-	-
11	-	41.56	41.56	-	-	-	41.56	-
12	-	38.83	38.83	-	-	-	-	38.83
13	-	38.17	-	38.17	-	38.17	-	-
14	-	36.30	-	36.30	-	-	36.30	-
15	-	33.79	-	33.79	-	-	-	33.79
16	-	35.81	-	-	35.81	35.81	-	-
17	-	36.38	-	-	36.38	-	36.38	-
18	-	34.01	-	-	34.01	-	-	34.01
Sum	320.27	332.67	232.30	209.87	210.77	219.70	220.33	212.91
Parameter-Effects [db]	35.59	36.96	**38.72**	34.98	35.13	36.62	36.72	35.49
D(SN) [db]	1.38		**-3.74**		0.15	0.10		-1.24

Table A- 10: (Signal/Noise) of roughness in milling Ti-MMC with PCD insert

No	(SN) vc [db]			(SN) fr [db]			(SN) ap [db]		
	Level1	**Level2**	**Level3**	**Level1**	**Level2**	**Level3**	**Level1**	**Level2**	**Level3**
1	67.99	-	-	67.99	-	-	67.99	-	-
2	66.45	-	-	-	66.45	-	-	66.45	-
3	58.94	-	-	-	-	58.94	-	-	58.94
4	-	74.25	-	74.25	-	-	-	-	74.25
5	-	66.48	-	-	66.48	-	66.48	-	-
6	-	68.10	-	-	-	68.10	-	68.10	-
7	-	-	55.79	55.79	-	-	-	-	55.79
8	-	-	60.59	-	60.59	-	60.59	-	-
9	-	-	56.42	-	-	56.42	-	56.42	-
Sum	193.38	**208.83**	172.80	198.03	193.53	183.46	195.07	190.97	188.98
Parameter-Effects[db]	64.46	**69.61**	57.60	66.01	64.51	61.15	65.02	63.66	62.99
D(SN) [db]	5.15	**-12.01**		-1.5	-3.36		-1.36	-0.67	

Table A- 11: (Signal/Noise) of tool wear ratio in milling Ti-MMC with PCD insert

No	(SN) vc [db]			(SN) fr [db]			(SN) ap [db]		
	Level1	**Level2**	**Level3**	**Level1**	**Level2**	**Level3**	**Level1**	**Level2**	**Level3**
1	14.57	-	-	14.57	-	-	14.57	-	-
2	15.18	-	-	-	15.18	-	-	15.18	-
3	12.65	-	-	-	-	12.65	-	-	12.65
4	-	11.94	-	11.94	-	-	-	-	11.94
5	-	12.09	-	-	12.09	-	12.09	-	-
6	-	12.57	-	-	-	12.57	-	12.57	-
7	-	-	9.34	9.34	-	-	-	-	9.34
8	-	-	10.34	-	10.34	-	10.34	-	-
9	-	-	10.20	-	-	10.20	-	10.20	-
Sum	42.3	36.6	29.9	35.5	37.8	35.5	37	37.9	33.9
Parameter-Effects[db]	**14.1**	12.2	10	11.8	12.6	11.8	12.3	12.6	11.3
D(SN) [db]	-1.9	-2.2		0.8	-0..8		**0.3**	-1.3	